CAPITAL UNIVERSITY OF SCIENCE AND TECHNOLOGY, ISLAMABAD

Design, Synthesis, Characterization and Pharmacological Evaluation of Novel Schiff Base Moieties

by

Noor ul Ain

A thesis submitted in partial fulfillment for the degree of Master of Philosophy

in the

Faculty of Pharmacy
Department of Pharmaceutical Chemistry

2025

I dedicate this thesis to my loving and supportive family and friends, whose unwavering support has been crucial in helping me achieve my life goals.

CERTIFICATE OF APPROVAL

Design, Synthesis, Characterization and Pharmacological Evaluation of Novel Schiff Base Moieties

by

Noor ul Ain

(MPH233011)

THESIS EXAMINING COMMITTEE

S. No.	Examiner	Name	Organization
(a)	External Examiner	Dr. Madiha Ahmed	STMU, Islamabad
(b)	Internal Examiner	Dr. Farman Ullah Khan	CUST, Islamabad
(c)	Supervisor	Dr. Siraj Khan	CUST, Islamabad

Dr. Siraj Khan
Thesis Supervisor
September, 2025

Dr. Reem
Head
Dept. of Pharmaceutical Chemistry
September, 2025

Dr. Muzaffar Abbas
Dean
Faculty of Pharmacy
September, 2025

Author's Declaration

I, **Noor ul Ain** hereby state that my MS thesis titled "**Design, Synthesis, Characterization and Pharmacological Evaluation of Novel Schiff Base Moieties**" is my own work and has not been submitted previously by me for taking any degree from Capital University of Science and Technology, Islamabad or anywhere else in the country/abroad.

At any time if my statement is found to be incorrect even after my graduation, the University has the right to withdraw my MPhill Degree.

(Noor ul Ain)

Registration No: MPH233011

Plagiarism Undertaking

I solemnly declare that research work presented in this thesis titled "**Design, Synthesis, Characterization and Pharmacological Evaluation of Novel Schiff Base Moieties**" is solely my research work with no significant contribution from any other person. Small contribution/help wherever taken has been duly acknowledged and that complete thesis has been written by me.

I understand the zero tolerance policy of the HEC and Capital University of Science and Technology towards plagiarism. Therefore, I as an author of the above titled thesis declare that no portion of my thesis has been plagiarized and any material used as reference is properly referred/cited.

I undertake that if I am found guilty of any formal plagiarism in the above titled thesis even after award of MPhill Degree, the University reserves the right to withdraw/revoke my MPhill degree and that HEC and the University have the right to publish my name on the HEC/University website on which names of students are placed who submitted plagiarized work.

(Noor ul Ain)

Registration No: MPH233011

Acknowledgement

In the name of **Allah**, the Most Gracious, the Most Merciful. Peace and blessings be upon His noble servant and final messenger, **Prophet Muhammad (S.A.W)**. Above all, I express my deepest gratitude to **Allah** Almighty and His beloved **Prophet Muhammad (S.A.W)**; without their divine guidance and blessings, the completion of this work would not have been possible. I owe a deep depth of gratitude to our University, **Capital University of Science & Technology (CUST)** for giving me such an opportunity to complete this work. A special thanks to the Dean D**r. Muzaffar Abbas** for encouraging throughout the entire process.

I would like to acknowledge and very grateful to my **Supervisor Dr. Siraj Khan** who has been always generous during all phases of the research and for all the valuable lessons that I learned during this period, I thank him from the bottom of my heart. I am sincerely grateful to **Mr. Muhammad Ibrar Khan** for their valuable guidance and contribution in part of this research.

My thanks and appreciation goes to my friend **Alina Javaid**. Last but not least, I want to express my wholehearted thanks to my **family specially my parents, sisters, and brother** who have provided me generous support throughout my life and specially in doing my research. Because of their unconditional love, support and prayers, I have completed this thesis.

(Noor ul Ain)

Abstract

Schiff bases are a versatile class of organic compounds with varied pharmacological actions. This study aims to design and synthesis a series of novel Schiff base derivatives (**1a**–**5a**) by reacting with sulfonamide drugs, particularly sulfamethoxypyridazine and sulfadimidine, with diverse aldehydes under mild acidic conditions in ethanol. The synthesized compounds were analyzed with Thin Layer Chromatography (TLC), Fourier Transform Infrared (FTIR) spectroscopy and Nuclear Magnetic Resonance (NMR) spectroscopy. The compounds were evaluated for their antioxidant potential by Total Antioxidant Capacity (TAC), Total Reducing Power (TRP), and DPPH assays. The compounds showed good antioxidant potential were further screened *in vivo*. FTIR confirmed characteristics imine peaks between 1636-1655 cm^{-1} and sulfonamide S=O stretches in the range of 1153-1282 cm^{-1}, validating successful condensation. The products were obtained in 71% to 79% yields. The compounds demonstrated good physiochemical characteristics. Compound **1a** exhibited the highest TAC and DPPH scavenging activity (89.3%), followed by **2a**, indicating their potential in mitigating oxidative stress. Compounds **1a** and **2a** demonstrated significant dose-dependent analgesic and anti-inflammatory effects in *in vivo* studies using acetic acid-induced writhing and carrageenan-induced paw edema models in BALB/c mice compared to standard diclofenac. Molecular docking studies, conducted using AutoDock Vina against COX-2 and NF-κB proteins, revealed strong binding affinities, with compound **4a** showing -9.9 kcal/mol and **5a** at -9.8kcal/mol against COX-2 surpassing diclofenac (-7.6kcal/mol). NF-κB docking also showed promising results, with 4a and 5a scoring -7.1 kcal/mol. All derivatives met Lipinski's Rule of Five such as appropriate molecular weight, lipophilicity (LogP ≤ 5), and topological polar surface area (TPSA < 140 $Å^2$). Toxicity predictions via ProTox- II classified compounds **3a-5a** as low toxicity (LD_{50}: 25,000 mg/kg), while **1a** and **2a** fell in GHS class 4 (LD_{50}: 1700 mg/kg). Organ-specific and systemic toxicities, including hepatotoxicity and carcinogenicity, were predicted only in **2a**, indicating a favorable safety profile for most derivatives. This study highlights that structural modifications of sulfonamides yields potent antioxidant and anti-inflammatory agents, supporting

their potential as preclinical candidates for safer, more effective anti-inflammatory therapies.

Keywords: Schiff bases, sulfonamides, anti-inflammatory activity. antioxidant potential, COX-2, NF-κB.

Contents

List of Figures

List of Tables

Abbreviations

ADME	Absorption, Distribution, Metabolism, and Excretion
ANOVA	Analysis of Variance
BBB	Blood-Brain Barrier
COX-2	Cyclooxygenase-2
DPPH	2,2-Diphenyl-1-picrylhydrazyl
FTIR	Fourier Transform Infrared Spectroscopy
i.p.	Intraperitoneal
i.pl.	Intraplanter
LD_{50}	Lethal Dose 50%
NF-κB	Nuclear Factor Kappa B
NMR	Nuclear Magnetic Resonance
NSAIDs	Non-Steroidal Anti-Inflammatory Drugs
PDB	Protein Data Bank
SAR	Structure-Activity Relationship
SD	Standard Deviation
TAC	Total Antioxidant Capacity
TLC	Thin Layer Chromatography
TRP	Total Reducing Power

Chapter 1

Introduction

1.1 Background

Synthetic chemistry links the structural properties and reactivity of organic compounds. This enables them to systematically design and synthesis novel compounds from simpler ones [1]. Physicochemical science investigates the structure of organic molecules and develops models that reflect their behavior utilizing chemical theories and experiments. A Schiff base is analogous to an aldehyde or ketone because the carbonyl group is substituted with an azomethine (-C=N-) or imine group [2]. Among organic molecules, Schiff base compounds have been found to be identified due to their significant and intriguing characteristics [3]. The privileged ligand Schiff bases [4] have been documented by HugoSchiff and are the condensation result of amines with carbonyl compounds [5] (Figure 1.1) . The presence of lone pairs is owing to sp2 hybridization, as the compound's carbon and nitrogen atoms are very reactive. These chemicals are crucial since they have strong features including flexibility, simplicity, and effectiveness [6].

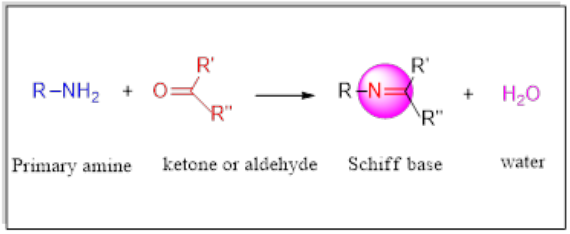

FIGURE 1.1: Synthesis of Schiff base [7].

Schiff bases exhibit a range of pharmacological and biological properties, including antioxidants [8], anthelmintic properties [9], anti-inflammatory [10], antifungal [11], antiviral [12], antibacterial [13], antispasmodic [14], anti-tuberculosis [15], and anticancer effects [16]. Schiff's base nucleus is present in the structures of a number of commercially available medications, such as the antibiotic nifuroxazide, the muscle relaxant dantrolene, and the antituberculosis medication thiacetazone, which are all shown in Figure 1.2.

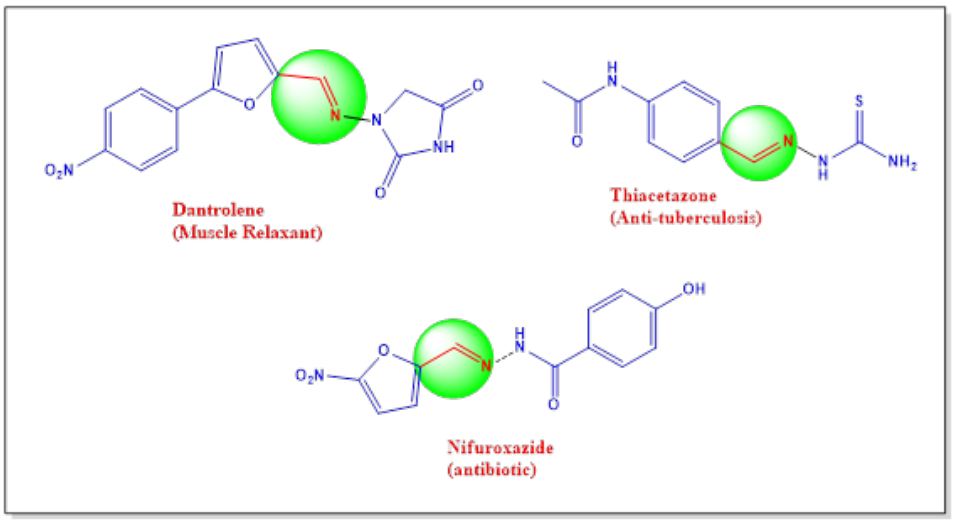

FIGURE 1.2: Marketed drugs with Schiff base nucleus [17].

The Schiff base formation requires a two-step reaction; Carbinolamine production, followed by dehydration [18]. When a primary amine is added nucleophilically to a carbonyl molecule, an unstable carbinolamine forms, which then dehydrates to form an imine, creating schiff bases. The type of amine and carbonyl components determines their reactivity [19]. The reactivity of benzaldehydes for Schiff base production varies; o-hydroxybenzaldehydes are more likely to produce Schiff

bases, whilst p-hydroxybenzaldehydes are less likely. In aqueous environments, Schiff bases can be unstable, but with subsequent reactions, they can form stable amide compounds [20]. The stability of Schiff bases throughout their development is significantly impacted by the presence of water. Structured water molecules attached to polar head groups aid in stabilizing the Schiff base in phosphatidylcholine (PC) reverse micelles. However, the Schiff foundation can break down if there is a larger amount of water. Since more co-solubilized water encourages protonation, the amount of water available also affects how much the Schiff base is protonated, indicating that water availability is essential for Schiff base stability and formation [21].

Sulphonamide-based Schiff bases are chemical compounds that emerge when sulphonamide derivatives condense with carbonyl compounds. The presence of an imine or azomethine (-C=N-) group distinguishes these compounds. Schiff bases were created by combining sulfonamides with vanillin, specifically sulfamethoxazole, sulfapyridine, sulfathiazole, sulfadiazine, and sulfisoxazole. In terms of antifungal activity against Candida albicans and antibacterial activity against *Staphylococcus* aureus and *Escherichia coli*, the synthesized Schiff bases performed better than the parent sulfonamides [22]. Schiff Base from Sulfamethoxypyridazine and 2-hydroxy-1-Naphthalene aldehyde assessed antibacterial activity against *Staphylococcus* aureus and *Escherichia coli* and showed varying effectiveness [23].

Due to their high affinity for biological targets and chemical versatility, sulfonamides and heterocycles are crucial functionalized scaffolds in contemporary medicinal chemistry. Over 362 FDA-approved pharmaceuticals contain sulfur-containing scaffolds, particularly sulfonamides, which are widely employed in a variety of therapeutic classes, including anti-infective, anticancer, metabolic, and central nervous system treatments. The development of drug candidates with enhanced pharmacokinetics and target selectivity is facilitated by their modular design [24]. These frameworks, which frequently play a crucial part in scaffold design workflows, improve lipophilicity and target binding affinity [25]. Simultaneously, sulfonamides function as pharmacophoric cores from which the development of more complex chemical series occurs, in addition to being bioactive agents

themselves. Since sulfonamide scaffolds can operate as bioisosteres for functional groups like carboxylic acids, they are of great importance in medicinal chemistry. This characteristic promotes the synthesis of structurally unique, drug-like compounds, improves metabolic stability, and makes it easier to adjust pKa [26]. The continued significance of sulfonamides in drug development is highlighted in a review published in Royal Society of Chemistry (RSC) Medicinal Chemistry. This has led to new synthetic techniques that employ sulfonamide moieties to produce molecules with a range of biological functions [27].

A comprehensive understanding of the inflammation cascade serves as a reason for using Schiff base derivatives as anti-inflammatory drugs [28].Inflammation is a prevalent indication of conditions such as rheumatoid arthritis, allergic asthma, and bacterial infections. It is marked by the percolation of lymphatic fluid, resulting in edema, erythema, and pain [29]. Infections generated by harmful bacteria induce complex inflammation in the body, a prevalent global issue that necessitates effective antibacterial medicines that promote antimicrobial defence [30]. The production of reactive oxygen species (ROS) results in oxidative stress, which harms the body's organ systems. This deterioration leads to more frequent inflammation [31]. NSAIDs are the most commonly prescribed medications for inflammation. It has been stated that NSAIDs work by inhibiting the activity of cyclooxygenase. COX comes in two forms: COX-1 and COX-2. The COX-1 enzyme produces prostaglandin, which promotes blood flow to the kidneys and helps to protect the stomach lining. COX-2 produces prostaglandins, which promote inflammation, resulting in discomfort, swelling, and fever [32]. Some NSAIDs are selective, inhibiting only COX-2; others are more typical, inhibiting both COX-1 and COX-2. NSAIDs are effective at reducing inflammation, but they are not without risks. Because NSAIDs inhibit COX-1 activity, prolonged use can induce gastrointestinal problems such as bleeding and stomach ulcers. Furthermore, several NSAIDs enhance cardiovascular risk for patients who already have heart problems [33]. Schiff bases produced from 2-(2,6-dichloroanilino) [34] and 4-amino-1,5-dimethyl-2-phenylpyrazol-3-one [10] have shown significant anti-inflammatory effects. Schiff bases have been employed extensively in recent years to formulate medications for a variety of biological activities [35]. The potential of Schiff bases to form various

functional groups is extremely important in biological research. Increasing the structural flexibility of Schiff bases can assist resolve current biological challenges while also improving the therapeutic efficacy of Schiff base-derived drugs [36].

1.2 Research Gap

Schiff bases are widely recognized for their diverse pharmacological activities, particularly antimicrobial and antioxidant properties, there is a notable lack of comprehensive studies on sulfonamide-based Schiff base derivatives. The incorporation of aromatic and heteroaromatic aldehydes in Schiff base synthesis is known to modulate biological efficacy. However, derivatives of sulfamethoxypyridazine and sulfadimidine have primarily been explored for antibacterial activity, with little attention to broader pharmacological profiling and minimal *in vivo*, computational, or ADME/toxicity evaluation. Thes limitation highlight the need for a more integrated and rational approach to advance such compounds toward therapeutic development.

1.3 Rationale of the Study

To address these constraints, the current study proposes the rational design and synthesis of a new series of Schiff base derivatives of sulfamethoxypyridazine and sulfadimidine employing a structurally diverse range of aromatic and heteroaromatic aldehydes. This method intends to examine the impact of aldehyde-derived structural alterations on the biological characteristics of the resulting compounds. The anti-inflammatory potential of the produced compounds will be comprehensively examined using well-established *in vivo* models, while antioxidant activity will be assessed using validated in vitro assays. Furthermore, *in silico* ADME (Absorption, Distribution, Metabolism, and Excretion) profiling will be used to predict pharmacokinetic behavior and drug-likeness. This collaborative work seeks to provide valuable SAR insights and expand the medicinal applications of sulfonamide-based Schiff bases.

1.4 Aim and Objectives

The aim of the project is to design and synthesize the pharmacologically active Schiff base derivatives.

The objective of this study are;

- The objective of this study is:
- To synthesize new Schiff base derivatives.
- To identify, purify, and characterize newly synthesized compounds.
- To evaluate the synthesized compounds anti-inflammatory and antioxidant potential.
- To perform molecular docking and ADME analysis for evaluating drug-likeness and interaction with inflammatory target proteins.

Chapter 2

Literature Review

2.1 Drug Discovery and Development

Drug discovery and development is a complicated and extensive process that involves identifying new medicinal compounds and then analysing their safety and efficacy [37]. Plant and animal products were important to early civilizations and valuable for medicinal uses [38]. Early in the 20^{th} century, systematic scientific study targeted at discovering new therapeutic agents marked the beginning of the shift towards modern drug discovery. A novel drugs development usually consists of a number of important steps [39]. In the pre-discovery stage, researchers focus on underlying a disease and identifying key targets, often proteins, that play role in progression. Once a promising target is confirmed, the drug discovery phase begins, involving the search for potential treatment, which are usually characterized as small molecules or biologics [37]. Drug discovery has used and continues to use natural product sources as well as synthetic organic chemistry to give appropriate starting points for future optimization [40]. Figure 2.1 schematically illustrates the step by step process involved in drug discovery.

Producing such molecules in a time, quality, and cost-effective manner has emerged as one of the most important applied issues in chemical sciences. Similarly, the progress of synthetic organic chemistry has been impacted by drug discovery. The area was revolutionized by the development of high-throughput screening (HTS)

equipment in the mid-1980s, which made it possible to screen thousands of compounds quickly [41]. Combinatorial chemistry emerged as a result of this development, which led to the development of massive and diverse chemical libraries [42]. Lead-oriented and fragment-based synthesis strategies have improved hit detection and lead optimization throughout time, therefore refining the drug development process. The ongoing integration of computational approaches, structure-based drug design, and artificial intelligence has sped the process, allowing for more efficient identification and validation of new drug candidates [43].

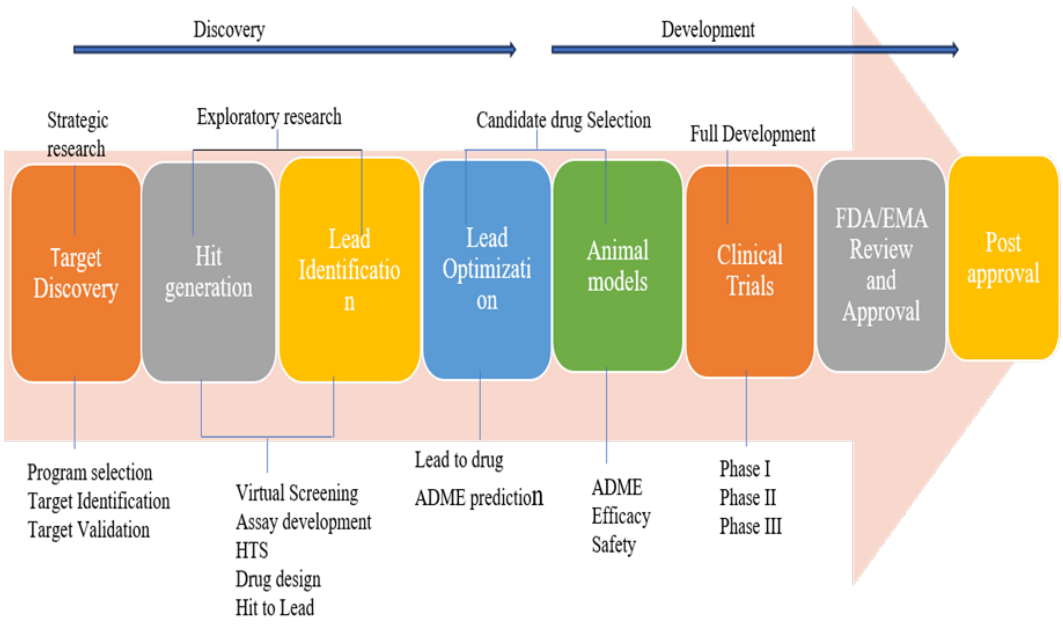

FIGURE 2.1: Schematic illustration of drug delivery process [44].

The pursuit for structurally varied and pharmacologically effective compounds has emerged as an important problem with modern drug discovery. To address the limits of traditional therapeutic drugs, researchers have increasingly concentrated on the development of hybrid designs and modular scaffolds that can interact with many biological targets. Schiff bases are a potential class of molecules with a variety of biological activities, structural diversity, and synthetic accessibility [44]. Their ability to incorporate a wide range of functional groups and form stable complexes with metal ions increases their utility in medicinal chemistry [45].

2.2 Schiff Bases as Potential Pharmacophores in Drug Design

Schiff bases, a significant class of compounds having an imine or azomethine moiety, have been utilized in the synthesis of several lead drugs with significant therapeutic benefits over the past few decades [46]. Hugo Schiff, a German scientist, was the first to report the findings of the reaction between primary amines and carbonyl compounds in 1864, which gave rise to the phrase Schiff's base. According to IUPAC rules, Schiff bases are imines containing a hydrocarbyl group on the nitrogen atom, represented by R2C = NR′ (R′ ≠ H) [47]. The presence of lone pairs is due to sp_2 hybridization, as the compound's carbon and nitrogen atoms are highly reactive [36]. A generalized structure of Schiff base is mentioned in Figure 2.2. Longer reaction periods and higher reaction temperatures are required because aliphatic ketones react with amines more slowly than aldehydes. Reaction yields can be increased from 80% to 95% by employing acid catalysts and excluding water from the reaction mixture. Aromatic ketones are less reactive than aliphatic ketones and require strong conditions to convert into imines [5].

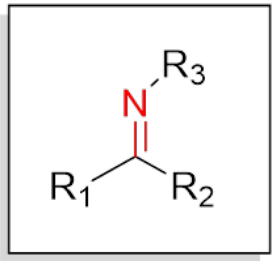

FIGURE 2.2: Structural representation of Schiff base R_1, R_2, R_3 are alkyl or aryl group [48].

2.3 Mechanistic Insights into Schiff Base Formation

The lone pair of electrons from the initial amine attack the electrophilic carbonyl nucleophilically in the Schiff base synthesis reaction. A 1,3-H shift takes place,

favoring the protonated imine's disassociation to yield the Schiff base after water is removed [49]. The complete mechanism is illustrated in Figure 2.3.

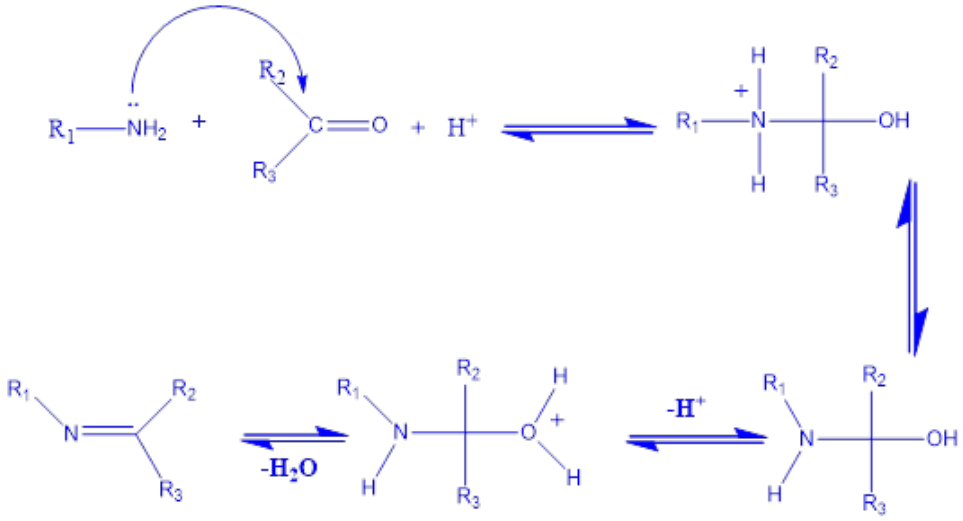

FIGURE 2.3: Mechanism of imine formation [50].

Typically, the product's separation, water elimination, or both enhance the formation's completion. Many Schiff bases can be hydrolysed by aqueous acids and bases into aldehydes, ketones, and amines [51]. Another variation on the theme of neutrophilic carbonyl group addition is the Schiff base generation mechanism. In this case, the amine functions as a neutrophil. During the first phase of the process, the amine reacts with the ketone or aldehyde to generate carbinolamine, an unstable addition product. An acid or a base catalyzes the carbinolamine's water loss mechanism [52]. Carbinolamine dehydration is catalyzed by an alcohol called acid. Since the rate-determining step in the formation of Schiff bases is often carbinolamine dehydration, acids catalyze the reaction. However, the acid concentration cannot be too high because amines are basic molecules. The balance moves to the left, limiting the synthesis of carbinolamines, when the amine is protonated and loses its neutrophilicity [53]. Therefore, a somewhat acidic pH can be used to produce a variety of Schiff bases. The dehydration of carbinolamines is accelerated by bases. The E2 elimination of alkyl halides is similar to this process, except for the lack of coordination. It goes in two steps through an anionic intermediate. The creation of Schiff bases actually entails a sequence of two types of reactions: addition and elimination [54].

2.4 Synthetic Route and Optimization of Schiff Bases

The elimination of a water molecule through the interaction of an aldehyde or ketone with a primary amine is the most widely used technique for producing imines, according to Schiff. The production of Schiff bases requires this condensation reaction, which can be accelerated by acid catalysis [55]. A Dean-Stark apparatus is commonly used to constantly drain water from the reaction under reflux conditions, shifting the balance in the direction of imine production [56, 57]. Several dewatering agents, including sodium sulfate and molecular sieves, have been used successfully to help with this transition [58]. To improve reaction efficiency, in situ dehydration techniques using solvents such as trimethyl orthoformate or tetramethyl orthosilicate have also been investigated. Acid catalysts are frequently necessary to encourage the production of imines [59]. There are many known catalysts, such as mineral acids like H_2SO_4 and HCl, organic acids like p-toluenesulfonic acid (PTSA) and pyridinium p-toluenesulfonate (PPTS), and solid-supported catalysts such acid resins and montmorillonite clay. Lewis acids like ZnCl are also used to improve reaction rates and selectivity [60], $TiCl_4$ [61], $SnCl_4$, $BF_3 \cdot Et_2O$, $MgSO_4$ [62], and Mg $(ClO_4)_2$ have been used. The scope of Schiff base synthesis has been greatly broadened by these developments in synthetic techniques, making it possible to prepare a variety of imine derivatives with a wide range of uses in coordination and medicinal chemistry [5]. The synthesis of Schiff bases is generally thought to be easy, cost-effective, and frequently provides the needed compounds in acceptable amounts [63–65].

2.5 Comparative Approaches to Schiff Base Synthesis

Four widely used techniques for synthesizing Schiff bases microwave, room temperature, grindstone, and reflux have been developed; they differ in reaction time,

product, and yield %. An overview of these methods is illustrated in Figure 2.4. The temperature-controlled microwave method of synthesis completes the process more quickly. A few drops of sodium hydroxide are added to an ethanolic solution of the aldehyde and the primary amine in a reaction vessel to change its pH. The combination is exposed to radiation for a few minutes while the reaction vessel is in a microwave. The mixture is immediately cooled by adding cold water after irradiation. The precipitate is collected through filtration and then dried and recrystallized from ethanol before being allowed to dry at room temperature [66].

Combine a primary amine with an aldehyde solution in a room-temperature ethanolic solution in a reaction vessel. Two to three drops of sodium hydroxide should be added to the finished liquid to change its pH. The product is precipitated out by adding cold water after the reaction mixture has been magnetically stirred for one to two hours at room temperature. Following filtration, the precipitate is dried, recrystallized from ethanol, and allowed to air dry at room temperature. The best results are obtained from this process, which also efficiently creates the product [67]. The Grindstone process allows for the creative and sustainable creation of Schiff bases. To adjust the pH of an ethanolic solution of aldehyde and primary amine in a mortar, add a few drops of citric acid. Then, for five to ten minutes, the mixture is mashed with a pestle. Applying cold water causes the product to precipitate out of the procedure. The precipitate is collected by filtering, dried, and recrystallized from ethanol before being allowed to dry at room temperature [68].

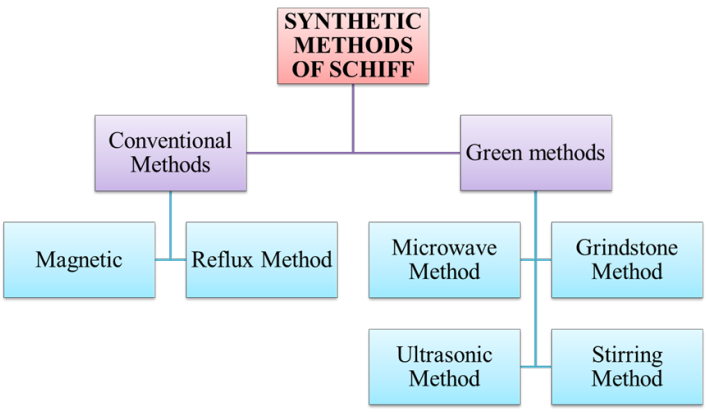

FIGURE 2.4: Synthetic Methods of Schiff Base [52].

The green technique lowers the cost of synthesis by lowering the reaction time from hours or days to minutes or seconds, carrying out the reaction at room temperature (RT), removing or substituting ecologically harmful solvents, etc [69]. However, obtaining azomethines via green methods is not always easy. When aliphatic Schiff bases are unstable in aqueous settings, an organic solvent, preferably anhydrous, is much more practical. Because aromatic Schiff bases are significantly less sensitive to the water in the reaction media than aliphatic imines, the green method is far easier to adopt in these cases [70].

Condensation of aldehydes and amines occurs under different reaction conditions and solvents. The Schiff Base is typically prepared using ethanol or methanol as solvents. Schiff bases can form in refluxing conditions or at room temperatures. Dehydrating substances like magnesium sulfate, which aid in removing water from the reaction environment, frequently promote the synthesis of these imines. A Dean–Stark apparatus can efficiently remove the produced water when non-polar solvents such as toluene or benzene are utilized, pushing the equilibrium in the direction of product production. Purification must be done carefully, though, because some methods, especially silica gel chromatography, might cause partial hydrolysis and degradation. Crystallization, on the other hand, provides a gentler and more dependable technique for separating pure products. These substances don't require particular storage conditions and are often stable in solid form. Furthermore, a broad variety of structurally varied derivatives can be produced thanks to the synthetic adaptability provided by different combinations of amines and aldehydes [54]. A summary of common synthetic strategies for Schiff base preparation is provided in Table 2.1.

TABLE 2.1: Schiff base can be made in four different ways: conventional (refluxed ethanol), mechanochemical (grinding), microwave-assisted, and combined procedures. Microwave radiation in grape juice [68]

Method	**Catalyst**	**Catalyst Quantity**	**Time**	**Yield**
Reflux	Glacial acetic acid	3-4 drops	360	80
Grinding	—	—	60	a
Microwave assisted	Glacial acetic acid	2 drops	14	80
Fruit juice	Lemon juice; pH=2.0 -2.8	0.5ml	7	88

Table 2.1 continued from previous page

Method	Catalyst	Catalyst Quantity	Time	Yield
	Orange juice; pH =2.8-3.1	0.5ml	10	76

2.6 Medicinal Relevance of Sulfonamide Scaffold

2.6.1 Chemical and Therapeutic Profile of Sulfonamides

In 1935, Gerhard Domagk identified the active component, sulfanilamide, after Prontosil, the sulfonamide prototype, was discovered [71]. Sulfonamide structures are organosulfur compounds with the -SO2NH2 and/or -SO2NH groups. They have a sulfanilamide group and distinctive 6- or 5-membered heterocyclic rings, as illustrated in Figure 2.5 [72].

Sulfonamides, the first synthetic chemotherapeutics, are important because they are powerful antimicrobials that inhibit some protozoa, such as coccidials, as well as gram-positive and gram-negative bacteria. By fully competitively binding the PABA, sulfonamides hinder the bacterial cell from multiplying and inhibit the generation of folic acid, which is required for DNA synthesis. Sulfonamides are often bacteriostatic [71].

Sulfonamides are typically weak organic acids that are more soluble at alkaline pH than acid pH and relatively insoluble in water. They vary in their degree of binding to plasma protein (15-90%) and have pKa values ranging from 2.65 to 10.4 [73]. Sulfonamide structures were utilized to develop a range of therapeutically effective medications, including sulfamethazine, sulfadiazine, sulfamethoxazole etc [72].

A key component of many significant bioactive and therapeutic substances, the main sulfonamide molecule has a variety of pharmacological medicine properties, including diuretic [74], hypoglycemic [75], antithyroid [76], antibacterial [77], antiviral [78], and anti-inflammatory activities [79].

Sulfonamides are not readily biodegradable and have the potential to cause a number of unwanted side effects, including digestive and respiratory problems [80], non-allergic effects to sulfonamide drugs include diarrhea, nausea, vomiting, dizziness, candidiasis, folate insufficiency, and migraines [81].

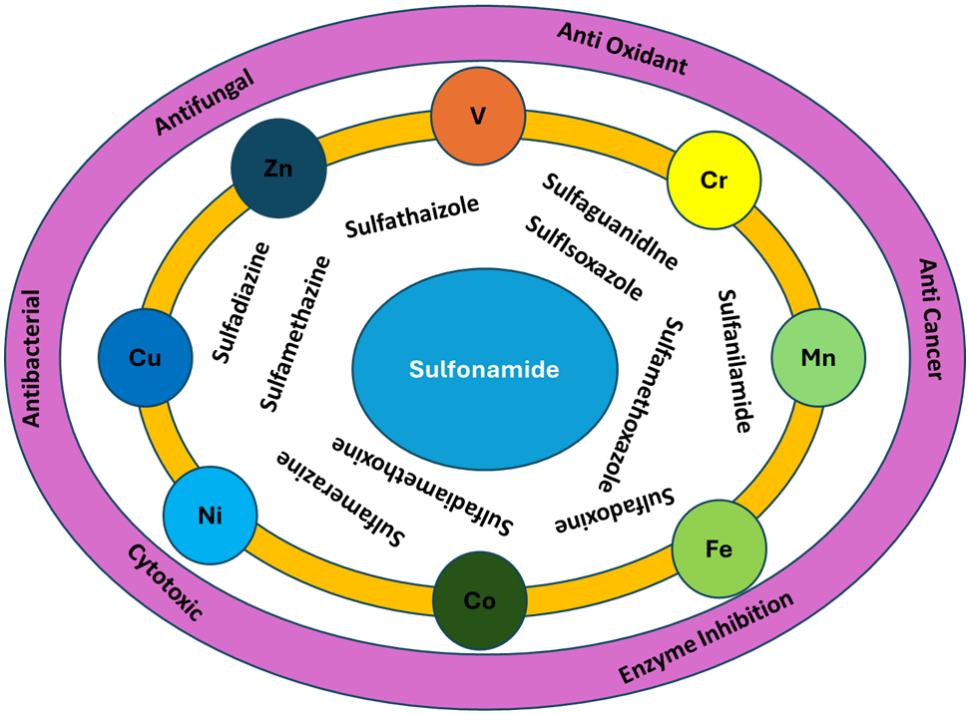

FIGURE 2.5: Characteristic features of sulfonamides.

2.6.2 Sulfadimidine

Sulfadimidine is a sulfa-based medication used to treat and prevent bacterial infections such as urinary tract infections, meningitis infections, influenza, eye infections, and actinomyces [82]. Sulfadimidine targets a crucial enzymatic process required for DNA synthesis, hence inhibiting bacterial folate synthesis. But resistance has restricted its efficacy, especially in species like *Pseudomonas aeruginosa*. These resistance mechanisms include target site alteration, active efflux of the antibiotic, and enzymatic drug inactivation [83].

They developed, produced, and tested sulfamethazine derivatives with high biological activity against *Salmonella typhi*, *Escherichia coli*, *P. aeruginosa*, *Staphylococcus aureus*, *Bacillus subtilis* and the common antibiotic ofloxacin; the findings

indicated that the majority of the newly synthesized compounds had moderate antibacterial activity against the tested pathogens [84]. Additionally, they can be used as model molecules to investigate the mechanisms of pharmacological action [85]. Sulfonamides chemical and pharmacological characteristics have been improved and increased by the addition of Schiff base moieties [86].

Promising antiviral and anticancer action has been demonstrated by sulfadimidine-based Schiff base metal complexes, which exhibit high binding to COVID-19 and liver cancer targets and considerable cytotoxicity against HEPG-2 cells [87]. The Schiff bases produced from sulfa medications have been widely employed as ligands for the creation of biologically active metal complexes because they have several donor sites, such as sulfonyl oxygen and amino, pyrimido, and sulfonamide nitrogen atoms [88]. The fundamental chemical and physiochemical properties of sulfadimidine are summarized in Table 2.2.

TABLE 2.2: Chemical information of sulfamethazine

Chemical structure	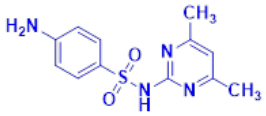
Nomenclature	2-(4-Aminobenzensulfonamido)-4,6-dimethylpyrimidine
Other names	Sulfamethazine, Sulfadimethylpyrimidine, Sulfamethiazine, Sulfadine, sulfodimesin, etc.
Formula	$C_{12}H_{14}N_4O_2S$
pKa value	7.45 ± 0.50 (most acid) 2.79 ± 0.24 (most basic)
K_{oc} value (L/kg)	1 at pH 1, 61.2 at pH 4, 48.2 at pH 7, 1 at pH 10

2.6.3 Sulfamethoxypyridazine

Sulfamethoxypyridazine is a long-acting sulfonamide antibiotic that is frequently used as an antibacterial and anti-inflammatory veterinary medication in cattle, pigs, and other animals. It has been used in combination with trimethoprim

and is just as effective as sulfamethoxazole [89]. The chemical structure of sulfamethoxypyridazine, illustrated in Figure 2.6. Chemically, sulfamethoxypyridazine is well-suited for derivatization and metal complexation because it contains multiple donor sites, including pyridazine nitrogen, aromatic amine, and sulfonyl oxygen. Through effective reflux-condition synthesis and structural confirmation using UV and IR spectroscopy, its Schiff base derivatives have validated imine formation [23]. Sulfamethoxypyridazine (SMPR) has been effectively altered by Schiff base formation with different aromatic aldehydes, resulting in improved pharmacological effects. These compounds outperformed the parent drug in terms of antibacterial, antioxidant, and anti-inflammatory activity [90].

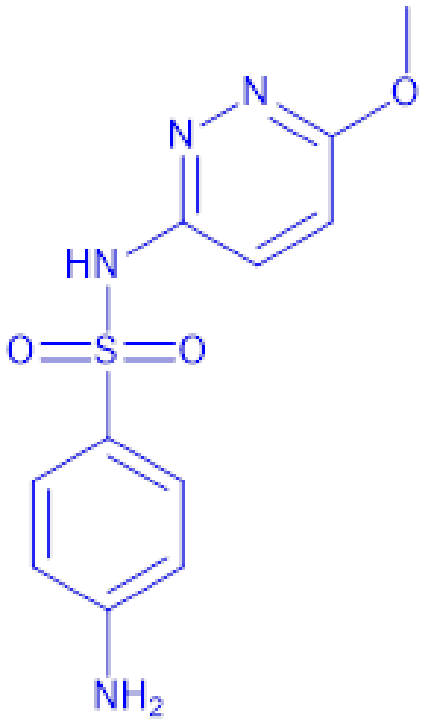

FIGURE 2.6: Structure of Sulphamethoxypyridaine.

2.7 Sulphonamide Schiff Bases: From Synthesis to Bioactivity

A comparative summary of various sulfonamide-aldehyde Schiff bases and their corresponding bioactivities is presented in Table 2.3.

TABLE 2.3: Sulfonamide- aldehyde Schiff Bases and their bioactivities

Compound	**Aldehyde Used**	**Type of complex**	**Evaluated bioactivities**	**Ref**
Sulfadimidine (sulfamethazine)	2-hydroxy- 1 -naphthaldehyde	Schiff base ligand +micro/ nano-metal complexes	Initial studies suggest that [aldehyde] Schiff bases have anticancer potential through DNA cleavage.	[87]
Sulfadimidine + Benzoin	Benzoin	Schiff base ligand + Cu, Co, Ni, Zn Cd complexes	Zinc and copper complexes demonstrated selective bioactivity, but their overall antibacterial efficacy was inferior to ciprofloxacin.	[91]
Sulfamethoxypyridazine	2-hydroxy-1 - naphthaldehyde	Schiff base+ transition metal (Mn, Ni, Cu, Zn) complexes	When it came to action against *S. aureus* and *E. coli*, Zn(II) fared better than the other metal complexes. Results from Cu(II) were similar to those from the parent ligand. None of them performed as well as the free Schiff base, although they were all more efficient than traditional antibiotics.	[23]
Sulfamethoxypyridazine	Various aromatic aldehydes	Schiff bases	With IC_{50} values of 12.18 and 49.37 μg/mL, respectively, the Schiff base demonstrated superior antioxidant and anti-inflammatory action compared to the parent molecule.	[90]

continued on next page

Table 2.3 continued from previous page

Compound	Aldehyde Used	Type of complex	Evaluated bioactivities	Ref
Sulfameth-oxypyridazine	Various aromatic aldehydes	Schiff bases	With IC_{50} values of 12.18 and 49.37 μg/mL, respectively, the Schiff base demonstrated superior antioxidant and anti-inflammatory action compared to the parent molecule.	[90]

2.8 Pharmacological Potential of Schiff Bases

Schiff bases and their metal complexes have proven to be appealing candidates for structural and synthetic research because of their structural diversity and ease of synthesis. Additionally, they have been the subject of extensive investigation due to their remarkable chemical properties and wide range of uses [92]. hrough the azomethine nitrogen of Schiff bases, metal ions can interact with many biomolecules in biological systems, such as proteins and amino acids, to provide antibacterial qualities.

Through the azomethine nitrogen of Schiff bases, metal ions can interact with many biomolecules in biological systems, such as proteins and amino acids, to provide antibacterial qualities. Our body manufactures Schiff bases, which accelerate a number of metabolic processes and lead to the synthesis of antimicrobial enzymes [93].

Schiff bases have acquired importance in the medicinal and pharmaceutical fields due to their broad range of biological actions, which include analgesia [94], anti-inflammatory [95], antimicrobial [96], anticonvulsant [97], anti-cancer [7], anti-oxidant [98], and anti-helminthic [9].

Heterocyclic aldehyde-derived Schiff bases have demonstrated potent antibacterial and antifungal properties [99].

Schiff bases are also employed as corrosion inhibitors [100], dyes [101], pigments [102], catalysts [103], solvents for polymers [104], and intermediates in organic synthesis [105]. Research revealed that metal complexes exhibit higher levels of biological activity compared to free organic molecules [106].

The development of coordination chemistry was influenced by Schiff bases, which were also crucial to the advancement of inorganic biochemistry and optical materials [107]. A visual overview of the major biological activities associated with Schiff bases is presented in Figure 2.7.

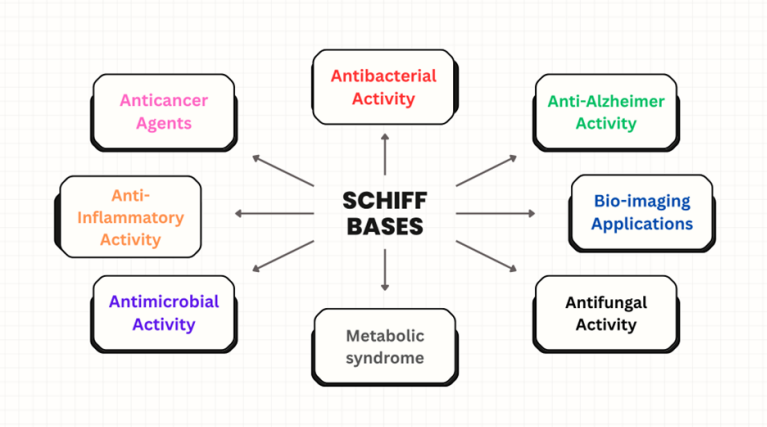

FIGURE 2.7: Biological Activities of Schiff Bases [108].

2.8.1 Antimicrobial Activity

Antimicrobials are widely used in healthcare, although their effectiveness is limited by antibiotic-resistant microbes [109]. Amino Acids Schiff bases are formed when simple amino acids with strong antibacterial qualities, such as glycine, valine, phenylalanine, cysteine, leucine, and alanine, condense with isatin. Cellulose-based Schiff bases, which exhibit antibacterial qualities against *Staphylococcus aureus*, *Enterococcus faecalis*, and *Escherichia coli*, are created when P-aminophenol combines with aldehyde groups [110]. A summary of Schiff bases with notable antimicrobial effects against various pathogens is provided in Table 2.4.

TABLE 2.4: Schiff bases have antibacterial properties with their effective microorganisms.

Compound Name	**Effective Microorganisms**	**Ref**
(E)-4-((benzo[d]thiazol-2- ylimino)methyl)-2-methoxyphenol	*S. aureus, Bacilus subtilis, E. coli*	[111]
2-[6-methylbenzothiazole-2-ylimino] methyl phenol	*Aspergillus niger, Candida albicans*	[112]
(E)-N-(2,4-dichlorobenzylidene)-4-methyl aniline	*S. aureus*	[113]
(Z)-2-(5-methyl-2-oxoindolin-3ylidene)hydrazinecarboxamide	*P. aeruginosa*	[114]
2,2'-(5,5-dimethyl cyclohexane-1,3'diylidene)bis(azan-1-yl1-ylidene) diphenol	*S. aureus*	[115]

2.8.2 Antioxidant Activity

Antioxidants are substances that prevent other molecules from oxidizing and causing damage to cells [116]. Oxidation is the process by which electrons are transferred from one molecule to the oxidizing product. Free radicals are formed during oxidation reactions.

Free radicals have unpaired electrons in their outermost shells, which makes them extremely reactive. The chain reaction begins as soon as they form. Antioxidants oxidize themselves to remove intermediate free radicals and prevent further oxidation processes [117].

Oxidative stress contributes significantly to a variety of human diseases, including cellular necrosis, CVS, cancer, neurological disorders, parkinson's dementia, alzheimer's disease, and inflammatory diseases [118]. Compounds having hydroxyl groups in the para position of an aromatic ring are more effective radical scavengers than those with hydroxyl groups in other places. Compounds containing the pyrazole moiety exhibit significant antioxidant activity [119]. Selected Schiff base derivatives known for their antioxidant properties, along with their structural features are summarized in Table 2.5.

TABLE 2.5: Schiff bases exhibit antioxidant activity

Structure	Compound Name	Ref
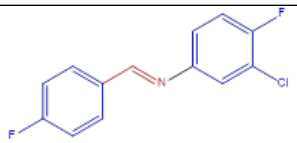	(E)-3-chloro-4-fluoro-N-(4-fluorobenzylidene)aniline	[113]
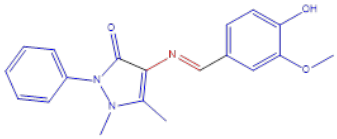	4-(4-hydroxy-3-methoxybenzylideneamino)-1,5-dimethyl-2-phenyl-1H-pyrazole-3-(2H)-one	[113]
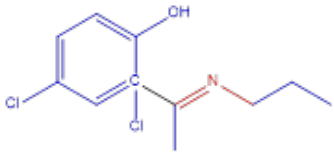	2,4-dichloro-2-[1-(propylimino)ethyl]phenol	[121]
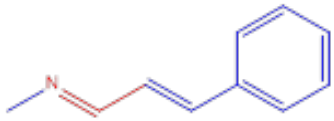	(1E,2E)-N-methyl-3-phenylprop-2-en-1-imine	[121]

2.8.3 Anti-inflammatory Activity

The FDA has approved NSAIDs as antipyretics, anti-inflammatory drugs, and pain relievers. NSAIDs are applied to counter multiple conditions, including pain in muscles, dysmenorrhea, rheumatic illnesses, pyrexia, gout, and used in severe injuries as opioid-sparing medications [123]. The synthesized products were created by the combination of aromatic aldehyde with a pyrazole derivative. They exhibit significant anti-inflammatory potential against COX1 and COX2. 2-(2-anilinophenyl)-N'-[(Z)-phenylmethylidene] Acetohydrazide is highly effective against COX-2 and 2-benzyl-4(E)-[(3,4-dihydroxyphenyl)methylidene].

The chemical amino-1,5-dimethyl-1,2-dihydro-3H-pyrazol-3-one lowers LPS-induced COX-2 mRNA levels [124]. Representative structures of Schiff base compounds with documented anti-inflammatory activity are illustrated in Figure 2.8.

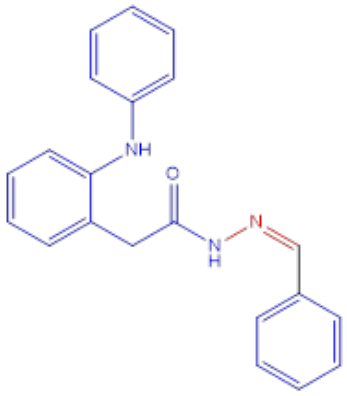

2-(2-anilinophenyl)-N'-[(Z)-phenylmethylidene] acetohydrazide

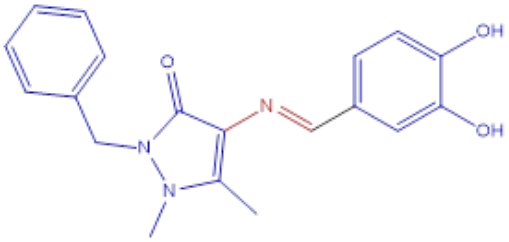

2-benzyl-4-{(E)-
[(3,4-dihydroxyphenyl)methylidene]amino}-1,5-dimethyl-1,2-dihydro-3H-pyrazol-3-one

FIGURE 2.8: Compounds possessing anti-inflammatory activity.

Chapter 3

Material and Methods

In this experimental study, analytical grade solvents were employed. A digital melting point device and thin-layer chromatography (TLC) were used to assess the purity of the synthesized compounds.

Silica gel aluminum plates that had already been coated were used for thin layer chromatography. The plates were 3×8 cm in size, and the chromatogram was seen under UV light at two different wavelengths: 254 and 365 nm. Clean glassware, specific catalysts, and basic or acidic conditions were used for the entire series of reactions.

Each synthesized compound was analyzed using several spectroscopic methods, such as FTIR, ^{1}H NMR, and ^{13}C NMR.

3.1 Materials

All of the analytical-grade chemicals and solvents (Tables 3.1 and 3.2) were purchased from Sigma-Aldrich and utilized exactly as supplied, requiring no further purification.

3.1.1 Chemicals

TABLE 3.1: List of Chemicals

Name of Chemical	**Molecular mass (g/mol)**
Sulfadimidine	278.33
Sulfamethoxypyridazine	280.304
4-dimethylaminobenzaldehyde	149.188
3-hydroxybenzaldehyde	122.12
3,4,5 trimethoxybenzaldehyde	196.20
Vanillin	152.15
4-hydroxybenzaldehyde	122.12
Glacial acetic acid	60.052
Sulphuric acid (H_2SO_4)	98.079

3.1.2 Solvents

A comprehensive list of solvents employed in this investigation have been displayed in Table 3.2

TABLE 3.2: List of solvents

Name of solvent	**Molar Mass (g/mol)**
Petroleum Ether(C_6H_{14})	82.2
Ethyl acetate (C_4H_{80})	88.11
Chloroform ($CHCl_3$)	119.38
Methanol (CH_2OH)	32.04
Ethanol (C_2H_5OH)	46.068

3.2 Apparatus and Equipment

In order to perform Thin Layer Chromatography, 2.50 x 5.0 cm plates covered with 0.25 mm thick silica gel (60 F-254) were subjected to iodine treatment and UV light exposure.

The column chromatography technique utilized silica gel with mesh sizes ranging from 60 to 120 or 100 to 200. The attenuated reflection of each generated molecule

was investigated using infrared spectroscopy on a Perkin Elmer Spectrum 100 spectrophotometer, with wave numbers represented in cm^{-1}.

The NMR spectra were obtained at 400 and 500 MHz for ^{1}H-NMR and 100, 125, or 300 MHz for ^{13}C-NMR using the Bruker Avance DPX 200 FT, Bruker Robotics, and Bruker DRX300 and 400 Spectrometers.The solvent used for the study was dimethylsulfoxide (DMSO-d6). Chemical shifts (δ) were measured in ppm for different types of protons and carbons in the structures.

3.3 Methods

3.3.1 General Reaction for the Synthesis of Schiff Bases

3.3.1.1 Synthesis of (Z) - 4 - ((4 (dimethylamino) benzylidene) amino) - N - (6 - methoxypyridazin - 3 - yl) benzenesulfonamide (1a)

The Schiff base was synthesized through a condensation reaction between equimolar amounts of a *4-dimethlyaminobenzaldehyde* and *Sulfamethoxypyridazine*. The *4-dimethylaminobenzaldehyde* (0.5 mmol, 74.594 mg) was dissolved in 15 ml of absolute ethanol, and *Sulfamethoxypyridazine* was separately dissolved in 15 ml of ethanol.

After that, the two solutions were mixed in a dry, clean round-bottom flask. After adding one drop of strong sulfuric acid to start the reaction, the liquid was magnetically agitated for three hours at room temperature. Using thin layer chromatography, the reaction in a 1:1 solvent mixture of petroleum ether and ethyl acetate was detected. Orange precipitate formed gradually, confirming the Schiff base's successful synthesis.

Following completion, the reaction mixture was allowed to cool to ambient temperature before the solid product was vacuum-filtered out. The product was left to air dry after contaminants were eliminated using ethanol, and then it was stored for further analysis.

3.3.1.2 Synthesis of (Z) - 4 - ((4 - hydroxy - 3 - methoxybenzylidene) amino)- N -(6 - methoxypyridazin - 3 - yl) benzenesulfonamide 2a

The Schiff base was synthesized through a condensation reaction between equimolar amounts of a *vanillin* and *sulfamethoxypyridazine*.

Vanillin(0.5 mmol,76.075 mg) was dissolved in 15 ml of absolute ethanol, and *Sulfamethoxypyridazine* was separately dissolved in 15 ml of ethanol. Both solutions were then combined in a clean, dry round bottom flask [22].

The reaction was started by adding one drop of sulfuric acid concentrate. The reaction mixture underwent 56 hours of refluxing at 80^{o}C.

Using a 1:1 ratio of petroleum ether to acetone as the mobile phase, thin-layer chromatography was employed to monitor the development of the reaction.

A rotary evaporator running at lower pressure was used to extract the solvent after the mixture had been allowed to cool to room temperature. This product was air-dried after being cleaned with ethanol. A collection of the colored solid was established [22].

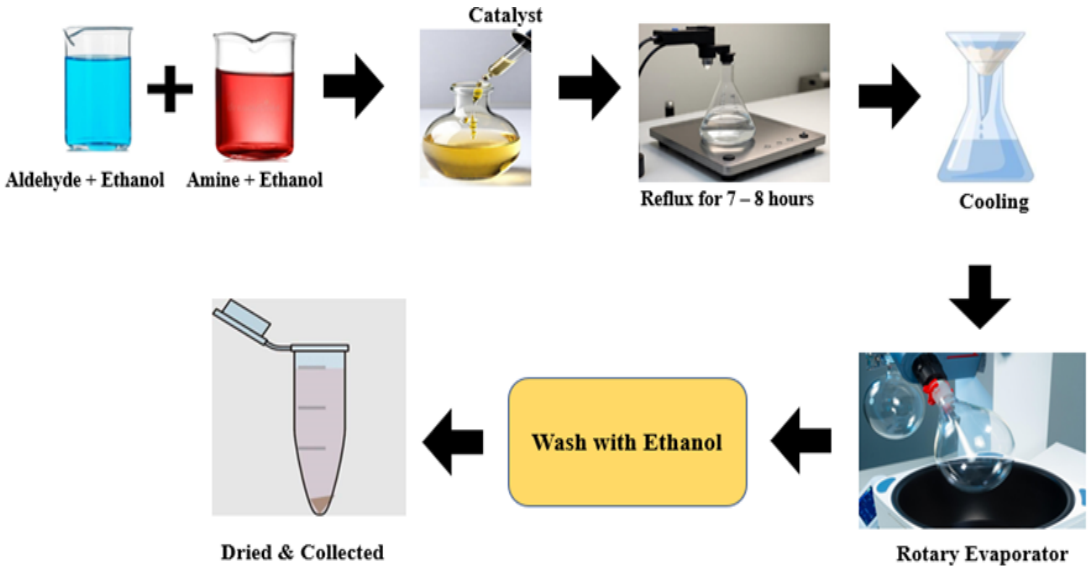

FIGURE 3.1: Schematic Representation of Schiff Base Formation

3.4 Synthesis Scheme

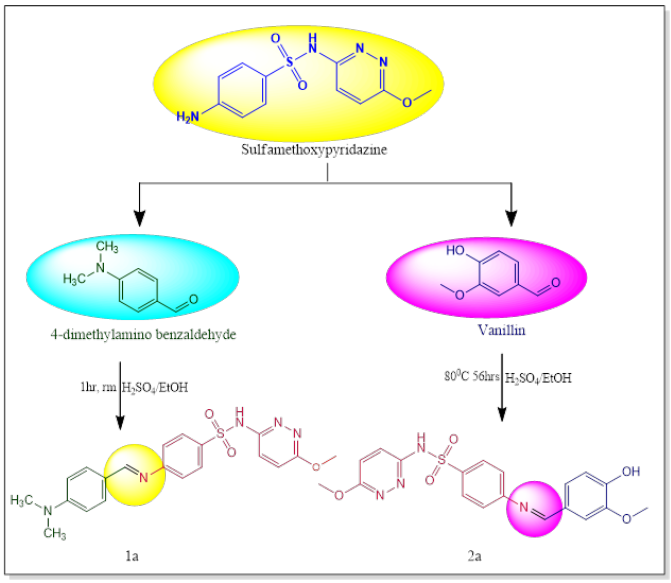

FIGURE 3.2: Synthesis Scheme of Schiff Bases (**1a, 2a**) rm: Room Temperature, hr: hour

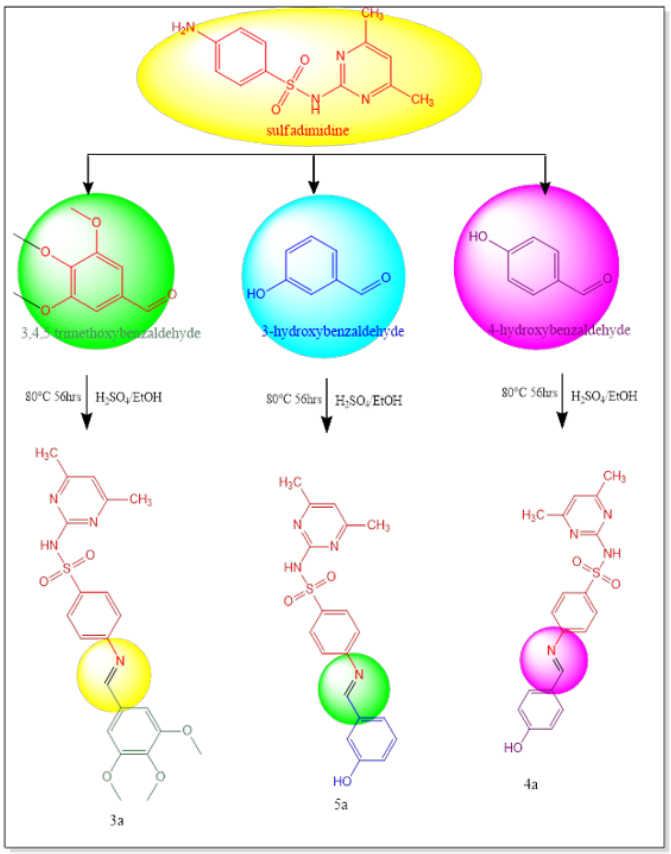

FIGURE 3.3: Synthesis Scheme of Schiff Bases (**3a, 4a,5a**) hr: hour

3.4.1 Characterization of Synthesized Compounds

3.4.1.1 Melting Point Determination

The melting point of the synthesized compounds was measured using both an electronic Gallenkamp melting point equipment and the capillary tube method. The substance was put into a capillary tube with one end closed off. The open end was gently tapped to ensure the compound was properly packed. After inserting a thermometer into the device's specified slot, the melting point mechanism was triggered. The capillary tube carrying the sample was put into the apparatus and examined with a lens until the compound melted. To reduce errors, this method was done three times, with the melting temperature recorded at each trial.

3.4.1.2 Solubility Testing

All of the synthesized organic compounds underwent solubility testing. To test the chemical product's solubility, a little amount was put in different Eppendorf tubes and mixed with different solvents. After shaking the tube's contents, they were left to stand so that any settled particles could be seen.

3.4.1.3 FTIR Analysis

The FTIR spectra of the synthesized compounds were acquired on an Agilent Technologies Cary 630 FTIR spectrometer (transmittance mode). The spectra were collected using a wavenumber range of 4000-650 cm^{-1} and a resolution of 1 cm^{-1}. The temperature at which all measurements were taken and documented was 25^{o}Celsius.

3.4.1.4 NMR Analysis

Nuclear Magnetic Resonance (NMR) spectroscopy was conducted by first dissolving the compound in a deuterated solvent (such as DMSO-d6 or $CDCl_3$) in order

to prevent hydrogen signals from interfering. The solution was transferred into a clean NMR tube and placed in the spectrometer, where it is subjected to a strong, uniform magnetic field. Radiofrequency (RF) pulses cause nuclei like ^{1}H or ^{13}C to absorb energy and transition from a lower to a higher spin state. As they relax, they release characteristic RF signals that are measured by the spectrometer.

These signals are processed using Fourier transformation to provide a spectrum in which chemical shifts, splitting patterns, and integration provide information about the number, type, and environment of nuclei in the molecule, allowing for exact structural elucidation.

3.5 *In silico* Studies

In silico studies on the synthesized compounds were performed to acquire insight into their potential interactions at the receptor's active region. The spatial orientation of the ligands within the target protein's active pocket was evaluated, binding affinities were predicted, and important amino acid residues implicated in interactions were identified using molecular docking.

These computational evaluations not only give the rational basis for understanding the compound's mechanism of action, but also support its potential as a lead candidate for future therapeutic development. Such approaches provide a cost-effective and time-saving alternative to early-stage experimental screening, hence increasing the efficiency of structure-based drug design efforts [125].

3.5.1 Molecular Docking Investigation

3.5.1.1 Recovering Protein Structure from Protein Data Bank (PDB)

The 3D structures of COX-2 and NF-κB receptor proteins were retrieved from PDB (www.rcsb.org) in PDB format. The PDB ID of both proteins were 1CX2 and 1VKX, respectively.

3.5.1.2 Preparation of Protein Macromolecule

The selected molecular proteins were arranged and docked for investigation using the Autodock Tools usage. The chosen proteins were then exposed to energy reduction and Gasteiger charge addition. After laying the foundation, protein structures were saved in pdbqt format. Ramachandran plots and hydrophobicity profiles were generated more quickly because to the use of Discovery Studio 4.1 Client (2012) for structural validation and visualization. Furthermore, the VADAR 1.8 web server was used to investigate the statistical distribution of tributary physical properties, including as coils, turns, β-helices, and β-sheets.

The hydrophobicity and ramachandran graphs were made with Discovery Studio 4.1 Client (2012). VADAR 1.8 provided access to the protein structure and statistical percentages of coils, twists, helices, and β-sheets [126].

3.5.1.3 Ligands-Proteins Molecular Docking

Following energy minimization, the compounds were drawn using Discovery Studio Client and stored as ligands in pdb format. Autodock Tools was used to prepare ligands in the most stable configuration. The ligands were saved in pdbqt format after the Kolman and Gasteiger charges were added. A virtual screening application that applies the Auto Dock Vina Wizard method [127]. The grid box center values (central X = 6.84, center Y = 38.644, center Z = 40.252) and size values (X = 52, Y = 54, Z = 88) were changed for COX-2, and the size values (X = 40, Y = 40, and Z = 40) and center X = 27.863 and center Y = 17.459 and center Z = 9.571 were changed for 1vkx.

For improved conformational placement in the target protein's active region. The selected protein targets were docked to individual compounds using the default exhaustiveness value of 100. The predicted docked complexes were evaluated using the lowest binding energy values (kcal/mol). Every docked complex was represented graphically in three dimensions using Discovery Studio (2.1.0) (Discovery Studio Visualizer Software, Version 4.0 2012).

3.5.2 ADME-T Assessment

The Swiss ADME prediction system (http://www.swissadme.ch/) was used to estimate the physiochemical properties and other pharmacokinetic parameters of the selected compounds in this study. The molecular weight (Mol. Wt.), number of rotatable bonds (NRB), number of hydrogen bond donors (HD), number of hydrogen bond acceptors (HA), Topological polar surface area (TPSA), and Log Po/w (iLOGP) were all estimated using Swiss ADME prediction. The drugs' carcinogenicity, inhibitory potential, plasma protein binding, and human intestinal absorption (HA) were evaluated using the PreADME-T server. TPSA stands for topological polar surface area.

The BOILED-Egg model was created using the SwissADME tool's online interface. The ProTox-II website was developed by Drwal *et al.* (2014) [128], was used for the in silico study. Parameters such as organ toxicity, specifically hepatotoxicity, immunotoxicity, genetic toxicity endpoints, specifically cytotoxicity, mutagenicity, and carcinogenicity, and oral acute toxicity, specifically with regard to median lethal dose (LD50) as mg/Kg, were predicted for established synthetic compounds. based on the protocol of Banerjee *et al.* (2018).

3.6 Biological Evaluation of the Synthesized Compounds

3.6.1 In-vitro Anti-oxidant Potential

3.6.1.1 Evaluation of Total Antioxidant Capacity (TAC) and Total Reducing Power (TRP)

To determine the total reducing power (TRP) and total antioxidant capacity (TAC) of the synthesized compounds (1**a-5a**), a sample solution containing 4 mg/ml in DMSO was combined with a reagent that contained ammonium molybdate, sodium phosphate, and sulfuric acid. The mixture was then incubated for 95

minutes at 90^{o}C. After that, the absorbance at 645 nm was measured using a spectrophotometer. The sample was further treated with 1% potassium ferricyanide and phosphate buffer (pH 6.6) prior to TRP measurements. The absorbance at 700 nm was determined after the addition of 10% ferric chloride and trichloroacetic acid. Both assays employed ascorbic acid as a positive control and DMSO as a negative control. Results for each milligram of material were represented as μg of ascorbic acid equivalent (AAE/mg of sample) [130].

3.6.1.2 DPPH Assay

The DPPH (1,1-diphenyl-2-picrylhydrazyl) test was used to assess the compounds (1a–5a) for their ability to scavenge free radicals. A 96-well plate was filled with the sample solutions (4 mg/ml in DMSO) and the DPPH reagent. After being incubated at 37^{o}C for an hour, the absorbance at 517 nm was measured. DMSO was used as the negative control, whereas ascorbic acid was used as the reference (positive) standard.

The radical scavenging activity of each sample was calculated using the following formula:

% Scavenging Activity = (1 − As / An) × 100 where As is the absorbance of the sample-treated DPPH solution, and An is the absorbance of the DPPH solution without sample (negative control) [131].

3.6.2 *In-vivo* Pharmacological Potential

3.6.2.1 Animals

In a recent study, male BALB/c mice weighing 30–35 g were used. The animals live in a controlled environment with a temperature of 24 ± 0.5^{o}C and a humidity of 40 ± 5%, and they are allowed free access to food and water. Animal testing for this study was carried out at the Capital University of Science and Technology (CUST), Islamabad, at the Faculty of Pharmacy. The animal activities were

authorized in accordance with the approvals of the bioethical committee of CUST in Islamabad (Approval number REC/FoP/F2024/08).

3.6.2.2 Acute Analgesic Potential of Compound 1a and 2a

The writhing test (acetic acid-induced) was preformed to investigate the particular drug's acute analgesic effect, with minor modifications to the guidelines. In brief, a 1% acetic acid solution was created to induce acute pain in mice. The animals were subjected into various groups of five each. The control group was given 1% acetic acid (10 ml/kg) intraperitoneally. The control group received no further treatments. The positive control group received 1% acetic acid (10 ml/kg i.p.) and diclofenac (5 mg/kg i.p.). The treatment group received 1% acetic acid (10 ml/kg, i.p.) and either compound 1a or compound 2a in three separate doses (1, 5, or 10 mg/kg, i.p.). The acetic acid-induced pain writhing response was observed for a period of 5 minutes [132].

3.6.2.3 Carrageenan Induced Inflammation Model

A carrageenan-induced acute inflammation pain model was used for this study to assess the anti-inflammatory activity of compounds **1a** and **2a** as reported [133]. The trial began after eight days of giving male BALB/c mice, who were 6–7 weeks old, enough food and water. Following that, the animals were split up into many groups, each consisting of five mice, as explained below. **Group I** (normal control) was given normal saline (10 ml/kg, i.p.) with no further treatment. **Group II** (negative control) received normal saline + 1% carrageenan (20 μl, intraplanter, i.pl). **Group III** (positive control) received diclofenac sodium (5 mg/kg, i.p.) and carrageenan. **Group IV** received compound **1a** (1 mg/kg, i.p.) together with carrageenan. **Group V** received compound **1a** (5 mg/kg, i.p.) along with carrageenan. **Group VI** received compound **1a** (10 mg/kg, i.p.) plus carrageenan. **Group VII** received compound **2a** (1 mg/kg, i.p.) plus carrageenan. **Group VII** received compound **2a** (5 mg/kg, i.p.) along with carrageenan. **Group VIII** received compound **2a** (10 mg/kg, i.p.) plus carrageenan. All treatments

were prepared in normal saline with 2% DMSO and administered 30 minutes before carrageenan administration. Paw edema was measured before and after carrageenan injection (0, 1, 2, 4, and 6 hours).

3.7 Statistical Analysis

One or two-way ANOVA was used in this study to examine the *in vitro* and *in vivo* results. Graph design and ANOVA analysis were performed using GraphPad Prism (version 8.0.2). At $p < 0.05$, the data was deemed statistically significant. The results were shown as mean ± SD.

Chapter 4

Results

4.1 Chemistry

The synthesis of Schiff base derivatives was accomplished by following Scheme 1 mentioned in section 3.4. The purity of synthesized compounds was confirmed with the help of TLC and structures were elucidated through FTIR and NMR spectroscopy. The successful formation of Schiff bases was indicated by a change in color, TLC pattern differences and presence of characteristic imine (C=N) stretching frequencies in FTIR spectra.

Furthermore, the ^{1}H NMR spectra displayed well defined signals corresponding to azomethine protons, while the ^{13}C NMR spectra revealed downfield shifts attributed to the imine carbon atoms, collectively confirming the structural integrity of the synthesized Schiff base derivatives.

The synthesis of Schiff bases was optimized under various reaction conditions, as summarized in Table 4.1. The optimization trials demonstrate that acidic conditions (H_2SO_4), lower pH, and extended reaction time were crucial for product formation.

The physical characteristics of synthesized compounds, including molecular formula, melting point, yield, and solubility, are presented in Table 4.2. Additionally, the chemical structures of all synthesized compounds are illustrated in Figure 4.1.

TABLE 4.1: Optimization of reaction conditions for the synthesis of compounds **1a-5a**

Compound	**Trial no.**	**Temp. (^{o}C)**	**Catalyst**	**Time (hr)**	**pH**	**Solvent**	**Molar Ratio**	**Product formed**
1a	1	rt	CH_3COOH	6	7	EtOH	1:01	No
1a	2	60	CH_3COOH	8	7	EtOH	1:01	No
1a	3	80	CH_3COOH	10	7	EtOH	1:01	No
1a	4	100	CH_3COOH	10	7	EtOH	1:01	No
1a	5	80	CH_3COOH	10	7	EtOH	2:01	No
1a	6	80	CH_3COOH	15	7	EtOH	1:01	No
1a	7	80	CH_3COOH	18	7	EtOH	1:01	No
1a	8	80	CH_3COOH	36	8	EtOH	1:01	No
1a	9	120	CH_3COOH	36	8	EtOH	1:01	No
1a	10	80	CH_3COOH	36	8	EtOH	1:01	No
1a	11	80	CH_3COOH	56	10	EtOH	1:02	No
1a	12	80	CH_3COOH	10	2	EtOH	1:01	No
1a	13	80	H_2SO_4	8	7	EtOH	1:01	No
1a	14	120	H_2SO_4	10	10	EtOH	1:01	No
1a	15	rt	H_2SO_4	1	3.5	EtOH	1:01	Yes
2a	1	rt	H_2SO_4	1	3.5	EtOH	1:01	No
2a	2	60	H_2SO_4	8	3.5	EtOH	1:01	No
2a	3	80	CH_3COOH	36	8	EtOH	1:01	No
2a	4	100	CH_3COOH	36	10	EtOH	1:01	No
2a	5	80	CH_3COOH	36	8	MeOH	1:03	No
2a	6	120	CH_3COOH	10	10	MeOH	1:02	No
2a	7	rt	CH_3COOH	3	8	MeOH	3:01	No
2a	8	120	H_2SO_4	8	6	EtOH	1:01	No
2a	9	100	H_2SO_4	24	5	EtOH	1:01	No
2a	10	60	H_2SO_4	36	4	EtOH	1:01	No
2a	11	80	H_2SO_4	56	4	EtOH	1:01	Yes
3a	1	rt	CH_3COOH	3	7	EtOH	1:01	No
3a	2	60	CH_3COOH	8	7	EtOH	1:01	No
3a	3	80	CH_3COOH	16	7	EtOH	1:02	No
3a	4	120	CH_3COOH	24	9	EtOH	1:01	No
3a	5	120	CH_3COOH	36	9	EtOH	1:01	No
3a	6	80	H_2SO_4	8	7	EtOH	1:01	No

continued on next page

Table 4.1 continued from previous page

Compound	Trial no.	Temp. (^oC)	Catalyst	Time (hr)	pH	Solvent	Molar Ratio	Product formed
3a	7	80	H_2SO_4	24	5	EtOH	1:01	No
3a	8	80	H_2SO_4	36	4	EtOH	1:01	No
3a	9	80	H_2SO_4	48	4	EtOH	1:01	No
3a	10	80	H_2SO_4	56	3	EtOH	1:01	Yes
4a	1	rt	H_2SO_4	3	3	EtOH	1:01	No
4a	2	60	CH_3COOH	8	3	MeOH	1:01	No
4a	3	80	CH_3COOH	24	4	MeOH	1:01	No
4a	4	120	CH_3COOH	36	5	MeOH	3:01	No
4a	5	80	H_2SO_4	24	5	MeOH	1:01	No
4a	6	80	H_2SO_4	10	5	MeOH	1:03	No
4a	7	80	H_2SO_4	36	8	EtOH	1:01	No
4a	8	80	H_2SO_4	56	8	EtOH	1:01	No
4a	9	80	H_2SO_4	24	7	EtOH	1:01	No
4a	10	80	H_2SO_4	56	3	EtOH	1:01	Yes
5a	1	rt	CH_3COOH	3	8	MeOH	1:03	No
5a	2	60	CH_3COOH	8	8	MeOH	1:01	No
5a	3	80	CH_3COOH	56	8	MeOH	2:01	No
5a	4	120	CH_3COOH	56	4	MeOH	1:02	No
5a	5	80	CH_3COOH	24	7	EtOH	1:01	No
5a	6	80	H_2SO_4	8	7	EtOH	1:01	No
5a	7	80	H_2SO_4	12	9	EtOH	1:01	No
5a	8	80	H_2SO_4	24	6	EtOH	1:01	No
5a	9	80	H_2SO_4	36	6	EtOH	1:01	No
5a	10	80	H_2SO_4	56	3	EtOH	1:01	Yes

rt; room temperature, EtOH; ethanol, MeOH; methanol

TABLE 4.2: Physical Data of Synthesized Compounds

Comp.	Mol formula	Mol Weight	Melting Point	Physical State	Color	% Yield	Solubility
1a	$C_{20}H_{21}N_5O_3S$	411.48	180	Solid	Orange	75	DMSO
2a	$C_{19}H_{18}N_4O_5S$	414.44	210	Solid	Goldenrod	79	DMSO
3a	$C_{22}H_{24}N_4O_5S$	456.51	195	Solid	Cinnamon	71	DMSO
4a	$C_{19}H_{18}N_4O_3S$	382.44	165	Solid	Brick Red	73	DMSO

continued on next page

Table 4.2 continued from previous page

Comp.	Mol formula	Mol Weight	Melting Point	Physical State	Color	% Yield	Solubility
5a	$C_{19}H_{18}N_4O_3S$	382.44	177	Solid	Saffron	72	DMSO

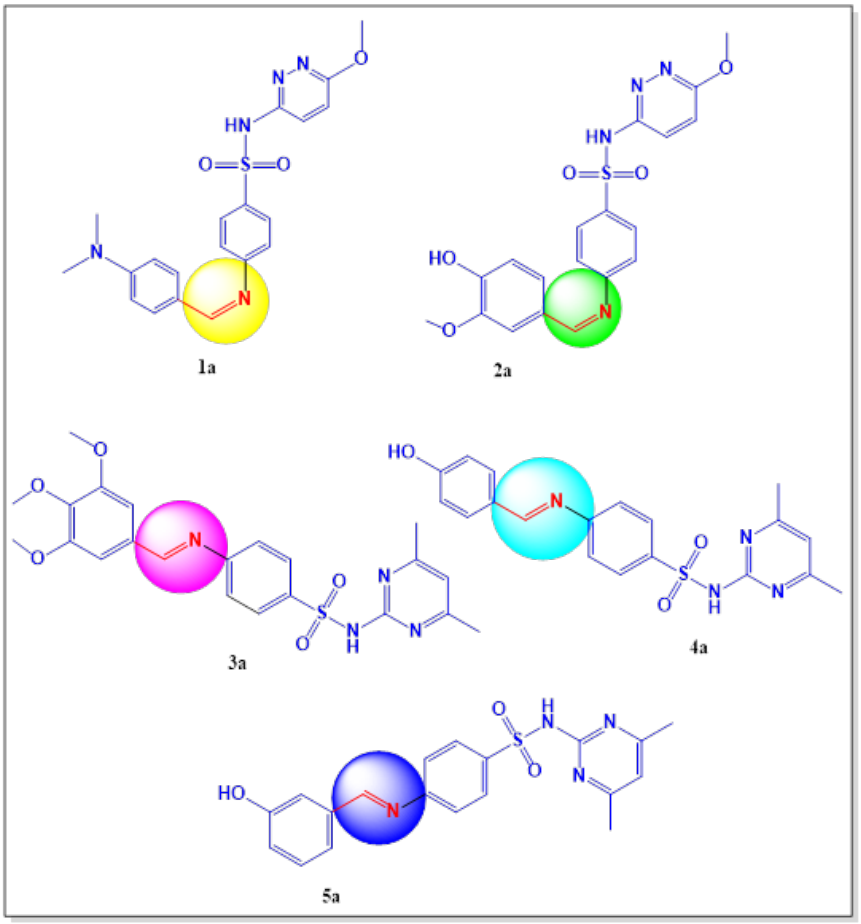

FIGURE 4.1: Structures of Synthesized Schiff Base Derivatives.

4.2 Synthesized Compounds FTIR Spectral Data

The compounds were synthesized based on literature-based reported procedures, and the desired products was obtained in good yield. Functional groups of the synthesized derivatives were verified by using FTIR spectroscopy. Stretching frequency for C=N were seen at the expected wavenumber in IR spectra which confirmed the synthesis of desired compound. C=N stretching was found at the range of 1610-1655 cm^{-1} consistent with the literature values for imine linkage.

4.2.1 FTIR Characterization of (Z)- 4 -((4 - (dimethylamino) benzylidene) amino) - N - (6 - methoxypyridazin - 3 - yl) benzenesulfonamide (1a)

The FTIR spectrum of compound 1a is shown in Figure 4.2. A notable sharp peak observed at 1651cm^{-1} is characteristic of C=N stretching, which indicates the presence of imine group. A broad absorption band around 3201.8cm^{-1} corresponds to N-H stretching vibrations indicative of a secondary amine. In the 3138-3063 cm^{-1} region, weak to moderate bands appear by aromatic C-H stretching vibrations, suggesting the presence of aromatic rings in the structure.

A methyl or methylene group is present because the peaks at 2903.6 cm^{-1} and 2821.6 cm^{-1} correspond to aliphatic C-H stretching. The existence of an amine or sulfonamide group is further supported by peaks in the range of 1572.9 to 1535.7 cm^{-1}, which can be attributed to N–H bending vibrations. These peaks could also indicate C=C stretching within the aromatic ring system.

In the fingerprint region, bands between 1341.8–1155.5 cm^{-1} correspond to the symmetric and asymmetric S=O stretching vibrations, (characteristic of the sulfonamide functional group). C–N stretching vibrations are represented by peaks located between 1211.9 and 1098.6 cm^{-1}, which support the presence of amines or substituted imines.

Aromatic C–H out-of-plane bending vibrations are present in the 939.3–805.1 cm^{-1} range, confirming the aromatic ring substitution pattern. The key FTIR absorption bands for compound 1a are presented in table 4.3

Table 4.3: FTIR Spectral data of Compound 1a

Compound 1a	**Wave number (cm^{-1})**
C=N	1651
NH	3201.8
S=O	1341.8
Aromatic CH stretch	3063.9

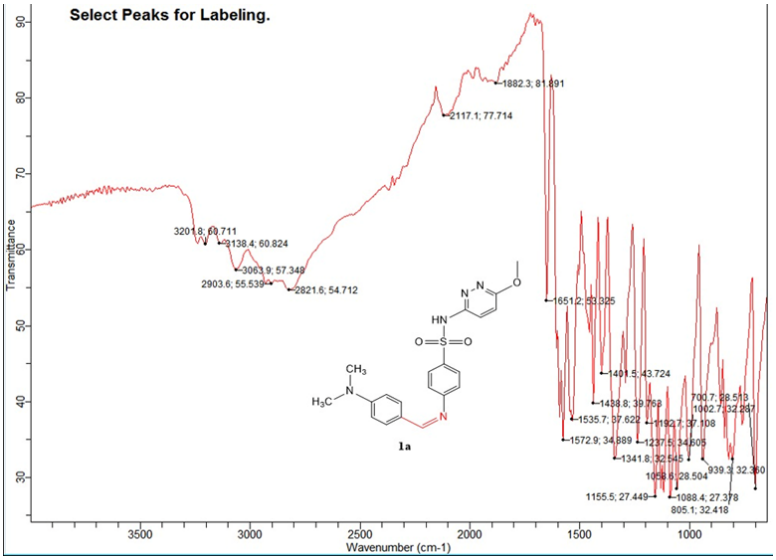

FIGURE 4.2: Shows the FTIR spectrum and all the related peaks of compound 1a.

4.2.2 FTIR Characterization of (Z) - 4 - ((4 - hydroxy - 3 - methoxybenzylidene) amino) - N - (6 - methoxypyridazin - 3 - yl) benzenesulfonamide (2a)

The FTIR spectrum of compound 2a is shown in Figure 4.3. A distinct absorption band at 1654.9 cm^{-1}, which is associated with the C=N stretching vibration, validates the imine group's formation. At 3406.8 cm^{-1}, a broad and intense peak denotes N–H stretching vibrations, which are indicative of the secondary amine. According to aliphatic C–H stretching vibrations, the peak at 2952.1 cm^{-1} indicates that the structure contains methyl or methylene groups.The peak at 1576.7 cm^{-1}, corresponding to N–H bending vibrations, typical for NH in sulfonamides or amines. Meanwhile, the peak at 1517.0 cm^{-1}, which may represent C=C stretching in an aromatic ring.

In the region below 1500 cm^{-1}, peaks at 1401.5 cm^{-1} and 1488.6 cm^{-1} are generally associated with aromatic skeletal vibrations and CH bending. The fingerprint region (1350–500 cm^{-1}) display several distinct peaks: 1174.1 cm^{-1}, 1125.7 cm^{-1}, and 995.2 cm^{-1} are likely due to S=O symmetric and asymmetric stretching of a sulfonamide group, confirming its presence. The peak at 1308.3 cm^{-1} may

also correspond to C–N stretching. The characteristic FTIR bands observed for compound 2a are summarized in table 4.4.

TABLE 4.4: FTIR Spectral data of Compound 2a

Compound 1a	**Wave number (cm^{-1})**
C=N	1654.9
NH	3406.8
Aromatic CH stretch	3071

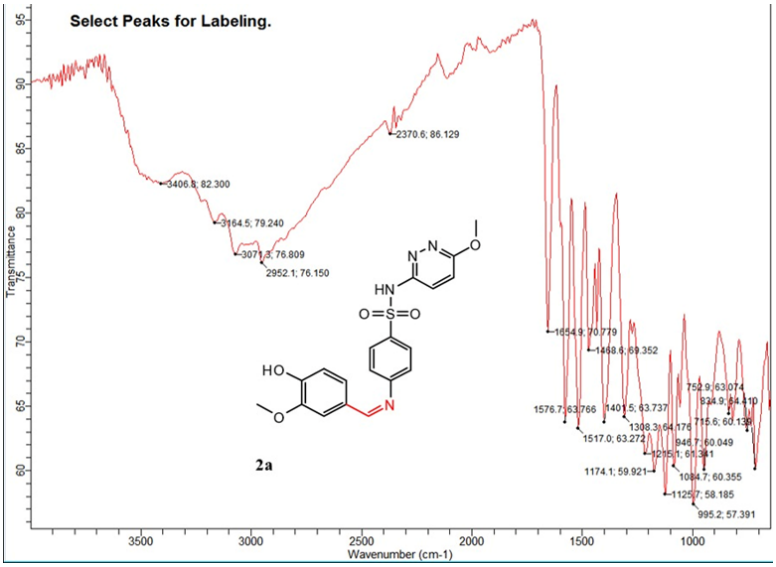

FIGURE 4.3: Shows the FTIR spectrum and all the related peaks of compound 2a.

4.2.3 FTIR Characterization of (E)-N-(4,6-dimethylpyrimidin-2-yl)-4-((3,4,5-trimethoxybenzylidene) amino) benzenesulfonamide (3a)

The FTIR spectrum of compound 3a is shown in Figure 4.4. The spectrum for compound 3a indicated the existence of the desired functional groups. A distinct band at 1652.4 cm^{-1} corresponds to C=N stretching, indicating formation of imine linkage. The broad band at 3399.4 cm^{-1} indicated overlapping N-H and O-H stretches, whereas aromatic and aliphatic C-H vibrations suggested the presence of methoxy and hydroxyl-substituted aromatic rings.

The major functional group frequencies in the FTIR spectrum of compound 3a are listed in table 4.5. The symmetric and asymmetric S=O and C-N vibrations characteristic of the sulfonamide moiety, hence verifying compound 3a structure.

TABLE 4.5: FTIR Spectral data of Compound 3a

Compound 1a	**Wave number (cm^{-1})**
C=N	1652.4
NH	3399.4
Aromatic CH stretch	2626.2
S=O	1163.7

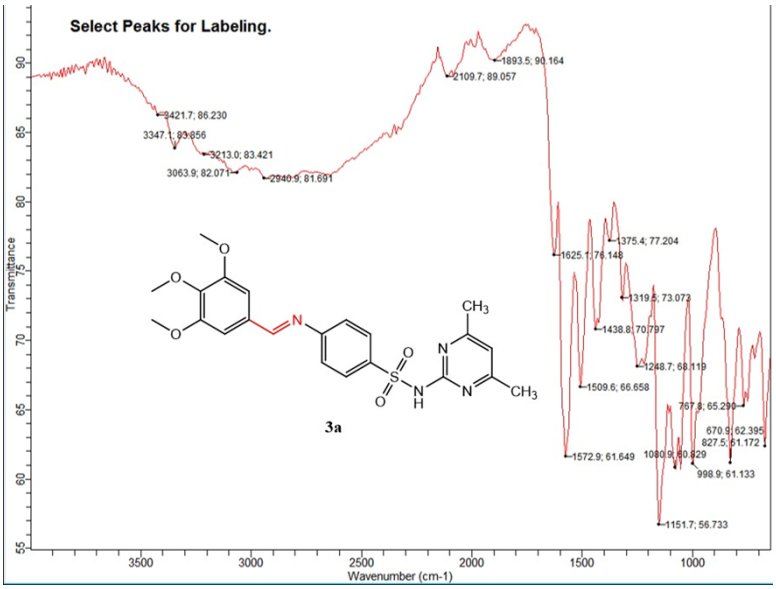

FIGURE 4.4: Shows the FTIR spectrum and all the related peaks of compound 3a.

4.2.4 FTIR Characterization of (E) - N - (4,6-dimethylpyrimidin-2-yl)- 4 -((4-hydroxybenzylidene) amino) benzenesulfonamide (4a)

The FTIR spectrum of compound 4a is shown in Figure 4.5. A sharp absorption band observed at 1636 cm^{-1}, which indicates the C=N stretching vibration of the imine group and broad absorption band around 3347.1 cm^{-1} is attributed to N–H stretching vibrations, The peak at 3071.3 cm^{-1} corresponds to aromatic C–H stretching, indicates the presence of aromatic rings. Peaks in the region of

1282.2 cm^{-1}, 1252.4 cm^{-1}, and 1155.5 cm^{-1} are characteristic of asymmetric and symmetric S=O stretching vibrations of the sulfonamide group.

In the fingerprint region, peaks at 1002.7 cm^{-1}, 827.5 cm^{-1}, and 767.8 cm^{-1} are assigned to C–H out-of-plane bending vibrations of substituted aromatic rings. These bands are consistent with para- and meta-substituted benzene derivatives commonly found in sulfa drugs. A summary of the significant IR absorption peaks for compound 4a is provided in Table 4.6.

TABLE 4.6: FTIR Spectral data of Compound 4a

Compound 1a	**Wave number (cm^{-1})**
C=N	1636.3
NH	3347.1
S=0	1371

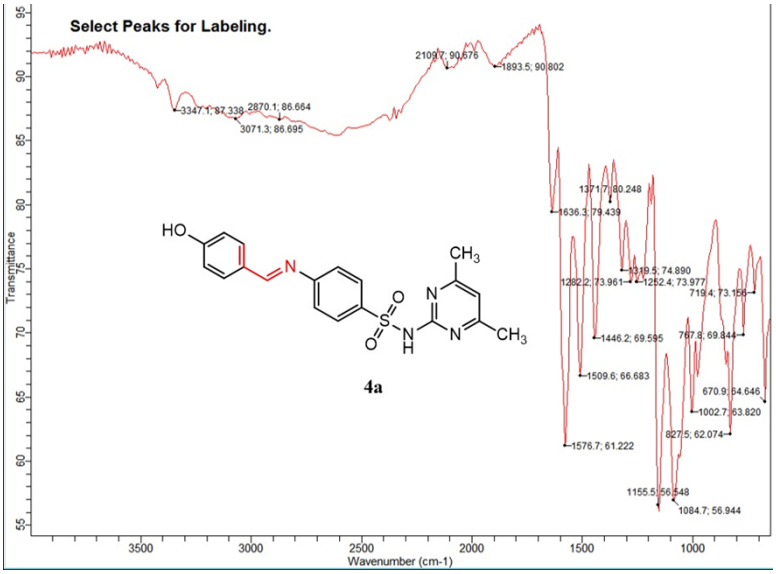

FIGURE 4.5: Shows the FTIR spectrum and all the related peaks of compound 4a.

4.2.5 FTIR Characterization of (E)- N -(4, 6 - dimethylpyri midin - 2-yl)- 4 s-((3-hydroxybenzylidene) amino) benzenesulfonamide (5a)

The FTIR spectrum of compound 5a is shown in Figure 4.6. C=N stretching corresponds to a strong peak observed at 1591.6 cm^{-1}, which shows the imine

functional group development. A wide absorption band at 3354.6 cm^{-1} supports the presence of a hydroxyl group by corresponding to OH stretching vibrations.

A peak at 2926.0 cm^{-1} suggests aliphatic CH stretching, typically attributed to methyl or methylene groups.

Aromatic skeletal vibrations are evident from peaks between 1498.4 and 1379.1 cm^{-1} while sulfonamide S=O stretching vibrations are observed near 1423.8 and 1379.1 cm^{-1} consistent with both symmetric and asymmetric S=O modes.

A summary of the significant IR absorption peaks for compound 5a is provided in Table 4.7.

TABLE 4.7: FTIR Spectral data of Compound 5a

Compound 1a	**Wave number (cm^{-1})**
C=N	1591.6
OH	3354.6
S=0	1423.8

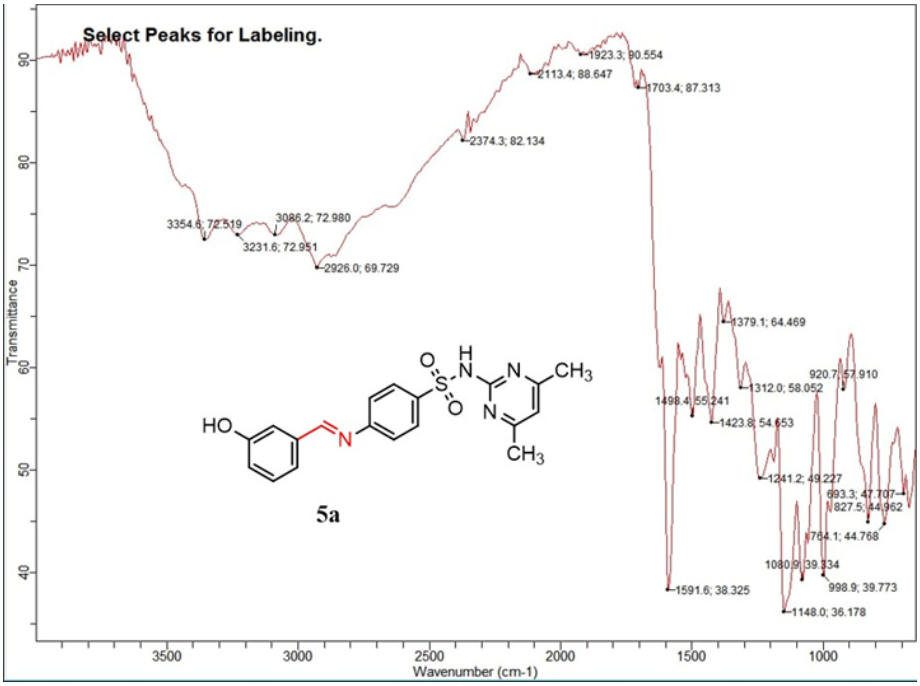

FIGURE 4.6: Shows the FTIR spectrum and all the related peaks of compound 5a.

4.3 NMR Spectra of the Synthesized Compounds (1a, 2a)

4.3.1 NMR spectra of (Z) - 4 - ((4 - (dimethylamino) benzylidene) amino)- N -(6 - methoxypyridazin - 3 - yl) benzenesulfonamide (1a)

^{1}H NMR (400 MHz, DMSO) 9.67 (s, ^{1}H), 7.99 (d, J = 8.8 Hz, ^{1}H), 7.82 (dd, J = 14.9, 9.3 Hz, ^{1}H), 7.68 (d, J = 9.0 Hz, 2H), 7.50 (d, J = 8.7 Hz, 2H), 7.26 (d, J = 9.7 Hz, ^{1}H), 6.79 (d, J = 8.9 Hz, 2H), 6.62 (d, J = 8.7 Hz, 2H), 3.86 (s, 3H), 3.04 (s, 6H). ^{13}C NMR (400 MHz, DMSO) δ 41.3, 54.37, 111.08, 120.1, 124.52, 128.43, 138.2, 149.6, 153.4, 155.2, 160.0.

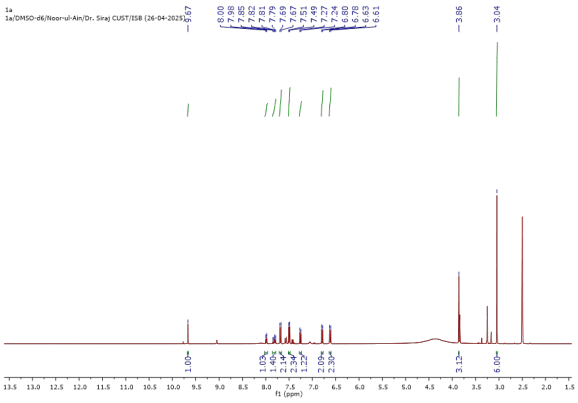

FIGURE 4.7: ^{1}H NMR of the Compound 1a

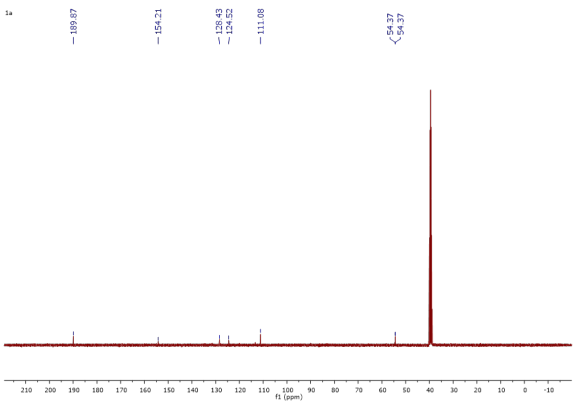

FIGURE 4.8: ^{13}C NMR of the Compound 1a

4.3.2 NMR Spectra of (Z)- 4 -((4 - hydroxy - 3 - methoxy-benzylidene) amino)- N -(6 - methoxypyridazin - 3 - yl) benzenesulfonamide 2a

^{1}H NMR (400 MHz, DMSO) δ 9.76 (s, ^{1}H), 7.64 (dd, J = 9.2, 4.3 Hz, 4H), 7.48 – 7.36 (m, 3H), 7.30 (d, J = 9.7 Hz, ^{1}H), 6.96 (d, J = 8.0 Hz, 2H), 6.87 (d, J = 8.6 Hz, ^{1}H), 3.84 (d, J = 5.3 Hz, 6H). ^{13}C NMR (400 MHz, DMSO) δ 52.94, 54.53, 55.64, 61.35, 110.74, 115.44, 126.12, 128.31, 128.75, 148.20, 153.07, 191.07.

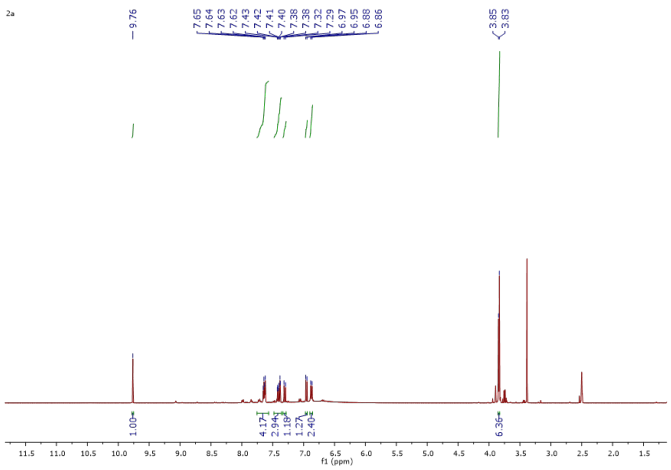

FIGURE 4.9: ^{1}H NMR of the Compound 2a

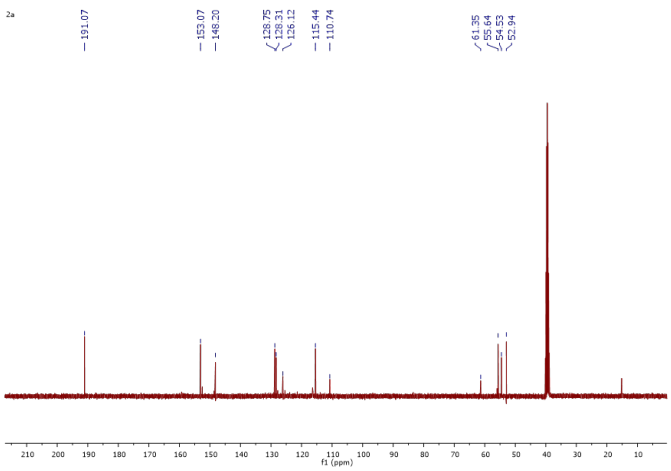

FIGURE 4.10: ^{13}C NMR of the Compound 2a

4.4 Physiochemical Evaluation

The physiochemical parameters of each synthesized compounds (**1a-5a**) were investigated using the SwissADME catalogue and the results are presented in Table 4.8. Every compound complies with Lipinski's Rule of Five, which is probably used for predicting a compound's oral bioavailability and drug likeness. Compounds with molecular weight (MW) $<$ 500 Da, logP (lipophilicity) 5, hydrogen bond donors (nHBD) 5, and hydrogen bond acceptors (nHBA) 10 are more likely to be orally active, according to Lipinski's criteria. According to Veber's Rule, other factors that are important in determining oral bioavailability include the number of rotatable bonds (nRB) and the Topological Polar Surface Area (TPSA 140Å^2). All five Schiff base derivatives met these criteria, indicating favorable properties for oral bioavailability and suggesting drug-like behavior similar to known therapeutic agents. For molecular weight, the number of hydrogen bond donors, topological polar surface area, logP, and the number of hydrogen bond acceptors, all of the Schiff base derivatives fall within the defined limits of 500, 5, 140 A2, and 10, respectively. Notably, compounds 2a, 4a, 5a exhibited identical F.Csp3 values of 0.11, reflecting a relatively low degree of saturation, which is typical for planar, aromatic rich molecules. Compound 3a had the highest F.Csp3 value of 0.23, suggesting increased sp3 carbon content, which may enhance solubility and reduce promiscuity in biological systems. Compound 1a and 2a each contain 7 rotatable bonds, while 4a and 5a have 5 rotatable bonds. There structural flexibilities contribute to their conformational adaptability, potentially aiding in receptor binding.

TABLE 4.8: Physiochemical property of derivatives calculated with SwissADME database

Ligands	**Molecular Formula**	**MW**	**nHA**	**nAHA**	**F.Csp^3**	**nRB**	**nHBA**	**nHBD**	**MR**	**TPSA (A²)**
1a	$C_{20}H_{21}N_5O_3S$	411.48	29	18	0.15	7	6	1	113.54	105.16Å^2
2a	$C_{19}H_{18}N_4O_5S$	414.44	29	18	0.11	7	8	2	107.85	131.38Å^2
3a	$C_{22}H_{24}N_4O_5S$	456.51	32	18	0.23	8	8	1	122.25	120.38Å^2

continued on next page

Table 4.8 continued from previous page

Ligands	Molecular Formula	MW	nHA	nAHA	F.Csp^3	nRB	nHBA	nHBD	MR	TPSA (A²)
4a	$C_{19}H_{18}N_4O_3S$	382.44	27	18	0.11	5	6	2	104.8	112.92Å^2
5a	$C_{19}H_{18}N_4O_3S$	382.44	27	18	0.11	5	6	2	104.8	112.92Å^2

4.4.1 Pharmacokinetics Evaluation

Pharmacokinetics is fundamental to attain the envisioned therapeutic consequence of a remedy. This proposes that every amalgam's pharmacokinetic distinguishing has the prospective to influence a drug's therapeutic profile. Pharmacokinetic profiles of the created derivatives were predicted using the SwissADME database.

Important factors were assessed, including cytochrome P450 (CYP) enzyme inhibition, P-gp substrate status, blood-brain barrier (BBB) permeability, gastrointestinal (GI) absorption, and bioavailability evaluations (Table 4.9). Compounds 1a, 4a, and 5a exhibited high gastrointestinal absorption, suggesting favorable oral uptake potential. In contrast, 2a and 3a showed low GI absorption, which may impact their systemic availability.

Since none of the compounds were found to be P-glycoprotein substrates, there may be a chance for increased bioavailability and a decreased probability of active efflux. All derivatives were anticipated to have low blood-brain barrier (BBB) permeability, which suggests a lesser chance of active efflux and the possibility of increased bioavailability. All derivatives were anticipated to have low blood-brain barrier (BBB) permeability, which would indicate less penetration of the central nervous system. Regarding metabolic interaction, CYP2C9 and CYP3a4 were inhibited by all derivatives, while CYP1a2 and CYP2D6 remained unaffected across the series. Inhibition of CYP2C19 was observed selectively in 1a and 3a. These finding suggest a shared CYP mediated metabolic profile, which potential implications for drug-drug interactions. The bioavailability score was uniform across all compounds at 0.55, indicative of moderate oral bioavailability.

TABLE 4.9: The bioavailability evaluations and pharmacokinetics of Schiff base derivatives calculated using the SwissADME database.

Ligands	**GI absorption Score**	**Bioavailability**	**BBB per**	**P-gp substrate**	**CYP1a2 Inh**	**CYP2C19 Inh**	**CYP2C9 Inh**	**CYP2D6 Inh**	**CYP3a4 Inh**
1a	High	0.55	No	No	No	Yes	Yes	No	Yes
2a	Low	0.55	No	No	No	No	Yes	No	Yes
3a	Low	0.55	No	No	No	Yes	Yes	No	Yes
4a	High	0.55	No	No	No	No	Yes	No	Yes
5a	High	0.55	No	No	No	No	Yes	No	Yes

4.4.2 Drug Likeness

Drug-likeness prediction serves as a vital step in early drug development by assessing whether a compound possesses properties consistent with known orally active drugs. Five commonly used rule-based filters were used to assess this: the Muegge, Veber, Ghose, and Lipinski's Rule of Five filters. In order to predict oral bioavailability, metabolic stability, and absorption, these computational filters evaluate a number of pharmacokinetic-relevant parameters, such as molecular weight, hydrogen bonding potential, lipophilicity (LogP), rotatable bonds, and topological polar surface area. As shown in Table 4.10 none of the synthesized Schiff base derivatives (**1a-5a**) violated any of the drug-likeness rules. This lack of violation suggests good alignment with the physiochemical space occupied by known oral drugs, supporting their potential as orally bioavailable therapeutic agent. Such favorable drug-likeness scores strongly justify further biological and pharmacokinetic evaluations.

TABLE 4.10: Drug Likeness Scores

Ligands	**Lipinski**	**Ghose**	**Veber**	**Egan**	**Muegge**
1a	Yes	Yes	Yes	Yes	Yes
2a	Yes	Yes	Yes	Yes	Yes
3a	Yes	Yes	Yes	Yes	Yes
4a	Yes	Yes	Yes	Yes	Yes
5a	Yes	Yes	Yes	Yes	Yes

4.4.3 Medicinal Chemistry

All compounds generated zero PAINS alerts, indicating a low risk of false positives in high-throughput biological screens. Each compound received one Brenk alert indicating the presence of an imine functional group (imine_1), which is common in Schiff bases. None of the compounds entirely met the lead-likeness requirements. Most failed due to molecular weight (MW > 350 Da), with compound 3a exhibiting an extra violation (number of rotatable bonds > 7). All compounds obtained synthetic accessibility values ranging from 3.13 to 3.59, indicating modest ease of synthesis. Table 4.11 provides a summary of the full PAINS Brenk, lead-likeness, and synthetic accessibility (SA) data.

TABLE 4.11: PAINS, Brenk, lead-likeness, and synthetic accessibility (SA) scores for synthesized Schiff base compounds

Ligands	**Pains**	**Brenk**	**Lead Likeness**	**Synthetic Accessibility**
1a	0 alert	1 alert: imine_1	No; 1 violation: MW>350	3.5
2a	0 alert	1 alert: imine_1	No; 1 violation: MW>350	3.47
3a	0 alert	1 alert: imine_1	No; 2 violations: MW > 350 , Rotors > 7	3.59
4a	0 alert	1 alert: imine_1	No; 1 violation: MW>350	3.13
5a	0 alert	1 alert: imine_1	No; 1 violation: MW>350	3.16

4.4.4 Lipophilicity

The lipophilic behavior of the synthesized derivatives was calculated using SwissADME a widely used *in silico* tool for ADME prediction. Additionally, the SwissADME offers five prediction models shown in Table 4.12.

TABLE 4.12: The calculated lipophilic parameters for derivatives using the database SwissADME

Compound	**ILogP ***	**XLOGP3**	**WlogP ***	**MlogP ***	**SILICOS-IT***
1a	2.74	2.42	3.99	1.83	2.09
2a	2.43	1.92	3.64	1.09	1.99

continued on next page

Table 4.12 continued from previous page

Compound	ILogP *	XLOGP3	WlogP *	MlogP *	SILICOS-IT*
3a	3.08	2.17	4.56	0.95	3.59
4a	2.37	1.91	4.24	1.31	2.9
5a	2.1	1.91	4.24	1.31	2.9

The ILogP values ranged from 2.10 (5a) to 3.08 (3a) indicating a moderate lipophilicity. XLOGP3 values indicating that compounds have similar structural hydrophobic features. WlogP, which tends to overestimate the lipophilicity with compound 3a showing the maximum lipophilicity (4.56). followed by the compound 1a (3.99). MlogP values were the lowest (0.95- 1.83). SILICOS-IT values which incorporate the topological and fragmental information varied from 1.99(2a) to 3.59(3a) suggesting the 3a as most lipophilic derivative.

4.4.5 Water Solubility Predictions

The aqueous solubility of the derivatives was also predicted using three SwissADME models: ESOL, Ali, and SILICOS-IT. The results, presented in Table 4.13, show that while all compounds fall within the soluble to moderately soluble range by the ESOL and Ali models, the SILICOS-IT model consistently classified them as poorly soluble. ESOL predictions indicated that all compounds were soluble (Log S 3.5 to 3.9), with compound 2a, 4a, and 5a exhibiting the highest predicted solubility. Ali model values generally agreed, although classed most compounds as moderately soluble. SILICOS-IT values were significantly lower, suggesting poor solubility for all derivatives. These discrepancies among models are expected due to differing computational approaches. However, the consensus suggests that the compounds possess acceptable solubility for further development, especially in formulation-optimized drug delivery systems.

TABLE 4.13: Water solubility prediction values, based on three alternative models

Compound	Log S (ESOL)	Solubility Class	Log S (Ali)	Solubility Class	Log S (SILICOSIT)	Solubility Class
1a	-3.91	Soluble	-4.27	Moderately soluble	-6.91	Poorly soluble

continued on next page

Table 4.13 continued from previous page

Compound	Log S (ESOL)	Solubility Class	Log S (Ali)	Solubility Class	Log S (SILICOSIT)	Solubility Class
2a	-3.62	Soluble	-4.3	Moderately soluble	-6.35	Poorly soluble
3a	-3.93	Soluble	-4.33	Moderately soluble	-7.78	Poorly soluble
4a	-3.58	Soluble	-3.9	Soluble	-6.89	Poorly soluble
5a	-3.58	Soluble	-3.9	Soluble	-6.89	Poorly soluble

4.5 Toxicological Evaluation

The ProTox-II, which uses machine learning models trained on large toxicological datasets, was used to perform the initial safety assessment of the synthesized compounds (1a–5a).

These *in silico* toxicity prediction provides insights into LD_{50} values, GHS toxicity classifications, organ specific toxicity, potential systemic effects carcinogenicity, and molecular bioavailability parameters such as blood brain barrier permeability. The predicted LD_{50} values and corresponding GHS classification are summarized in Table 4.14.

Table 4.14: Acute Toxicity and Toxicity Class

Compound	LD_{50}(mg/kg)	GHS Toxicity Class	Toxicity Interpretation
1a	1700	4	Harmful if swallowed
2a	1700	4	Harmful if swallowed
3a	25000	6	Non-toxic
4a	25000	6	Non-toxic
5a	25000	6	Non-toxic

According to GHS (Globally Harmonized System) guidelines, Compound 1a and 2a were classified as toxicity class 4 due to their predicted LD_{50} values of 1700 mg/kg.

With considerably higher estimated LD_{50} values of 25,000 mg/kg, compounds 3a, 4a, and 5a have been classified in toxicity class 6, which indicates low toxicity.

4.5.1 Organ Toxicity Prediction

All compounds were predicted inactive for neurotoxicity, nephrotoxicity, and cardiotoxicity (Table 4.15).

However respiratory toxicity was predicted to be active across all five compounds, suggesting a potential caution for pulmonary exposure. Hepatotoxicity was predicted only in compound 2a, with a moderate probability (0.58), indicating a potential for liver-related adverse effects.

TABLE 4.15: Organ toxicity prediction

Compound	**Hepato toxicity**	**Neuro toxicity**	**Nephro toxicity**	**Respiratory toxicity**	**Cardio toxicity**
1a	Not active (0.51)	Not active (0.72)	Not active (0.67)	Active (0.72)	Not active (0.73)
2a	Active (0.58)	Not active (0.79)	Not active (0.62)	Active (0.67)	Not active (0.69)
3a	Not active (0.51)	Not active (0.73)	Not active (0.53)	Active (0.71)	Not active (0.64)
4a	Not active (0.57)	Not active (0.71)	Not active (0.53)	Active (0.74)	Not active (0.78)
5a	Not active (0.57)	Not active (0.71)	Not active (0.53)	Active (0.74)	Not active (0.78)

4.5.2 Systemic and Genetic Toxicity

Carcinogenicity was predicted to be active in compounds 2a-5a, indicating a potential risk for long-term exposure. Compound 1a was found to be inactive for all systemic toxicity endpoints. All compounds were inactive for mutagenicity and cytotoxicity. Immunotoxicity, ecotoxicity and clinical toxicity were predicted inactive across all derivatives.

All compounds were inactive for mutagenicity and cytotoxicity. Immunotoxicity, ecotoxicity and clinical toxicity were predicted inactive across all derivatives.

These results collectively indicate a relatively favorable systemic safety profile, with the exception of carcinogenic potential in compound 2a-5a (Table 4.16).

TABLE 4.16: Systemic and Genetic Toxicity

Compound	**Carcino genicity**	**Muta genicity**	**Cyto toxi-city**	**Immuno toxicity**	**Clinical toxicity**
1a	Inactive (0.54)	Inactive (0.70)	Inactive (0.69)	Inactive (0.99)	Inactive (0.52)
2a	Active (0.58)	Inactive (0.72)	Inactive (0.96)	Inactive (0.97)	Inactive (0.57)
3a	Active (0.60)	Inactive (0.68)	Inactive (0.94)	Inactive (0.81)	Inactive (0.54)
4a	Active (0.66)	Inactive (0.80)	Inactive (0.88)	Inactive (0.99)	Inactive (0.51)
5a	Active (0.66)	Inactive (0.80)	Inactive (0.88)	Inactive (0.99)	Inactive (0.51)

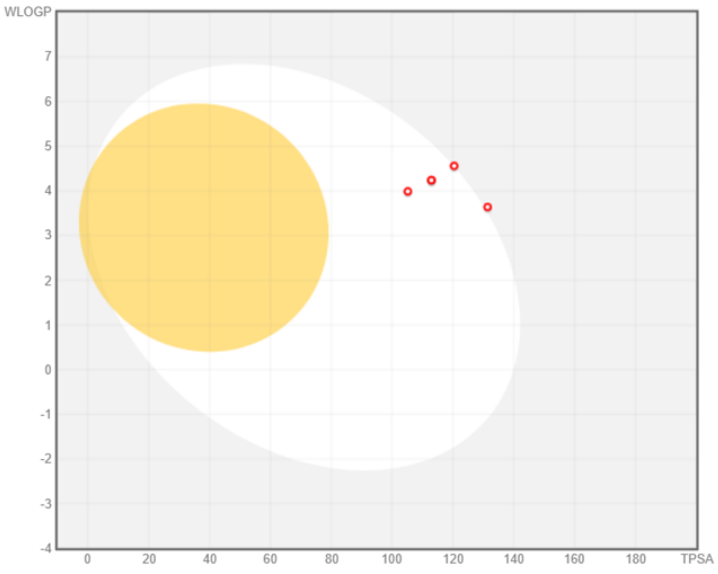

FIGURE 4.11: The boiled egg analysis of produced derivatives

When assessing a compound's fundamental pharmacokinetic characteristics, computer-guided techniques provide a dependable alternative to previous testing, saving time and money. A web-based SwissADME was utilized to ascertain the ADME profile

of the created compounds. SwissADME boiled-egg plot is a rapid, easy to use, and remarkably reliable way to forecast a compound's passive gastrointestinal absorption [129, 130]. With the white portion of the egg representing gastrointestinal absorption and the interior yolk-like portion representing BBB penetration, the egg-shaped plot offers a visual description of the process. The synthesized derivatives Boiled-Egg plot is shown in Figure 4.11. The graph makes it clear that none of the synthetic compounds penetrate the brain. Nonetheless, every chemical has the ability to pass through the gastrointestinal tract.

4.6 Structural Analysis of Target Proteins

4.6.1 COX-2 (PDB ID: 1CX2)

The selected protein has a resolution of 3.00, and an R-value of 0.216. With a 90^o angle for α, β, and γ, the unit cell dimensions for the lengths were found to be a = 180.34, b = 133.92, and c = 121.14. 98.0% of the amino acids were found to be within the permitted ranges for the phi (ϕ) and psi (ψ) angles, according to the Ramachandran plot.

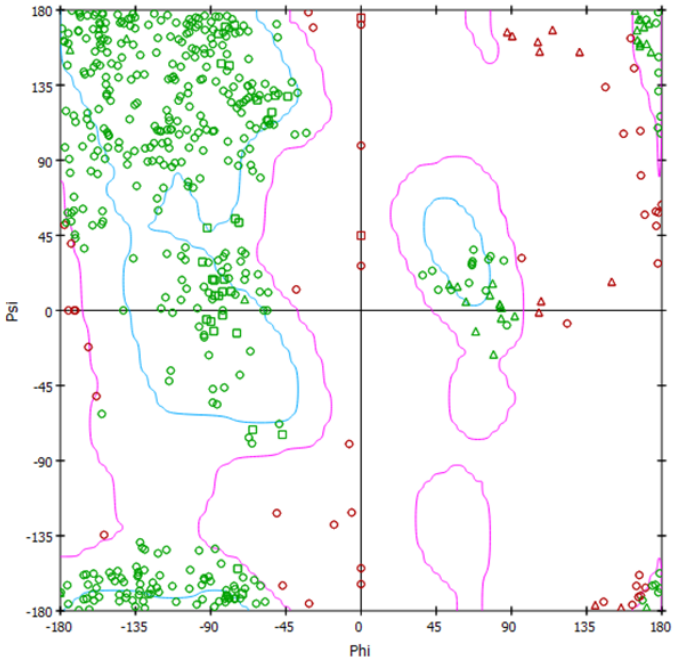

FIGURE 4.12: Structural analysis of COX-2

4.6.2 NF-κB (PDB ID: 1VK X)

The selected protein displayed a resolution of 2.90 Åand an R-value of 0.208. The lengths' unit cell dimensions were determined to be a=106.61, b=106.61, and c=206.56, with α, β, and γ at a 90^o angle. 98.0% of the amino acids were found to be within the permitted ranges for the phi (ϕ) and psi (ψ) angles, according to the Ramachandran plot.

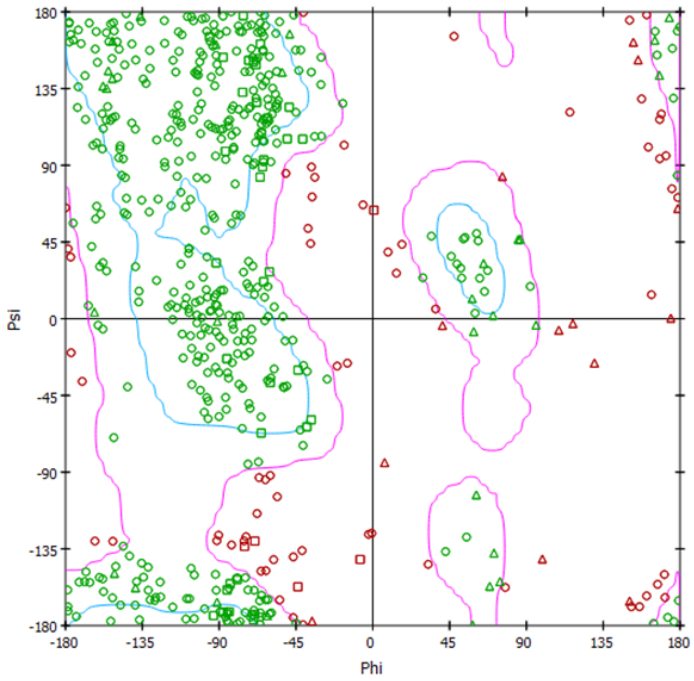

FIGURE 4.13: Structural analysis of NF-κB.

4.7 Evaluation of Binding Affinity and Interaction Against COX-2 and NF-κB

Molecular docking studies were used to assess how the produced ligands interacted with the target proteins. Docking was done using AutoDock Vina [131] and the binding affinity was assessed based on the predicted binding free energy values (kcal/mol). These values reflect the stability of the ligand protein complex and serve as an indicator of binding strength. The docking study also revealed potential constants for binding and interaction patterns of the ligands within the active

sites. The synthesized compounds showed promising binding affinities against NF-κB and COX-2, as shown in Tables 4.17 and 4.18. These findings highlight their potential as anti-inflammatory agents. The favorable binding energies and non-covalent interactions observed suggest that these compounds mat effectively modulate inflammatory pathways through strong and specific protein-ligand interactions.

TABLE 4.17: Docking analysis of compounds in COX-2 active site: Binding affinity, interaction residues and bond types

Compound	**Binding Affinity**	**Bonding Interaction**	**Interacting Amino acid residue**	**Bond Type with**
1a	-9.1	Hydrogen bond, Carbon hydrogen bond, Unfavorable Acceptor Acceptor, Pi-alkyl, Amide-Pi Stacked, Van der Waals.	ARG A:469, TYR A:130, CYS A:41, PRO A:153, MET A:48, ARG A:44, GLY A:135 LYS A:468, ASN A:43, LEU A:152, GLN A:42, GLU A:465, GLN A: 461, GLY A:45, ASN A:39, CYS A:36, GLU A:46, LYS A:137, CYS A:47, TYR A: 136	OCH_3 C_6H_6 S=O
2a	-8.9	Conventional Hydrogen Bond, Carbon Hydrogen Bond, Pi Alkyl.	ARG A:44, TYR A:136, CYS A:41, TYR A:136, ARG A:469, MET A:48, CYS A:47,	OH, C_6H_6
3a	-9.5	Conventional Hydrogen Bond, Pi-Pi T-Shaped, Pi-Alkyl, Carbon Hydrogen Bond	ARG A:44, GLY A :135,TYR A:136, LEU A-152, PRO A-153, CYS A:36, TYR A:134, ALA A:44, GLU A:465	OCH_3, C_6H_6

continued on next page

Table 4.17 continued from previous page

Compound	**Binding Affinity**	**Bonding Interaction**	**Interacting Amino acid residue**	**Bond Type with**
4a	-9.9	Conventional Hydrogen Bond, Amide-Pi Stacked, Pi-Sulfur, Pi Alkyl, Carbon Hydrogen Bond pi- donor hydrogen Bond	GLY A:45, ARG A:44, GLY A:135, MET A:48, LYS A:468, LEU A:152, PRO A:153, ALA A:156,ASN A:34, TYR A 136	CH_3, S=O, C_6H_6, NH
5a	-9.8	Conventional Hydrogen bond, Pi-Sigma, Pi-Alkyl	ARG A:44, GLY A:45, CYS A:41, ASN A:34, LEU A:152, ALA A:156, TYR A:136 , PRO A:153, CYS A:36	CH_3, C_6H_6, S=O, OH,
Diclofenac	-7.6	Conventional Hydrogen Bond, amide-Pi Stacked, Pi Sulfur, Pi-Alkyl	GLN A:461, LEU A:152, CYS A:36, CYS A:47, CYS A:41	OH, S=O

Molecular docking studies were performed out to determine the binding affinities and interaction patterns of the synthesized compounds (**1a-5a**) with the cyclo-oxygenase-2 (COX-2) enzyme. The docking scores, interaction types, and key amino acid residues involved are summarized in Table 4.17.

According to the current docking results, compound 4a had the highest binding affinity among the synthesized compounds, with a docking score of -9.9 kcal/mol, followed by compounds 5a (-9.8 kcal/mol) and 3a (-9.5 kcal/mol).

These compounds showed much higher binding affinities than diclofenac, a standard drug with a binding energy of -7.6 kcal/mol.

Every compound has non-covalent interactions within the COX-2 active site, such as hydrogen bonds, π-alkyl interactions, π-sulfur bonding, π-π stacking, and amide-π stacking. Key residues such as ARG44, TYR136, GLY135, LEU152, PRO153, and CYS41 were found to be crucial for ligand anchoring in the COX-2 active site.

Compound 1a had a binding affinity of -9.1kcal/mol and formed interactions with multiple COX-2 residues through hydrogen bonding, van der Waals force, and π-type interactions.

Compound 2a demonstrated a slightly reduced binding affinity (-8.9kcal/mol), but it maintained stable links, mostly through hydrogen bonding and π-alkyl interactions.

Compound 3a demonstrated favorable π-π T-shaped, hydrogen bonding, and π-alkyl interactions. Compound 3a demonstrated excellent π-π T-shaped and hydrogen bonding interactions, with a binding score of -9.5 kcal/mol.

Compound 4a formed hydrogen bonds, amide-π stacking, and π-sulfur interactions with key residues such GLY45, ARG44, MET48, and TYR136. Compound 5a demonstrated significant π-sigma and hydrogen bonding interactions with several residues, indicating a high affinity of -9.8 kcal/mol.

Diclofenac had lower binding affinity and fewer interactions with GLN461, LEU152, and cysteine residues through hydrogen bonding and π-sulfur interactions. Schiff base derivatives, particularly 4a and 5a, may be more effective COX-2 inhibitors with stronger binding interactions.

These findings suggest that Schiff base derivatives particularly compounds 4a and 5a demonstrate stronger and more diverse binding interactions with COX-2, indicating their potential as more effective COX-2 inhibitors.

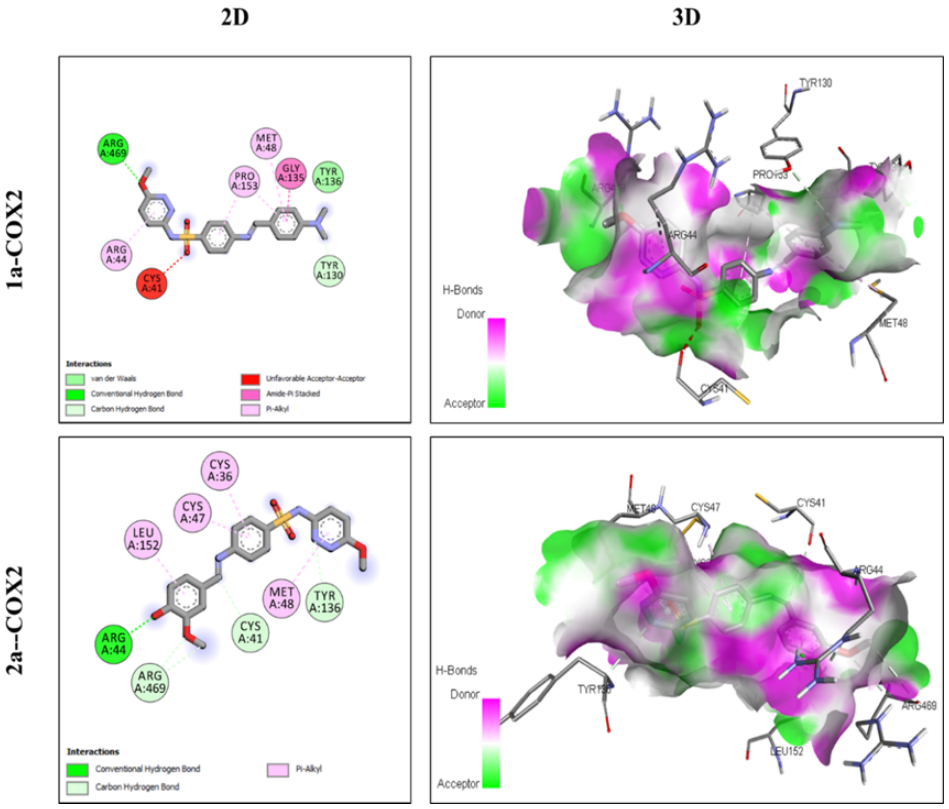

FIGURE 4.14: Molecular docking representation of 1a and 2a against COX-2

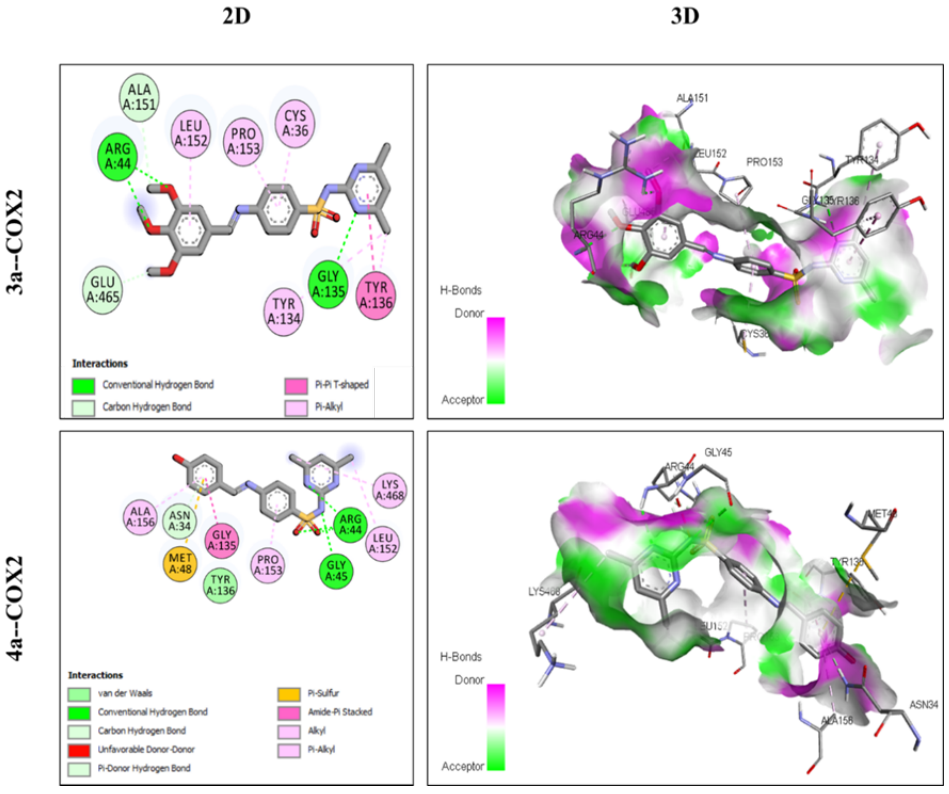

FIGURE 4.15: Molecular docking representation of 3a and 4a against COX-2.

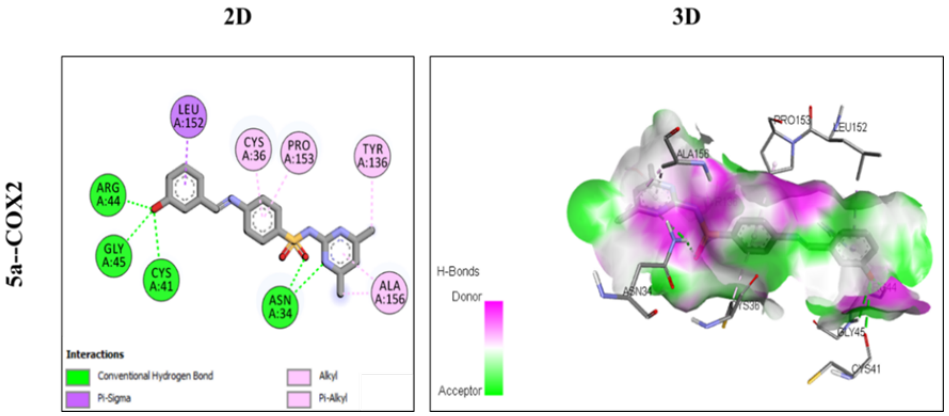

FIGURE 4.16: Molecular docking representation of 5a against COX-2.

TABLE 4.18: Docking analysis of compounds in NF-κB active site: Binding affinity, interaction residues and bond types

Compound	**Binding Affinity**	**Bonding Interaction**	**Interacting Amino acid residue**	**Bond Type with**
1a	-5.8	Conventional Hydrogen Bond, C-H bond, Pi-Alkyl	THR B:639, GLU B:641, LYS B:549	S=O, C6H6, CH3
2a	-6.1	Amide-Pi Stacked, conventional Hydrogen Bond, Pi-Anion, Pi-Alkyl	GLU B:641, THR B:639, ARG B:351, LYS B:549, GLU B:638, ILE B:550	OH, C_6H_6, S=O, OCH_3
3a	-6.1	Conventional Hydrogen Bond, C-H bond, Pi-Cation, Pi-Donor Hydrogen Bond, Alkyl, Pi-Alkyl	ARG B:354, GLY B:365, HIS B:364, SER B:546, ARG A:246, PHE B:353, PHE B:607, LYS B:572, LYS B:549	S=O, C_6H_6. OCH_3, CH_3

continued on next page

Table 4.18 continued from previous page

Compound	**Binding Affinity**	**Bonding Interaction**	**Interacting Amino acid residue**	**Bond Type with**
4a	-7.1	Pi-Donor Hydrogen Bond, conventional Hydrogen Bonds, Pi-Sigma, Alkyl Pi-Alkyl	GLU B:504, THR B:399, TYR B:538, ALA B:545	OH, CH_3, $C_4H_4N_2$
5a	-7.1	Pi-Donor H-Bond, Pi-Sigma, Pi-Pi Stacked, Alkyl, Pi-Alkyl	THR B:399, TYR B:538, ALA B:545	C_6H_6, CH_3
Diclofenac	-7.6	Amide-Pi Stacked, conventional Hydrogen Bond, Pi Sulfur, Pi-Alkyl	GLN A:461, LEU A:152, CYS A:36, CYS A:47, CYS A:41	OH, S=O

Table 4.18 summarizes the binding affinities and interaction patterns of the synthesized compounds (**1a-5a**) and the NF-κB receptor. The synthetic ligands 4a and 5a have the greatest binding affinity (-7.1 kcal/mol), followed by 2a and 3a (both -6.1 kcal/mol).

Compound 1a has the lowest binding energy (-5.8 kcal/mole). In comparison, diclofenac exhibited a binding affinity of -7.6 kcal/mol, which was somewhat better than all of the ligands. Compound 4a has strong binding affinity due to advantageous interactions such as conventional hydrogen bonding, π-donor hydrogen bonding, π-sigma, and π-alkyl interactions. GLU B:504, THR B:399, TYR B:538, and ALA B:545 interact with functional groups such -OH, -CH , and C H N ,

resulting in improved molecular stability within the NF-κB binding pocket. Compound 5a has a similar binding affinity (-7.1 kcal/mol) through interactions such as π-donor hydrogen bonds, π-π stacking, and π-alkyl contacts. It involved residues including THR B:399, TYR B:538, and ALA B:545, assisted by aromatic rings (C_6H_6) and alkyl substituents (-CH_3).

The inclusion of hydrophobic and π-interacting groups likely increased the binding complementarity. Compounds 2a and 3a had identical binding affinities of -6.1 kcal/mol, but their interaction patterns vary. Compound 2a exhibited typical hydrogen bonding, amide-π stacking, and π-anion interactions with GLU B:641, THR B:639, ARG B:351, LYS B:549, and ILE B:550. Polar groups such as -OH, -OCH_3, and S=O, along with aromatic systems, likely contributed to the moderate binding.

Compound 3a exhibited a wider range of contacts, including π-cation, π-donor hydrogen bond, π-π T-shaped, and alkyl interactions with residues such as ARG B:354, GLY B:365, HIS B:364, PHE B:353, and LYS B:549. The inclusion of -OCH_3, S=O, aromatic, and alkyl groups allowed it to occupy the active site in a stable state.

Compound 1a had the lowest binding affinity (-5.8 kcal/mol) and only generated a few interactions with THR B:639, GLU B:641, and LYS B:549. These interactions included hydrogen bonding and π-alkylation. This lesser interaction variety could explain for its weaker binding.

Diclofenac, the reference drug, showed the strongest binding (-7.6 kcal/mol), creating interactions such as conventional hydrogen bonding, amide-π stacking, and π-sulfur interactions with key residues GLN A:461, LEU A:152, and CYS.

This shows that, while compounds 4a and 5a have promise action, additional structural optimization could improve their binding which suggest that both compounds either comparable potential or outperform diclofenac. It suggests that structural characteristics such as heteroaromatic rings, hydrogen bond donors/acceptors, and π-conjugated systems are crucial for increasing binding affinity to NF-κB. The synthetic ligands 4a and 5a show promise as NF-κB inhibitors.

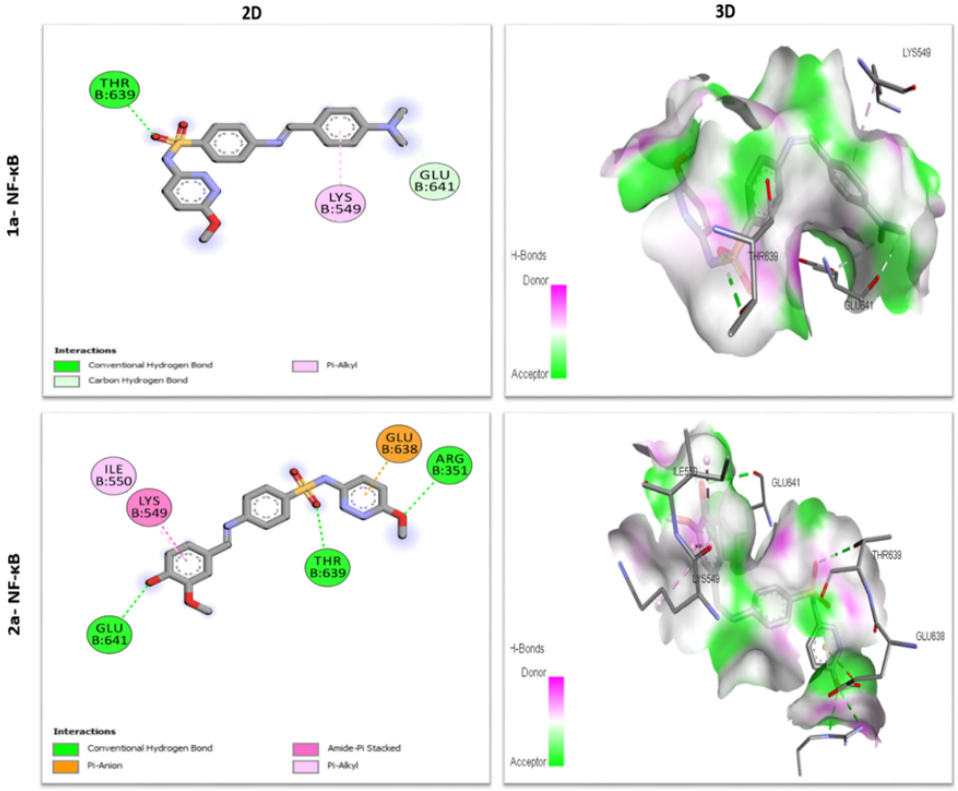

FIGURE 4.17: Molecular docking representation of 1a and 2a against NF-κB

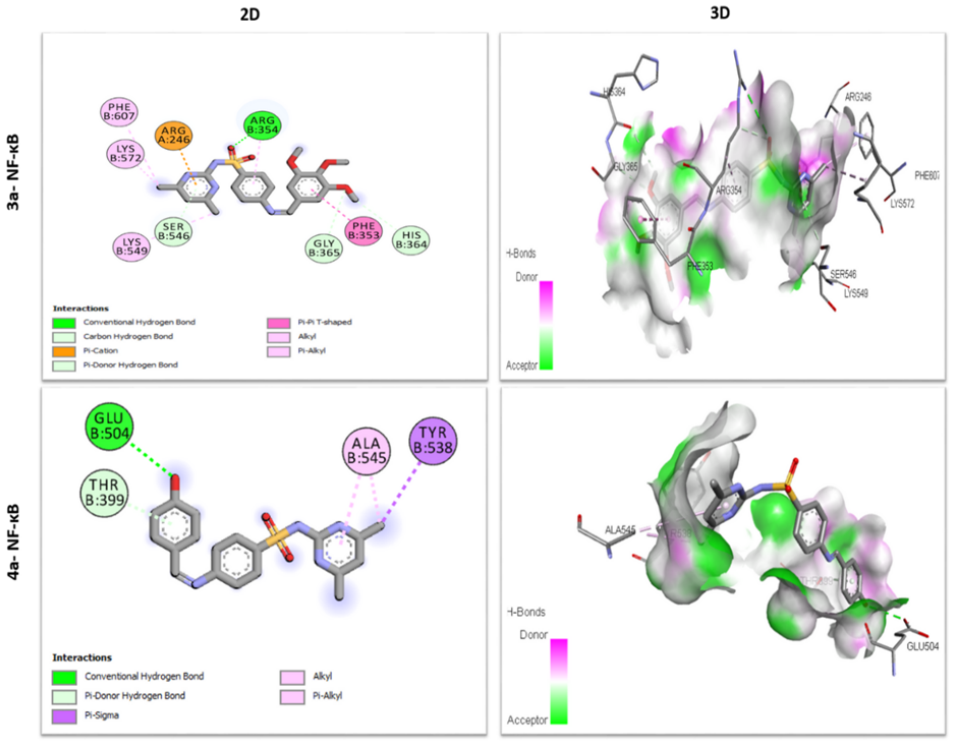

FIGURE 4.18: Molecular docking representation of 3a and 4a against NF-κB

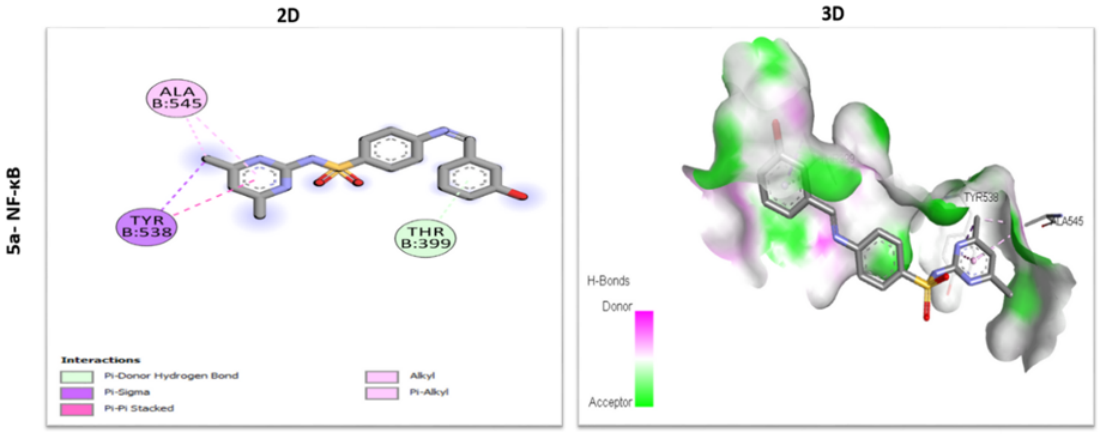

FIGURE 4.19: Molecular docking representation of 5a against NF-κB

4.8 *In-vitro* Antioxidant Evaluation of Synthesized Compounds

4.8.1 Total Antioxidant Capacity (TAC) and Total Reducing Power (TRP) of Synthesized Compounds (1a-5a)

The antioxidant potential of the synthesized Schiff base derivatives (**1a-5a**) was determined using the Total Antioxidant Capacity (TAC) and Total Reducing Power (TRP) assays. The TAC and TRP assays demonstrated that the synthesized compounds have variable amounts of antioxidant capacity.

Compound 1a demonstrated the highest TAC and TRP potential, indicating strong anti-oxidant activities. Compound 2a also showed significant activity, though slightly lower than 1a. Compound 4a presented a moderate level of antioxidant potential, while compounds 3a and 5a exhibited only weak activity. These observations suggest that compounds 1a and 2a possess superior antioxidant properties, whereas the others may have limited effectiveness in contributing to antioxidant defence. The results are shown in Figure 4.20.

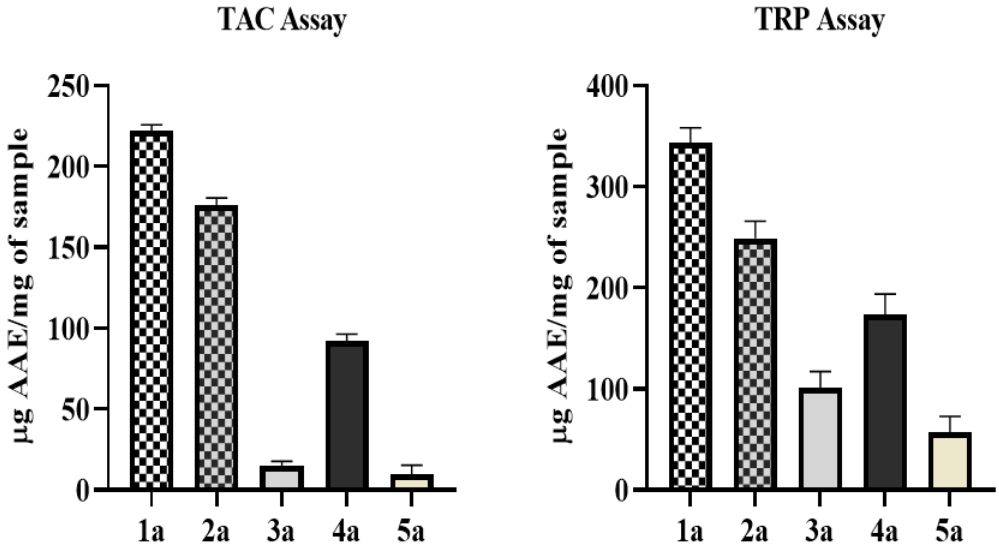

FIGURE 4.20: Evaluation of anti-oxidant potential of synthesized compounds using TAC and TRP assay

4.8.2 Free Radical Scavenging Effects of Synthesized Compounds (1a-5a)

The antioxidant activity of the produced Schiff base derivatives (**1a-5a**) was assessed using the DPPH free radical scavenging test. The DPPH assay findings revealed significant differences in the antioxidant activity of the five newly synthesized compounds.

Among them, compound 1a exhibited the strongest free radical scavenging activity, indicating its potential as a powerful antioxidant agent. Compounds 2a and 4a showed moderate antioxidant effects, suggesting a fair capacity to neutralize free radicals.

In contrast, compound 3a demonstrated relatively low activity, while compound 5a displayed only minimal scavenging ability. These findings suggest that structural variations among the compounds may significantly influence their antioxidant potential. The results are depicted in Figure 4.21.

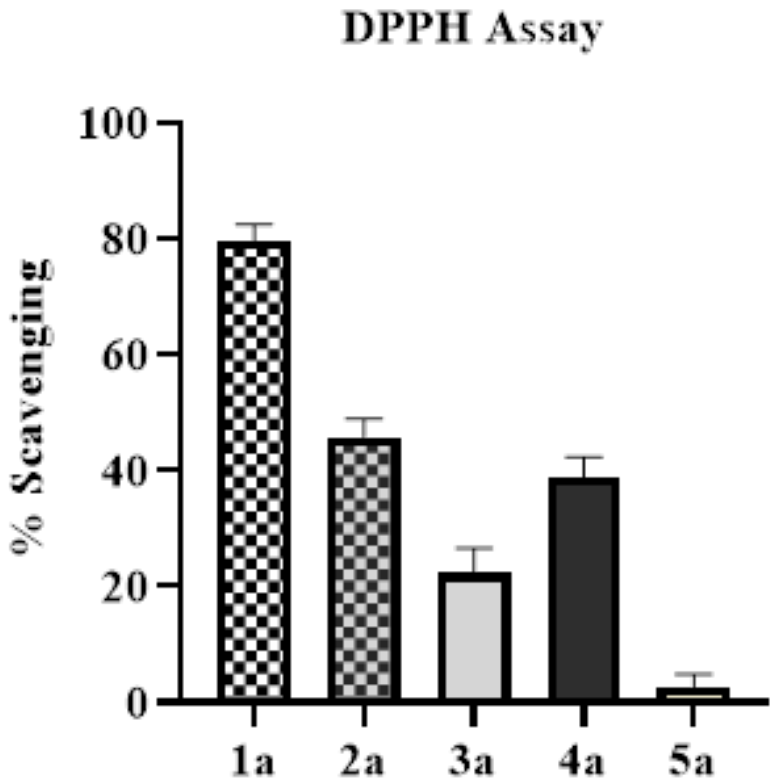

FIGURE 4.21: Evaluation of antioxidant potential of synthesized compounds using DPPH assay

4.9 *In-vivo* Evaluation

4.9.1 Acute Analgesic Effect of 1a and 2a

In a recent study, all mice in each group received acetic acid (1%, 10 ml/kg, i.p.) to induce writhing pain behavior. The control group, which received acetic acid (10 ml/kg, i.p.) and normal saline, had a considerable number of writhing behaviour. However, pre-treatment with 1a or 2a (1, 5, 10 mg/kg. i.p.) may reduce acetic acid-induced writhing pain behavior as compared to the saline treated group. Furthermore, the pain inhibitory effects were dose-dependent. Similarly, previous tramadol administration (1 mg/kg, i.p.) significantly suppressed the acetic acid-induced writhing response in compared to the control group. Figure 4.22 shows the results for compound 1a or compound 2a.

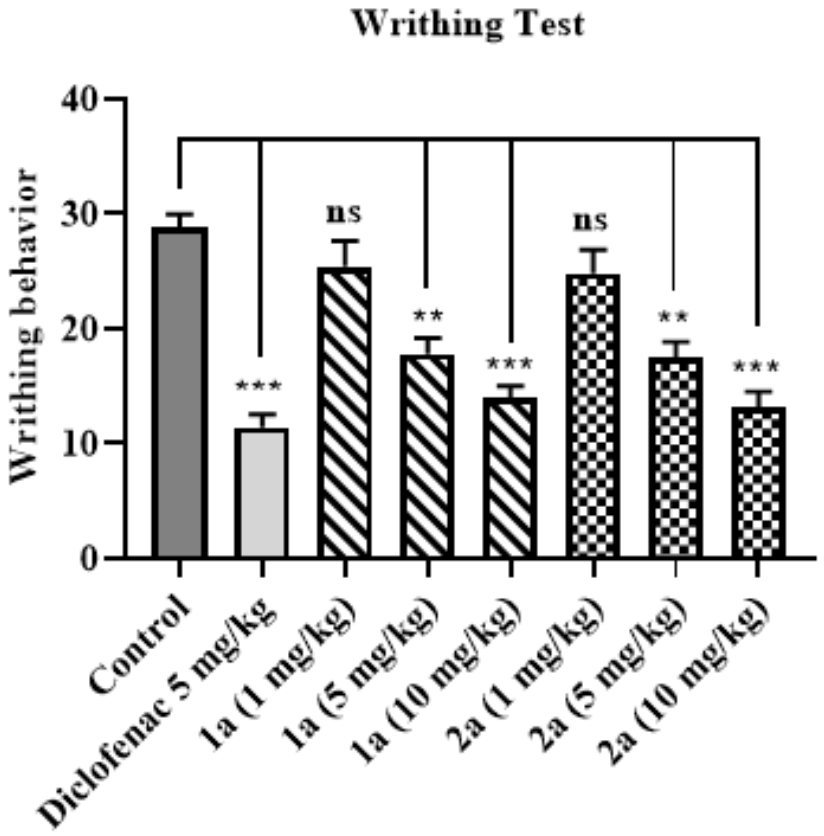

FIGURE 4.22: Effect of 1a or 2a on acetic acid induced pain behaviour. Both compounds show marked analgesic effect (**p<0.01, ***p<0.001) in dose dependant manner against acetic acid induced pain behaviour. The results were displayed as mean±SD (n=5).

4.9.2 Acute Inflammatory Effect of Compound 1a and Compound 2a Iin Carrageenan Induced Paw Edema

The present investigation evaluates the inhibitory activity of compound 1a or compound 2a in carrageenan induced inflammation model. The results demonstrated that administration of 1% carrageenan (40 μl, i.pl.) into the right hind paw significantly increased paw edema in saline treated (10 ml/kg, i.p.) negative control group as compared to the normal group. The paw edema in treatment group were markedly reduced by compound 1a or compound 2a as compared to negative control. The response produced by compound 1a or compound 2a were observed in dose dependant manner. The results are indicated in Figure 4.23.

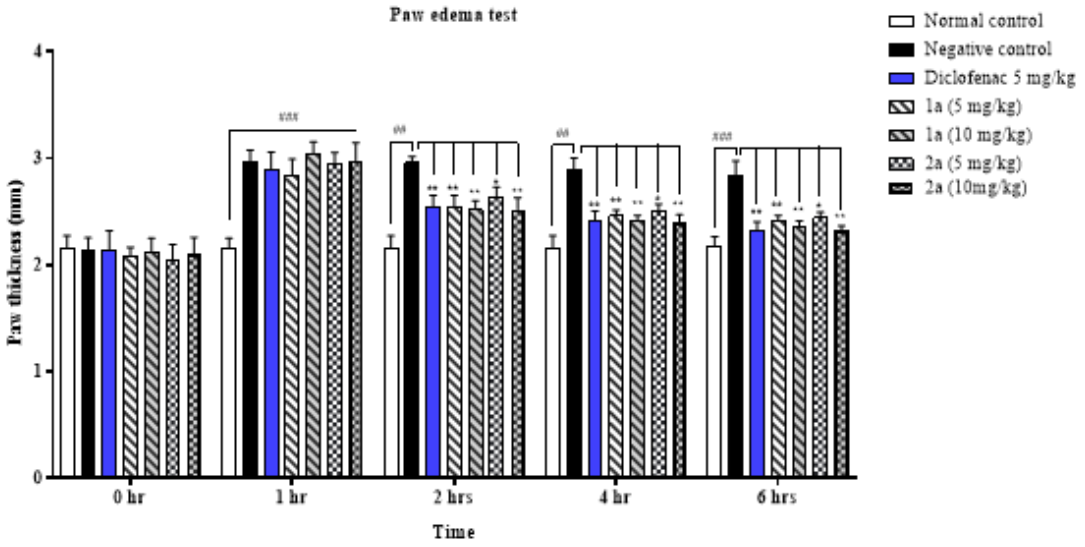

FIGURE 4.23: Anti-inflammatory effect of synthesized derivative on carrageenan induced edema. The results indicate both compounds show promising decrease (*p<0.05, **p<0.01)) in paw edema after carrageenan induction. The results were presented as mean±SD (n=5).

Chapter 5

Discussion

Schiff bases are a well-known class of compounds with numerous pharmacological activities. These include protective role against inflammation, bacterial infections, oxidative stress, and anticancer effects. Their biological significance is largely related to the existence of the azomethine (C=N) functional group, which plays an important role in facilitating biochemical interactions and target binding [132]. Numerous studies have documented the straightforward synthesis of Schiff base derivatives via condensation reactions between primary amines and carbonyl compounds, yielding structural diverse compounds with considerable therapeutic potential [133, 134]. In particular, aromatic and sulfonamide-modified Schiff bases have fascinated growing consideration in part to their enhanced biological activities and improved affinity for pharmacologically relevant targets [135]. In the current investigation, a series of Schiff base derivatives (**1a-5a**) were synthesized and thoroughly analyzed using structural, computational, and pharmacological methods. Spectroscopic techniques such as FTIR and NMR were employed for structural confirmation, while in silico ADMET profiling and molecular docking studies provided insights into pharmacokinetic properties and target interactions. Furthermore, the in vitro antioxidant assays (TAC, TRP, and DPPH) and in vivo anti-inflammatory evaluation using the carrageenan-induced model validated the biological relevance of the synthesized compounds. The integration of these multidisciplinary findings offers a critical assessment of the compounds therapeutic

potential, particularly highlighting compounds (**1a-5a**) as promising candidates for further development.

Schiff bases are well known for their structural diversity and diverse pharmacological applications. Their effective synthesis tends to validated by FTIR spectroscopy [136], which is an effective method for identifying important functional groups such as imines (C=N), sulfonamides (S=O), and amines (N-H). In the present study, the synthesized Schiff base derivatives (**1a-5a**) were identified by their different FTIR absorption bands. All compounds showed distinctive imine (C=N) stretching bands between 1636-1655 cm^{-1}, indicating effective condensation of aromatic aldehydes and sulfonamide precursors [137]. The presence of all anticipated functional groups was also verified by the FTIR analysis of compound **5a**. The imine group was identified by a C=N stretching vibration at 1591 cm^{-1}, which is marginally below the usual range but still in line with reports from the literature for azomethine bonds in Schiff bases [138]. This shift can be explained by intramolecular hydrogen bonding or conjugation with aromatic rings, which tend to delocalize the electron density and weaken the azomethine linkage's interaction and lowering its wavenumber [139].Sulfonamide functional groups were consistently indicated by asymmetric and symmetric S=O stretching bands in the range of 1153-1282 cm^{-1} [140]. N-H and O-H groups were confirmed by broad absorption bands about 3200-3400 cm^{-1}. Compound-specific analysis confirmed these findings. Compound **1a** showed a distinct C=N peak at 1651 cm^{-1}, N-H stretching at 3201.8 cm^{-1}, and sulfonamide S=O vibrations between 1341.8 and 1155.5 cm^{-1}. Compound **2a** exhibited similar tendencies, with an imine peak at 1654.9 cm^{-1} and phenolic O-H stretching at 3406.8 cm^{-1}, indicating that hydroxyl groups contribute to hydrogen bonding and resonance effects [141]. These FTIR results collectively validate the successful formation of Schiff base derivatives and the presence of the anticipated functional groups.

Lead optimization necessitates a detailed grasp of the physiochemical and pharmacokinetic aspects of drug candidates, from administration to elimination. These parameters are essential for ensuring drug safety, therapeutic efficacy, and effective metabolism in vivo [142]. All synthesized compounds were therefore evaluated

for the ADMET properties using reliable in silico tools. The ideal drugs candidate should be nontoxic, easily absorbed into the bloodstream, and eliminated from the body without interfering with normal biological function. In this context, in silico ADMET analysis provides a cost-effective and time-efficient alternative to traditional in vivo and in vitro studies [130]. SwissADME is commonly used in early-stage drug discovery to assess absorption, distribution, metabolism, and excretion. By analyzing important physiochemical properties, it helps forecast the drug-likeness and bioavailability of compounds [143]. Due to toxicity risk and negative ADME, many new medications fail clinical trials. As a result, knowing pharmacokinetic properties is critical for designing and developing new drugs. Two well-known recommendations, (1) Veber's rule and (2) Lipinski's rule of five, were useful for predicting the oral bioavailability of drugs.

Lipinski's rule states that in the context of drug discovery, if there are more than ten H-bond acceptors (HBA), five H-bond donors (HBD), lipophilicity (cLogP) greater than five, and a molecular weight larger than five hundred, there is a higher likelihood of poor penetration or absorption. In contrast, Veber's rule indicates that if a molecule maintains a number of rotatable bonds (NROTB) and a topological polar surface area (TPSA) of 10 or fewer, oral bioavailability is preferred [144].The physiochemical belongings of the composites are revealed in Table 4.8 . All Schiff base derivatives satisfied Lipinski's criteria indicating acceptable oral drug likeness. Each compound had MW $\leq$ 500 Da, HB donor $\leq$ 5, HB acceptor $\leq$ 10, and log p$\leq$5 confirming their favorable absorption profile [145]. Any remedy molecule that fails at least one of the requirements can have limited penetrability or deprived absorption [146]. F.Csp3 is the definition of the proportion of sp3 hybridized Cs in the entire sum of carbon atoms. It depicts the carbon capacity and shows the intricacy of the molecular spatial structure. Since 84% of commercially available medications meet this criteria, F.Csp3 should be $>$ 0.42. A greater F.Csp3 score does not necessarily indicate excellent quality and may complicate chemical production, thus the sp3 content must be raised, but only to a limited degree [147]. All compounds showed Fsp3 $<$ 0.42, which is typical for synthetic molecules. However, this lower Fsp3 does not disqualify the compounds, as many marketed drugs fall below this threshold.Because synthetic

items frequently contain a lower percentage of F.Csp3 than organic substances, natural goods are therefore a possible source of therapies [148]. It is generally known that rotatable bonds with more than 10 tend to be more flexible and have higher entropy, which makes it harder for the body to absorb them [149]. Its method of action is still unknown, despite the fact that the number of "rotatable bond filters" has not been clearly linked to the rate of clearance in vivo. However, this filter is justified by the possibility of in vitro screening because ligand affinity decreases at a rate of, on average, 0.5 kcal for each pair of rotatable bonds [150]. All derivatives remained within acceptable limits, except **3a**, which showed higher flexibility and may require optimization. Rotatable bonds, donors, and H-bond acceptors are less common in oral medications since both the donor and the H-bond acceptor are still within range [151]. These three elements support the idea that oral delivery is flexible, useful, and simple.

Specific molecular systems with TPSAs larger than 140Å2 are known to exhibit limited absorption with fractional absorption below 10%, while those with TPSAs of 60Å2 exhibit significant absorption with fractional absorption above 90% [130]. Accordingly, the Schiff base derivatives (**1a-5a**) TPSA values between 105-131 Å2 suggesting good to moderate GI absorption.

Lipophilicity is a key physiochemical property in molecular discovery. The partition coefficient P is a classic quantitative indicator of lipophilicity that is widely utilized in pharmaceutical and biological research. Because of its amphiphilic nature, octanol is regarded to be an effective phospholipid membrane mimic [152]. The consensus Log Po/w, also known as the octanol/water partition coefficient, is the average of Log Po/w estimates obtained by iLOGP, XLOGP3, WLOGP, MLOGP, and SILICOS-IT techniques. Higher Log Po/w values suggest increased lipophilicity due to polarity, molecule size, and hydrogen bonding. Compound **3a** showed the highest lipophilicity in all models (highest ILogP, XLOGP3, WlogP, MlogP, SILICOS-IT) indicating a highly hydrophobic nature. Compound **2a** displayed the lowest lipophilicity in most models, implying it may be more polar or more hydrophilic substituents. Compound **4a** and **5a** shared identical values

for XLOGP3, WlogP, MlogP, SILICOS-IT suggesting structural similarity or isomerism.

Compound **3a**, with WlogP= 4.56 and SILICOS-IT = 3.59, approaches this threshold and solubility and metabolic stability. Compound **1a**, **2a**, **4a**, and **5a** fall within desirable range in most models, especially for oral drugs. Compound **3a**'s comparatively low MlogP (0.95) in contrast to its high WlogP and SILICOS-IT values indicates some model inconsistencies, most likely as a result of divergent structural feature weighting (e.g., molecular volume vs. Functional group types). The nearly identical lipophilic values of compounds **4a** and **5a** across all models demonstrate their structural closeness and suggest similar hydrophobic interactions.However, the relatively good bioavailability scores of 0.55 indicate that these drugs are promising candidates for additional optimization and experimental validation to improve their medicinal efficacy.

Lipophilicity affects various pharmacokinetic parameters. Low lipophilicity results in high water solubility, which is an important quality for drug resemblance; however, very low lipophilicity may impair the medication's ability to reach its physiological target. Highly soluble compounds, on the other hand, have minimal permeability through biological membranes, limiting absorption in the gastrointestinal tract and passing through the blood-brain barrier. As a result, the optimal requirements for efficient solubility and permeability qualities are limited to a very restricted range of lipophilicity [153]. Compound **3a**, consistently showed the highest logP values, indicating high hydrophobicity and potential for membrane permeability. Compound **2a** had the lowest lipophilicity, suggesting a more polar character. Compounds **4a** and **5a** exhibited nearly identical lipophilic profiles across all models, reflecting structural similarity or isomerism.

Furthermore, solubility is an important property to consider while designing drugs. Poor potential to absorb and attain bioavailability orally can be attributed to inadequate solubility in water. The solubility of a derivative in water has a significant impact on drug design and behavior, hence it is critical in drug discovery and development. Three models were used to calculate the molar solubility of water (logS). The chemical was subjected into six different categories: intractable (Log

S < -10), poorly soluble (Log S < -6), moderately soluble (Log S < -2), soluble (Log S < -4), very soluble (Log S < -2), and highly soluble (Log S 0) [154]. According to ESOL model all five compounds are classified as soluble indicating good water solubility. In the Ali Log S model, compound **1a**, **2a** ,**3a** classified as moderately soluble while **4a** and **5a** remain soluble. The SILICOS-IT model classifies all compounds as poorly soluble. Overall ESOL and Ali model suggests better solubility profiles than the SILICOS-IT model.

The human GIT absorption (HIA), substrate glycoprotein (P-gp) and non-substrate permeability, blood-brain barrier (BBB) dissemination, the contact of molecules with cytochromes P450 isomers (CYP) are shown in Table 4.9. Compounds **1a**, **4a**, and **5a** had high gastrointestinal (GI) absorption, indicating good oral availability while **2a** and **3a** had limited GI absorption, likely due to higher polarity or TPSA which could affect their oral efficacy. Compounds **1a**, **4a**, and **5a** because of good gastrointestinal (GI) absorption, making them ideal for oral delivery. In contrast, **2a** and **3a** due to reduced GI absorption, potentially due to physicochemical features such as higher molecular weight, hydrogen bonding potential, or polarity, which may limit passive diffusion across the intestinal epithelium.

None of the drugs were anticipated to cross the blood-brain barrier (BBB) or act as P-glycoprotein (P-gp) substrates, thereby alleviating concerns about CNS adverse effects and efflux-related bioavailability issues. In terms of cytochrome P450 (CYP) enzyme inhibition, the compounds most typically inhibited CYP2C9 and CYP3a4. **1a** and **3a** inhibited both CYP2C9 and CYP1a2, but the other drugs did not inhibit CYP1a2. compound **1a** was the only chemical that inhibited CYP2C19.

These findings indicate that Schiff base derivatives may have good oral bioavailability and few CNS side effects; however, potential CYP-mediated drug-drug interactions, notably with CYP3a4 and CYP2C9, should be explored in future research phases. The Schiff base derivatives (**1a-5a**) have favorable pharmacokinetic characteristics, with all compounds scoring a bioavailability score of 0.55, which is compatible with the oral drug-likeness criteria provided by Martin [155].

The Schiff base derivatives had promising medicinal chemistry characteristics. The absence of PAINS alerts for any compounds indicates that these ligands are unlikely to interfere with biological tests nonspecifically, which is an important criterion for hit-to-lead optimization [156]. Because of the nature of Schiff base structures, all compounds should have a single Brenk alert (imine_1). While imines may be highlighted for reactivity or instability, they are also vital for biological action and can be stabilized in drug design through careful optimization [157]. Lead-likeness is a desirable feature for selecting drug candidates with the right size and flexibility for future development. The breaches identified (mainly MW $>$ 350 Da) are not necessarily unacceptable, but they do indicate that the molecules are reaching the upper limit of optimal physicochemical attributes. Compound **3a**, with two violations (high MW and excessive flexibility), may require structural adjustment to improve developability [158].

Overall, these findings support the medicinal chemistry viability of Schiff base derivatives, specifically **1a**, **4a**, and **5a**, which exhibit fewer lead-likeness violations and acceptable synthetic accessibility values.

Compound **1a** and **2a** were predicted to have LD values of 1700mg/kg, placing them in GHS class 4, denoting moderate acute oral toxicity and categorizing them as harmful if swallowed. The GHS system defines these toxicity categories, which are used in computational models like as ProTox-II to classify chemicals based on LD levels [159].Compound **3a-5a** showed markedly LD values (25,000 mg/kg) and were categorized as GHS class 6, indicating low toxicity. These results suggest that the structural changes effectively minimized systemic toxic effects [160].

All of the compounds showed reasonably high probabilities ($\geq$0.62) for inactive predictions of neurotoxicity, nephrotoxicity, and cardiotoxicity, suggesting good safety profiles for these organ systems. Nonetheless, all compounds were predicted to be active in terms of respiratory toxicity (probability range: 0.67–0.74).The presence of structural motifs or functional groups linked to lung irritancy or bronchoconstrictive potential may be the cause of this observation. Similar indications have been seen for compounds that include amines or halogenated phenyl rings,

which are known to disrupt airway reactivity [161].Only compound **2a** was identified as hepatotoxic (0.58). Hepatotoxicity, one of the primary causes of medication withdrawal, is frequently linked to the bioactivation of reactive intermediates that covalently bind to liver proteins [162].

While no compounds were projected to be mutagenic or cytotoxic, compounds **2a**-**5a** were predicted to be carcinogenic, with probabilities ranging from 0.58 to 0.66. This supports a non-genotoxic carcinogenic pathway, which may involve prolonged receptor activation, oxidative stress, or hormone disturbance. Immunotoxicity, ecotoxicity, and overall clinical toxicity were all expected to be inactive, suggesting low adverse impacts on immune function, environmental impact, and overall systemic health.

The molecular docking results of the synthesized Schiff base compounds (**1a**-**5a**) against the COX-2 receptor provide significant details about their potential as anti-inflammatory agents. The binding affinities found in this study indicate that the structural characteristics put into these compounds greatly improve their interactions with the COX-2 active site when compared to the standard drug, diclofenac. Compound **4a** had the most binding affinity (-9.9 kcal/mol), followed by **5a** (-9.8 kcal/mol) and **3a** (-9.5 kcal/mol). These binding affinities are much better than the binding energy of diclofenac (-7.6 kcal/mol), a commonly used non-steroidal anti-inflammatory drug (NSAID), indicating superior binding potential and maybe improved inhibitory efficacy of the novel ligands [163]. Compound **4a**'s improved binding is due to its varies interactions, which include typical hydrogen bonds, amide-π stacking, π-sulfur interactions, and π-alkyl contacts. These interactions involved important residues such as GLY45, ARG44, GLY135, MET48, and TYR136, which are well-known contributors to COX-2 ligand binding [164]. The introduction of functional groups (-CH , -NH, S=O, and aromatic rings) in **4a** likely encouraged a range of bonding mechanisms, increasing the specificity and stability of the ligand-protein interaction. Compound **5a** formed strong connections with CYS41, ASN34, TYR136, and PRO153 by hydrogen bonding and π-sigma contacts. A number of hydrogen-bond donor groups (-OH and S=O)

probably aided in the ligand's proper positioning and anchoring inside the COX-2 binding pocket, which is consistent with previously reported COX-2 inhibitors that take advantage of comparable pharmacophoric characteristics [165].

NF-κB regulates genes involved in inflammation, immunity, and cell viability. Its dysregulation has been linked to various chronic inflammatory illnesses and malignancies, making it a prospective therapeutic target for anti-inflammatory drug development [166].

Molecular docking to examine the binding interactions between synthesized Schiff base derivatives (**1a-5a**) and the NF-κB receptor. Among the synthesized ligands, **4a** and **5a** had the highest binding affinities (-7.1 kcal/mol), which were similar to those of diclofenac (-7.6 kcal/mol), a therapeutically proven anti-inflammatory drug. This shows that these compounds may have equivalent or enhanced inhibitory activity against NF-κB.

Compound **4a** improves binding by creating stabilizing contacts in the NF-κB binding pocket, including hydrogen bonds, π-sigma, π-donor hydrogen bonds, and π-alkyl interactions. GLU B:504, THR B:399, TYR B:538, and ALA B:545, located near NF-κB's DNA-binding and dimerization domains, play a significant role in transcriptional activity [167]. Polar groups such as -OH and nitrogen-containing heterocycles ($C_4H_4N_2$) enhance the compound's orientation and interaction depth in the active site. Compound **5a**, which contains aromatic rings and methyl groups, also generated stable π-interactions with the crucial residues. The π-π stacking with TYR B:538 and π-sigma interaction patterns indicate advantageous non-covalent interactions that promote ligand-receptor stability. The approach is also used in previously reported NF-κB inhibitors [168].

Despite their moderate binding affinities (-6.1 kcal/mol), compounds **2a** and **3a** showed vast and diversified bonding patterns. For example, **3a** exhibited π-cation and π-π T-shaped interactions, which are crucial for stabilizing ligand-protein complexes, particularly in transcription factor binding sites [169]. These compounds' functional groups, including -OCH_3, S=O, and aromatic rings, play a

role in hydrophobic and hydrogen bonding interactions, providing opportunities for optimization.

Compound **1a**, on the other hand, demonstrated the lowest binding affinity (-5.8 kcal/mol) and fewer interaction types, most likely due to its inability to create persistent interaction with crucial active site residues. Minor structural variations, like lower hydrogen bonding or π-interaction capacity, can greatly impact a compound's ability to effectively suppress NF-κB.

The reference medication diclofenac showed strong binding (-7.6 kcal/mol) with interactions such as amide-π stacking, π-sulfur, and hydrogen bonding, involving key residues like GLN A:461 and CYS A:41. These findings support the docking methodology and highlight the necessity of include π-interacting and polar functions in ligand scaffolds to increase NF-κB inhibition [170]. The docking analysis suggests that **4a** and **5a** are promising NF-κB inhibitors.

The antioxidant activities of the synthesized derivatives evaluated by TAC and TRP assays demonstrated a vibrant difference in activity among all the derivatives. It was noted that compound (**1a** & **2a**) confirmed the highest antioxidant potential suggesting these molecules hold structural characteristics favorable to free radical scavenging or electron donation. However, compounds (**3a** & **5a**) showed weak activity, while **4a** revealed moderate antioxidant potential. These findings are associated with previous reports showing that specific structural features can markedly augment antioxidant activity. The strong antioxidant potential of compounds **1a** and **2a** may be ascribed to such structural features, potentially permitting more effective stabilization of radical species or reduction of free radicals. Inclusive, the current results focus the significance of designing novel compounds to strengthen their antioxidant properties. The promising activity of **1a** and **2a** proposes that these compounds could be auspicious candidates for further development as antioxidant agents [171–173]. These findings align with recent studies demonstrating that Schiff bases bearing electron-donating substituents such as hydroxyl and methoxy groups, along with extended conjugation, exhibit enhanced antioxidant activity through mechanisms including hydrogen atom transfer (HAT) and single-electron transfer (SET) [174]. The superior activity of compound **1a**

and **2a** can be attributed to comparable structural characteristics, simple resonance stabilization, and effective electron or hydrogen donation that promote interaction with and quenching of reactive oxygen species.

Pain and inflammation are considered one of the serious problems which occurs in response to injury, diseased, or during infection [175]. In acute phase both are considered protective responses of the body to avoid any damage. However, persistent pain or inflammation significantly disturb quality of life and routine daily activities. Inflammation is also considered one of the major problems associated with pathophysiology of various conditions in the body [176].

The current study aimed to evaluate the analgesic and anti-inflammatory properties of **1a** and **2a** using acetic acid-induced writhing and carrageenan-induced inflammation. The acetic acid-induced writhing test is a well-established model to evaluate peripheral analgesic activity. It reflects sensory neuron sensitization and visceral inflammation caused by the release of pro-inflammatory mediators like prostaglandins (PGE2), bradykinin, and cytokines (e.g., IL-1β, TNF-α) [177]. Injecting 1% acetic acid (10 mL/kg) intraperitoneally resulted in significant writhing responses in the control group treated with normal saline, indicating the activation of peripheral chemosensitive nociceptors and subsequent release of inflammatory cytokines like TNF-α and IL-1β. Pre-treatment with Compound **1a** and Compound **2a** at doses of 1, 5, and 10 mg/kg resulted in a significant and dose-dependent reduction in the number of writhes compared to the saline-treated control group. The considerable and dose-dependent reduction in writhing responses after treatment with compounds shows that nociceptive signaling is effectively inhibited at the peripheral level. The carrageenan-induced paw edema paradigm, which mimics acute inflammation through a biphasic response: an early phase mediated by histamine and serotonin, and a late phase dominated by prostaglandins and neutrophil infiltration, provides insight into anti-inflammatory efficacy [178]. Similarly, compound **1a** and Compound **2a** at doses (5, and 10 mg/kg) significantly suppress paw edema in carrageenan model. The substantial edema inhibition observed particularly during the later phase suggests that compounds

1a and **2a** may suppress cyclooxygenase (COX-2) activity or downstream pro-inflammatory mediator release, aligning with the in silico docking results that indicate strong binding affinities COX-2 and NF-κB. This indicates that both compounds possess notable analgesic and anti-inflammatory effects and may constrain with the peripheral mechanisms of pain, possibly through inhibition of inflammatory mediator synthesis or receptor antagonism. The dose-dependent response further supports the pharmacological relevance of these compounds and suggests a correlation between concentration and efficacy.

Tramadol (1 mg/kg, i.p.) was employed as the standard reference drug [179], also significantly reduced the acetic acid-induced writhing responses, consistent with its known analgesic action that involves both opioid receptor agonism and inhibition of monoamine reuptake. The analgesic effect observed with Compound **1a** and Compound **2a** at higher doses was comparable to that of tramadol, suggesting these compounds may possess a potent antinociceptive profile. These findings collectively suggest that Compound **1a** and Compound **2a** exhibit analgesic and anti-inflammatory activity. Moreover, the dose dependent trends observed in both analgesic and anti-inflammatory activities suggest that these Schiff base derivatives likely engage molecular targets in a concentration-responsive fashion potentially via COX inhibition, NF-κB pathway modulation, or interactions with other receptor sites. Structural elements such as azomethine (C=N) linkage, aromatic moieties, and sulfonamide functional groups may collectively enhance lipophilicity and strengthen target binding, thereby contributing to their pharmacological effectiveness. These findings align with earlier literature highlighting the potential of Schiff bases as multi-target anti-inflammatory and analgesic agents, especially those bearing electron-donating groups and sulfonamide pharmacophores [124].

Chapter 6

Conclusion

A new series of Schiff base derivatives generated from sulfonamide scaffolds sulfamethoxypyridazine and sulfadimidine condensed with different aromatic and heteroaromatic aldehydes were effectively designed, synthesized, and thoroughly evaluated pharmacologically in this study. The primary objective of this study was to create new compounds with better safety and efficacy profiles in order to overcome the drawbacks of the anti-inflammatory drugs. A thorough characterization of all synthesized Schiff base compounds (**1a-5a**) using standard analytical techniques such as TLC, FTIR, and NMR confirmed the successful formation of the imine (-C=N-) linkage and the validation of the intended structural framework. The biological screening of the synthesized compounds revealed high pharmacological potential. In vitro antioxidant assays (TAC, TRP, and DPPH) demonstrated that the compounds, notably 2a, had substantial radical scavenging activity, implying a potential function in alleviating oxidative stress, which is a major contributor to chronic inflammation and degenerative illnesses. Furthermore, in vivo testing of compounds **1a** and **2a** utilizing used of acetic acid to induced writhing and carrageenan to induce model of paw edema revealed that both derivatives had significant analgesic and anti-inflammatory properties that are comparable to or exceed those of typical NSAIDs such as diclofenac. Molecular docking revealed significant interactions between the synthesized compounds and two important inflammatory targets, COX-2 and NF-κB. Notably, compounds 4a and 5a demonstrated higher binding affinities than the reference drugs, implying improved target

selectivity and the possibility for fewer adverse effects. The presence of important amino acid residues in hydrogen bonding, π-stacking, and hydrophobic interactions contributes to the observed pharmaceutical efficacy. Furthermore, *in silico* ADME and toxicity profiling demonstrated that the developed compounds have desirable drug-like features, such as excellent lipophilicity, blood-brain barrier permeability, and low toxicity profiles, indicating their viability for future pharmaceutical development. This study shows the successful synthesis and validation of structurally diverse and physiologically active Schiff base derivatives with substantial anti-inflammatory and antioxidant properties. The combination of synthetic chemistry, spectroscopic characterization, biological studies, and computational modeling has laid a solid platform for the rational development of Schiff base-based drugs. The favorable outcomes indicate that these compounds could be useful lead molecules for the creation of safer, more tailored anti-inflammatory medicines. Further pharmacokinetic, mechanistic, and clinical investigations are required to demonstrate therapeutic usefulness and advance to preclinical studies.

6.1 Future Perspectives

Further *in vivo* pharmacokinetics and bioavailability studies should be carried out to determine systemic exposure and metabolism.

A more thorough SAR study should be conducted to modify pharmacophore characteristics for increased potency and selectivity.

Exploring metal-Schiff base compounds may improve bioactivity through enhanced target affinity and stability.

Additional biological targets (such as anticancer and antibacterial) should be investigated to broaden the therapeutic profile.

Molecular dynamics (MD) simulations should be performed to gain deeper insights into the confirmational behavior and binding stability of ligand-target complexes over time.

Bibliography

[1] K. Nicolaou, "Organic synthesis: the art and science of replicating the molecules of living nature and creating others like them in the laboratory," Proceedings of the Royal Society A: Mathematical, Physical and Engineering Sciences, vol. 470, no. 2163, p. 20130690, 2014.

[2] A. M. Abu-Dief and I. M. Mohamed, "A review on versatile applications of transition metal complexes incorporating Schiff bases," Beni-suef university journal of basic and applied sciences, vol. 4, no. 2, pp. 119-133, 2015.

[3] S. T. Tsantis, D. I. Tzimopoulos, M. Holynska, and S. P. Perlepes, "Oligonuclear actinoid complexes with Schiff bases as ligands—older achievements and recent progress," International Journal of Molecular Sciences, vol. 21, no. 2, p. 555, 2020.

[4] P. G. Cozzi, "Metal–Salen Schiff base complexes in catalysis: practical aspects," Chemical Society Reviews, vol. 33, no. 7, pp. 410-421, 2004.

[5] W. Qin, S. Long, M. Panunzio, and S. Biondi, "Schiff bases: A short survey on an evergreen chemistry tool," Molecules, vol. 18, no. 10, pp. 12264-12289, 2013.

[6] M. Yadav, D. Yadav, D. P. Singh, and J. K. Kapoor, "Pharmaceutical properties of macrocyclic Schiff base transition metal complexes: urgent need in today's world," Inorganica Chimica Acta, vol. 546, p. 121300, 2023.

[7] N. Uddin et al., "Synthesis, characterization, and anticancer activity of Schiff bases," Journal of Biomolecular Structure and Dynamics, vol. 38, no. 11, pp. 3246-3259, 2020.

[8] R. M. Wang, J. J. Mao, J. F. Song, C. X. Huo, and Y. F. He, "Antioxidant activity of bovine serum albumin binding amino acid Schiff-bases metal complexes," Chinese Chemical Letters, vol. 18, no. 11, pp. 1416-1418, 2007.

[9] S. Kaliyaperumal and P. Pattanayak, "Synthesis, Characterization and In Vitro Evaluation for Antimicrobial and Anthelmintic Activity of Novel Benzimidazole Substituted 1, 3, 4-Thiadiazole Schiff's Bases," FABAD Journal of Pharmaceutical Sciences, vol. 46, no. 3, pp. 261-270, 2021.

[10] M. S. Alam, J.-H. Choi, and D.-U. Lee, "Synthesis of novel Schiff base analogues of 4-amino-1, 5-dimethyl-2-phenylpyrazol-3-one and their evaluation for antioxidant and anti-inflammatory activity," Bioorganic & medicinal chemistry, vol. 20, no. 13, pp. 4103-4108, 2012.

[11] L. Li, Z. Li, K. Wang, Y. Liu, Y. Li, and Q. Wang, "Synthesis and antiviral, insecticidal, and fungicidal activities of gossypol derivatives containing alkylimine, oxime or hydrazine moiety," Bioorganic & Medicinal Chemistry, vol. 24, no. 3, pp. 474-483, 2016.

[12] K. Khaldoune et al., "New Schiff bases and their vanadium complexes: Synthesis, characterization, and biological assessment for antibacterial and antiviral action," Applied Organometallic Chemistry, vol. 38, no. 7, p. e7534, 2024.

[13] X. Xu et al., "High-performance, command-degradable, antibacterial Schiff base epoxy thermosets: synthesis and properties," Journal of Materials Chemistry A, vol. 7, no. 25, pp. 15420-15431, 2019.

[14] S. N. Pandeya and N. Rajput, "Synthesis and Anticonvulsant Activity of Various Mannich and Schiff Bases of 1, 5-Benzodiazepines," International Journal of Medicinal Chemistry, vol. 2012, no. 1, p. 237965, 2012.

[15] I. S. Meeran, S. S. Tajudeen, V. A. Dusthakeer, and T. Shabeer, "An insight into the anti-tubercular potential of Schiff bases," J Pharma Chem Bio Sci, vol. 6, no. 3, pp. 158-177, 2018.

[16] D. Sunil, A. M. Isloor, P. Shetty, P. G. Nayak, and K. Pai, "*in vivo* anticancer and histopathology studies of Schiff bases on Ehrlich ascitic carcinoma cells: 1st cancer update," Arabian Journal of Chemistry, vol. 6, no. 1, pp. 25-33, 2013.

[17] A. Khan et al., "Exploration for the opioidergic, GABAergic and histaminergic potentials of synthesized Schiff's base derivatives: An in-vivo approach," Results in Chemistry, vol. 10, p. 101716, 2024.

[18] C. Solis-Calero, J. Ortega-Castro, and F. Munoz, "Reactivity of a phospholipid monolayer model under periodic boundary conditions: a density functional theory study of the schiff base formation between phosphatidylethanolamine and acetaldehyde," The Journal of Physical Chemistry B, vol. 114, no. 48, pp. 15879-15885, 2010.

[19] A. D. Adesina, "Synthesis of Schiff bases by non-conventional methods," in Schiff Base in Organic, Inorganic and Physical Chemistry: IntechOpen, 2022.

[20] A. Natsch, H. Gfeller, T. Haupt, and G. Brunner, "Chemical reactivity and skin sensitization potential for benzaldehydes: can Schiff base formation explain everything?," Chemical Research in Toxicology, vol. 25, no. 10, pp. 2203-2215, 2012.

[21] M. M. Kapil and A. K. Singh, "Retinylidene Schiff bases in phosphatidylcholine reverse micelles: formation, protonation and stability," Journal of the Chemical Society, Perkin Transactions 2, no. 11, pp. 1785-1789, 1991.

[22] D. Ameen and S. Hayyas, "Synthesis, characterization and antimicrobial evaluation of schiff base derived from sulfonamides and vanillin," Zanco Journal of Medical Sciences (Zanco J Med Sci), vol. 28, no. 1, pp. 9-18, 2024.

[23] M. N. Khan, A. M. Khan, H. Ullah, S. Hussain, and A. K. Khattak, "Synthesis and antibacterial activity of the sulfonamide based schiff base and its transition metal (II) complexes," Pak. J. Pharm. Sci, vol. 31, no. 1, pp. 103-111, 2018.

[24] M. Feng, B. Tang, S. H Liang, and X. Jiang, "Sulfur containing scaffolds in drugs: synthesis and application in medicinal chemistry," Current topics in medicinal chemistry, vol. 16, no. 11, pp. 1200-1216, 2016.

[25] J. A. Arnott and S. L. Planey, "The influence of lipophilicity in drug discovery and design," Expert opinion on drug discovery, vol. 7, no. 10, pp. 863-875, 2012.

[26] C. Ballatore, D. M. Huryn, and A. B. Smith III, "Carboxylic acid (bio) isosteres in drug design," ChemMedChem, vol. 8, no. 3, pp. 385-395, 2013.

[27] Y. K. Chong, Y. S. Ong, and K. Y. Yeong, "Unveiling sultam in drug discovery: spotlight on the underexplored scaffold," RSC Medicinal Chemistry, 2024.

[28] K. Rana, A. Pandurangan, N. Singh, and A. K. Tiwari, "A systemic review of schiff bases as an analgesic, anti-inflammatory," Int. J. Curr. Pharm. Res, vol. 4, no. 2, pp. 5-11, 2012.

[29] E. F. McNaughton et al., "Novel anti-inflammatory peptides based on chemokine–glycosaminoglycan interactions reduce leukocyte migration and disease severity in a model of rheumatoid arthritis," The Journal of Immunology, vol. 200, no. 9, pp. 3201-3217, 2018.

[30] C. S. Sit and J. C. Vederas, "Approaches to the discovery of new antibacterial agents based on bacteriocins," Biochemistry and Cell Biology, vol. 86, no. 2, pp. 116-123, 2008.

[31] X.-L. Li, A.-G. Zhou, L. Zhang, and W.-J. Chen, "Antioxidant status and immune activity of glycyrrhizin in allergic rhinitis mice," International journal of molecular sciences, vol. 12, no. 2, pp. 905-916, 2011.

[32] R. A. Jones Lipinski et al., "Molecular docking-guided synthesis of NSAID–glucosamine bioconjugates and their evaluation as COX-1/COX-2 inhibitors with potentially reduced gastric toxicity," Chemical biology & drug design, vol. 98, no. 1, pp. 102-113, 2021.

[33] C. O. Stiller and P. Hjemdahl, "Lessons from 20 years with COX-2 inhibitors: Importance of dose–response considerations and fair play in comparative trials," Journal of internal medicine, vol. 292, no. 4, pp. 557-574, 2022.

[34] S. V. Bhandari, K. G. Bothara, M. K. Raut, A. A. Patil, A. P. Sarkate, and V. J. Mokale, "Design, synthesis and evaluation of antiinflammatory, analgesic and ulcerogenicity studies of novel S-substituted phenacyl-1, 3, 4-oxadiazole-2-thiol and Schiff bases of diclofenac acid as nonulcerogenic derivatives," Bioorganic & medicinal chemistry, vol. 16, no. 4, pp. 1822-1831, 2008.

[35] A. Xavier and N. Srividhya, "Synthesis and study of Schiff base ligands," IOSR Journal of Applied Chemistry, vol. 7, no. 11, pp. 06-15, 2014.

[36] I. Mushtaq, M. Ahmad, M. Saleem, and A. Ahmed, "Pharmaceutical significance of Schiff bases: an overview," Future Journal of Pharmaceutical Sciences, vol. 10, no. 1, p. 16, 2024.

[37] N. Singh, P. Vayer, S. Tanwar, J.-L. Poyet, K. Tsaioun, and B. O. Villoutreix, "Drug discovery and development: introduction to the general public and patient groups," Frontiers in Drug Discovery, vol. 3, p. 1201419, 2023.

[38] N. Chaachouay and L. Zidane, "Plant-derived natural products: a source for drug discovery and development," Drugs and Drug Candidates, vol. 3, no. 1, pp. 184-207, 2024.

[39] Ž. Šantić, N. Pravdić, M. Bevanda, and K. Galić, "The historical use of medicinal plants in traditional and scientific medicine," Psychiatria Danubina, vol. 29, no. suppl. 4, pp. 69-74, 2017.

[40] A. G. Atanasov, S. B. Zotchev, V. M. Dirsch, and C. T. Supuran, "Natural products in drug discovery: advances and opportunities," Nature reviews Drug discovery, vol. 20, no. 3, pp. 200-216, 2021.

[41] R. Nsouli, G. Galiyan, and L. K. Ackerman-Biegasiewicz, "Advancing Organic Chemistry Using High-Throughput Experimentation."

[42] R. Liu, X. Li, and K. S. Lam, "Combinatorial chemistry in drug discovery," Current opinion in chemical biology, vol. 38, pp. 117-126, 2017.

[43] O. O. Grygorenko, D. M. Volochnyuk, S. V. Ryabukhin, and D. B. Judd, "The symbiotic relationship between drug discovery and organic chemistry," Chemistry–A European Journal, vol. 26, no. 6, pp. 1196-1237, 2020.

[44] S. Rollas and Ş. Güniz Küçükgüzel, "Biological activities of hydrazone derivatives," Molecules, vol. 12, no. 8, pp. 1910-1939, 2007.

[45] M. Yadav, S. Sharma, and J. Devi, "Designing, spectroscopic characterization, biological screening and antioxidant activity of mononuclear transition metal complexes of bidentate Schiff base hydrazones," Journal of Chemical Sciences, vol. 133, pp. 1-22, 2021.

[46] H. R. Afzal et al., "Schiff bases of pioglitazone provide better antidiabetic and potent antioxidant effect in a streptozotocin–nicotinamide-induced diabetic rodent model," ACS omega, vol. 6, no. 6, pp. 4470-4479, 2021.

[47] E. Raczuk, B. Dmochowska, J. Samaszko-Fiertek, and J. Madaj, "Different Schiff bases—structure, importance and classification," Molecules, vol. 27, no. 3, p. 787, 2022.

[48] D. Iacopetta et al., "Schiff bases: Interesting scaffolds with promising antitumoral properties," Applied Sciences, vol. 11, no. 4, p. 1877, 2021.

[49] N. Aljamali, M. Hadi, M. Mohamad, L. Salih, and N. Aljamali, "Review on Imine Derivatives and Their Applications," vol. 5, pp. 20-32, 08/10 2019.

[50] N. T. Subasi, "Overview of Schiff Bases," in Schiff Base in Organic, Inorganic and Physical Chemistry: IntechOpen, 2022.

[51] S. S. Mukhtar, A. S. Hassan, N. M. Morsy, T. S. Hafez, H. M. Hassaneen, and F. M. Saleh, "Overview on synthesis, reactions, applications, and biological activities of Schiff bases," Egyptian Journal of Chemistry, vol. 64, no. 11, pp. 6541-6554, 2021.

[52] M. Achparaki et al., "Schiff Bases and Their Metal Complexes: Synthesis, Structural Characteristics and Applications.‖," Intech, vol. 1, p. 13, 2012.

[53] R. Shivhare et al., "Schiff base as multifaceted bioactive core," in Schiff Base in Organic, Inorganic and Physical Chemistry: IntechOpen, 2022.

[54] S. A. Dalia et al., "A short review on chemistry of schiff base metal complexes and their catalytic application," Int. J. Chem. Stud, vol. 6, no. 3, pp. 2859-2867, 2018.

[55] P. J. Silva, "New insights into the mechanism of Schiff base synthesis from aromatic amines in the absence of acid catalyst or polar solvents," PeerJ Organic Chemistry, vol. 2, p. e4, 2020.

[56] R. D. Patil and S. Adimurthy, "Catalytic methods for imine synthesis," Asian Journal of Organic Chemistry, vol. 2, no. 9, pp. 726-744, 2013.

[57] N. S. Radulović, A. B. Miltojević, and R. D. Vukićević, "Simple and efficient one-pot solvent-free synthesis of N-methyl imines of aromatic aldehydes," Comptes Rendus Chimie, vol. 16, no. 3, pp. 257-270, 2013.

[58] T. Dechasa, P. T. Arasu, and A. Lealem, "A review on the synthesis, characterization and application of Schiff bases containing resorcinol moieties and their first row transition metal complexes," Results in Chemistry, p. 101596, 2024.

[59] J. P. Reid, L. Simón, and J. M. Goodman, "A practical guide for predicting the stereochemistry of bifunctional phosphoric acid catalyzed reactions of imines," Accounts of Chemical Research, vol. 49, no. 5, pp. 1029-1041, 2016.

[60] A. K. Chakraborti, S. Bhagat, and S. Rudrawar, "Magnesium perchlorate as an efficient catalyst for the synthesis of imines and phenylhydrazones," Tetrahedron letters, vol. 45, no. 41, pp. 7641-7644, 2004.

[61] J. H. BILLMAN and K. M. TAI, "Reduction of schiff bases. II. Benzhydrylamines and structurally related compounds1a, b," The Journal of Organic Chemistry, vol. 23, no. 4, pp. 535-539, 1958.

[62] J. S. Samec and J. E. Bäckvall, "Ruthenium-Catalyzed Transfer Hydrogenation of Imines by Propan-2-ol in Benzene," Chemistry–A European Journal, vol. 8, no. 13, pp. 2955-2961, 2002.

[63] I. R. Pathan and M. K. Patel, "A comprehensive review on the synthesis and applications of Schiff base ligand and metal complexes: A comparative study of conventional heating, microwave heating, and sonochemical methods," Inorganic Chemistry Communications, p. 111464, 2023.

[64] N. E. Borisova, M. D. Reshetova, and Y. A. Ustynyuk, "Metal-free methods in the synthesis of macrocyclic Schiff bases," Chemical reviews, vol. 107, no. 1, pp. 46-79, 2007.

[65] N. T. Subasi, "Overview of schiff bases," Schiff Base in Organic, Inorganic and Physical Chemistry, 2022.

[66] S. Nagar, S. Raizada, and N. Tripathee, "A review on various green methods for synthesis of Schiff base ligands and their metal complexes," Results in Chemistry, vol. 6, p. 101153, 2023.

[67] V. K. Rao, S. S. Reddy, B. S. Krishna, K. R. M. Naidu, C. N. Raju, and S. Ghosh, "Synthesis of Schiff's bases in aqueous medium: a green alternative approach with effective mass yield and high reaction rates," Green Chemistry Letters and Reviews, vol. 3, no. 3, pp. 217-223, 2010.

[68] B. Kołodziej, "Comparison of conventional and green approaches to the synthesis of aromatic Schiff bases," Polish Journal of Chemical Technology, vol. 26, no. 4, 2024.

[69] S. Hussain and S. Berry, "A review study on green synthesis of chitosan derived schiff bases and their applications," Carbohydrate Research, vol. 535, p. 109002, 2024.

[70] K. Sunil, T. P. Kumara, B. A. Kumar, and S. Patel, "Synthesis, Characterization and Antiioxidant Activity of Schiff Base Compounds Obtained Using Green Chemistry Techniques," Pharmaceutical Chemistry Journal, vol. 55, no. 1, pp. 46-53, 2021.

[71] J. E. Lesch, The first miracle drugs: how the sulfa drugs transformed medicine. Oxford University Press, 2006.

[72] A. Ovung and J. Bhattacharyya, "Sulfonamide drugs: Structure, antibacterial property, toxicity, and biophysical interactions," Biophysical reviews, vol. 13, no. 2, pp. 259-272, 2021.

[73] N. Tansakul, F. Niedorf, and M. Kietzmann, "A sulfadimidine model to evaluate pharmacokinetics and residues at various concentrations in laying hen," Food additives and contaminants, vol. 24, no. 6, pp. 598-604, 2007.

[74] I. Ukrainets and N. Bereznyakova, "Heterocyclic diuretics," Chemistry of Heterocyclic Compounds, vol. 48, pp. 155-165, 2012.

[75] M. S. Ayoup et al., "Novel sulfonamide derivatives as multitarget antidiabetic agents: design, synthesis, and biological evaluation," RSC advances, vol. 14, no. 11, pp. 7664-7675, 2024.

[76] G. M. Gaddi et al., "Phosphatase Alkaline Inhibition and Antithyroid Activity of Acetylacetone Sulfonamide Derived Schiff Base. In Vitro and In Silico Studies," ChemistrySelect, vol. 9, no. 23, p. e202401342, 2024.

[77] A. K. Bishoyi, M. Mahapatra, C. R. Sahoo, S. K. Paidesetty, and R. N. Padhy, "Design, molecular docking and antimicrobial assessment of newly synthesized p-cuminal-sulfonamide Schiff base derivatives," Journal of Molecular Structure, vol. 1250, p. 131824, 2022.

[78] M. Chalkha et al., "Crystallographic study, biological assessment and POM/-Docking studies of pyrazoles-sulfonamide hybrids (PSH): Identification of a combined Antibacterial/Antiviral pharmacophore sites leading to in-silico screening the anti-Covid-19 activity," Journal of Molecular Structure, vol. 1267, p. 133605, 2022.

[79] A.-M. Alaa, A. Angeli, A. S. El-Azab, M. E. Hammouda, M. A. El-Sherbeny, and C. T. Supuran, "Synthesis and anti-inflammatory activity of sulfonamides and carboxylates incorporating trimellitimides: Dual cyclooxygenase/carbonic anhydrase inhibitory actions," Bioorganic chemistry, vol. 84, pp. 260-268, 2019.

[80] E. A. Sultan, "Pathophysiologic mechanisms of immune-mediated drug hypersensitivity reactions to sulfonamides," The University of Western Ontario (Canada), 2015.

[81] S. M. Mathews, V. Jiju, I. Thomas, J. T. Panicker, and L. S. Kuriakose, "Sulfa drugs and the skin," World J Pharm Res, vol. 4, no. 10, pp. 382-390, 2015.

[82] M.-K. Yun et al., "Catalysis and sulfa drug resistance in dihydropteroate synthase," Science, vol. 335, no. 6072, pp. 1110-1114, 2012.

[83] J. Botelho, F. Grosso, and L. Peixe, "Antibiotic resistance in Pseudomonas aeruginosa–Mechanisms, epidemiology and evolution," Drug resistance updates, vol. 44, p. 100640, 2019.

[84] H. Siddiqui, H. M. Haniffa, A. Jabeen, A.-u. -Rahman, and M. I. Choudhary, "Sulphamethazine derivatives as immunomodulating agents: New therapeutic strategies for inflammatory diseases," Plos one, vol. 13, no. 12, p. e0208933, 2018.

[85] A. M. Tawfik, M. A. El-Ghamry, S. M. Abu-El-Wafa, and N. M. Ahmed, "A new bioactive Schiff base ligands derived from propylazo-N-pyrimidin-2-yl-benzenesulfonamides Mn (II) and Cu (II) complexes: Synthesis, thermal and spectroscopic characterization biological studies and 3D modeling structures," Spectrochimica Acta Part A: Molecular and Biomolecular Spectroscopy, vol. 97, pp. 1172-1180, 2012.

[86] A. M. Mansour and N. T. A. Ghani, "Hydrogen-bond effect, spectroscopic and molecular structure investigation of sulfamethazine Schiff-base: Experimental and quantum chemical calculations," Journal of Molecular Structure, vol. 1040, pp. 226-237, 2013.

[87] S. Hosny, M. S. Ragab, and R. F. Abd El-Baki, "Synthesis of a new sulfadimidine Schiff base and their nano complexes as potential anti-COVID-19 and anti-cancer activity," Scientific Reports, vol. 13, no. 1, p. 1502, 2023.

[88] A. M. Mansour, N. T. Abdel-Ghani, and M. S. Ragab, "DNA/bovine serum albumin binding and cytotoxicity of transition metal ternary complexes based on sulfamethazine and bromazepam drugs," Applied Organometallic Chemistry, vol. 34, no. 12, p. e5995, 2020.

[89] A. Sarkar, S. Gupta, T. Banerjee, K. Manjaiah, and N. Narayanan, "Development of a GREEN analytical technique for detecting sulfamethoxypyridazine in soil and water by QuEChERS/SPE-ESI-LC/MS/MS," Chemical Papers, vol. 78, no. 10, pp. 6115-6126, 2024.

[90] M. Wajid et al., "Biological activities, DFT and molecular docking studies of novel schiff bases derived from sulfamethoxypyridazine," ChemistrySelect, vol. 9, no. 15, p. e202400675, 2024.

[91] K. Buran, "Metal complexes of sulfamethazine/benzoin-based Schiff base ligand: synthesis, characterization, DFT calculations, and antimicrobial activities," Turkish Journal of Biology, vol. 49, no. 1, pp. 118-126, 2025.

[92] E. N. Md Yusof et al., "Synthesis, characterization and biological evaluation of transition metal complexes derived from N, S bidentate ligands," International journal of molecular sciences, vol. 16, no. 5, pp. 11034-11054, 2015.

[93] M. N. Uddin, S. S. Ahmed, and S. R. Alam, "Biomedical applications of Schiff base metal complexes," Journal of Coordination Chemistry, vol. 73, no. 23, pp. 3109-3149, 2020.

[94] H. H. Afridi et al., "Synthesis and investigation of the analgesic potential of enantiomerically pure schiff bases: a mechanistic approach," Molecules, vol. 27, no. 16, p. 5206, 2022.

[95] S. J. Hamid and T. Salih, "Design, synthesis, and anti-inflammatory activity of some coumarin Schiff base derivatives: In silico and in vitro study," Drug Design, Development and Therapy, pp. 2275-2288, 2022.

[96] J. Ceramella, D. Iacopetta, A. Catalano, F. Cirillo, R. Lappano, and M. S. Sinicropi, "A review on the antimicrobial activity of Schiff bases: Data collection and recent studies," Antibiotics, vol. 11, no. 2, p. 191, 2022.

[97] R. Sahu and K. Shah, "Schiff Bases: A Captivating Scaffold with Potential Anticonvulsant Activity," Mini Reviews in Medicinal Chemistry, vol. 24, no. 18, pp. 1632-1650, 2024.

[98] H. Kizilkaya, B. Dag, T. Aral, N. Genc, and R. Erenler, "Synthesis, characterization, and antioxidant activity of heterocyclic Schiff bases," Journal of the Chinese Chemical Society, vol. 67, no. 9, pp. 1696-1701, 2020.

[99] M. Mesbah, T. Douadi, F. Sahli, S. Issaadi, S. Boukazoula, and S. Chafaa, "Synthesis, characterization, spectroscopic studies and antimicrobial activity of three new Schiff bases derived from Heterocyclic moiety," Journal of Molecular Structure, vol. 1151, pp. 41-48, 2018.

[100] D. M. Jamil et al., "Experimental and theoretical studies of Schiff bases as corrosion inhibitors," Chemistry Central Journal, vol. 12, pp. 1-9, 2018.

[101] D. A. Safin, M. G. Babashkina, M. Bolte, A. L. Ptaszek, M. Kukułka, and M. P. Mitoraj, "Novel sterically demanding Schiff base dyes: An insight from experimental and theoretical calculations," Journal of Luminescence, vol. 238, p. 118264, 2021.

[102] O. Wahba, A. M. Hassan, A. Naser, and A. Hanafi, "Preparation and spectroscopic studies of some copper and nickel Schiff base complexes and their applications as colouring pigments in protective paints industry," Egyptian Journal of Chemistry, vol. 60, no. 1, pp. 25-40, 2017.

[103] V. K. Juyal et al., "Schiff base metal complexes as a versatile catalyst: A review," Journal of organometallic chemistry, vol. 999, p. 122825, 2023.

[104] H. Mighani, "Schiff Base polymers: synthesis and characterization," Journal of Polymer Research, vol. 27, pp. 1-18, 2020.

[105] W. Al Zoubi and Y. G. Ko, "Schiff base complexes and their versatile applications as catalysts in oxidation of organic compounds: part I," Applied Organometallic Chemistry, vol. 31, no. 3, p. e3574, 2017.

[106] F. T. Esmadi, O. F. Khabour, K. Abbas, A. E. Mohammad, R. a. T. Obeidat, and D. a. Mfady, "Synthesis, characterization and biological activity of some unsymmetrical Schiff base transition metal complexes," Drug and Chemical Toxicology, vol. 39, no. 1, pp. 41-47, 2016.

[107] A. Kajal, S. Bala, S. Kamboj, N. Sharma, and V. Saini, "Schiff bases: a versatile pharmacophore," Journal of Catalysts, vol. 2013, no. 1, p. 893512, 2013.

[108] H. A. Younus et al., "Part-II: an update of Schiff bases synthesis and applications in medicinal chemistry-a patent review (2016-2023)," Expert Opinion on Therapeutic Patents, vol. 33, no. 12, pp. 841-864, 2023.

[109] M. Shoeb, R. Islam, and N. Parvin, "Antibiotic resistance: a global threat to humanity," in Transcending Humanitarian Engineering Strategies for Sustainable Futures: IGI Global, 2023, pp. 82-105.

[110] Y. Xu, Y. Shi, F. Lei, and L. Dai, "A novel and green cellulose-based Schiff base-Cu (II) complex and its excellent antibacterial activity," Carbohydrate polymers, vol. 230, p. 115671, 2020.

[111] M. A. Ashraf, K. Mahmood, A. Wajid, M. J. Maah, and I. Yusoff, "Synthesis, characterization and biological activity of Schiff bases," IPCBEE, vol. 10, no. 1, p. 185, 2011.

[112] J. K. Suyambulingam et al., "Synthesis, structure, biological/chemosensor evaluation and molecular docking studies of aminobenzothiazole Schiff bases," Journal of Adhesion Science and Technology, vol. 34, no. 23, pp. 2590-2612, 2020.

[113] A. Mermer, N. Demirbas, H. Uslu, A. Demirbas, S. Ceylan, and Y. Sirin, "Synthesis of novel Schiff bases using green chemistry techniques; antimicrobial, antioxidant, antiurease activity screening and molecular docking studies," Journal of Molecular Structure, vol. 1181, pp. 412-422, 2019.

[114] K. H. M. E. Tehrani, M. Hashemi, M. Hassan, F. Kobarfard, and S. Mohebbi, "Synthesis and antibacterial activity of Schiff bases of 5-substituted isatins," Chinese Chemical Letters, vol. 27, no. 2, pp. 221-225, 2016.

[115] J. T. Kakkassery, V. P. Raphael, and R. Johnson, "In vitro antibacterial and in silico docking studies of two Schiff bases on Staphylococcus aureus and its target proteins," Future Journal of Pharmaceutical Sciences, vol. 7, no. 1, pp. 1-9, 2021.

[116] A. Bratovcic, "Antioxidant enzymes and their role in preventing cell damage," Acta Sci. Nutr. Health, vol. 4, no. 3, pp. 01-07, 2020.

[117] S. Di Meo and P. Venditti, "Evolution of the knowledge of free radicals and other oxidants," Oxidative medicine and cellular longevity, vol. 2020, no. 1, p. 9829176, 2020.

[118] D. M. Teleanu et al., "An overview of oxidative stress, neuroinflammation, and neurodegenerative diseases," International journal of molecular sciences, vol. 23, no. 11, p. 5938, 2022.

[119] C. R. Amorim et al., "Schiff bases of 4-phenyl-2-aminothiazoles as hits to new antischistosomals: synthesis, in vitro, *in vivo* and in silico studies," European Journal of Pharmaceutical Sciences, vol. 150, p. 105371, 2020.

[120] R. Teran et al., "Characterization of antimicrobial, antioxidant, and leishmanicidal activities of Schiff base derivatives of 4-aminoantipyrine," Molecules, vol. 24, no. 15, p. 2696, 2019.

[121] B. B. Singh, N. A. Shakil, J. Kumar, V. S. Rana, and A. Mishra, "Microwave synthesis, characterization, and bio-efficacy of novel halogenated Schiff bases," Journal of Environmental Science and Health, Part B, vol. 51, no. 8, pp. 558-570, 2016.

[122] Z. Hussain, Z. Fadhil, H. Adil, M. Khalaf, B. Abdullah, and E. Yousif, "Schiff's bases containing sulphamethoxazole nucleus," Research Journal of Pharmaceutical Biological And Chemical Sciences, vol. 7, no. 3, pp. 1500-1510, 2016.

[123] J. W. Atchison, C. M. Herndon, and E. Rusie, "NSAIDs for musculoskeletal pain management: current perspectives and novel strategies to improve safety," Journal of Managed Care Pharmacy, vol. 19, no. 9 Supp A, pp. 1-19, 2013.

[124] S. K. Raju, A. Settu, A. Thiyagarajan, D. Rama, P. Sekar, and S. Kumar, "Biological applications of Schiff bases: An overview," GSC Biol. Pharm. Sci, vol. 21, no. 3, pp. 203-215, 2022.

[125] D. B. Kitchen, H. Decornez, J. R. Furr, and J. Bajorath, "Docking and scoring in virtual screening for drug discovery: methods and applications," Nature reviews Drug discovery, vol. 3, no. 11, pp. 935-949, 2004.

[126] L. Willard et al., "VADAR: a web server for quantitative evaluation of protein structure quality," Nucleic acids research, vol. 31, no. 13, pp. 3316-3319, 2003.

[127] O. Trott and A. J. Olson, "AutoDock Vina: improving the speed and accuracy of docking with a new scoring function, efficient optimization, and multithreading," Journal of computational chemistry, vol. 31, no. 2, pp. 455-461, 2010.

[128] M. N. Drwal, P. Banerjee, M. Dunkel, M. R. Wettig, and R. Preissner, "ProTox: a web server for the in silico prediction of rodent oral toxicity," Nucleic acids research, vol. 42, no. W1, pp. W53-W58, 2014.

[129] A. Daina and V. Zoete, "A boiled-egg to predict gastrointestinal absorption and brain penetration of small molecules," ChemMedChem, vol. 11, no. 11, pp. 1117-1121, 2016.

[130] A. Daina, O. Michielin, and V. Zoete, "SwissADME: a free web tool to evaluate pharmacokinetics, drug-likeness and medicinal chemistry friendliness of small molecules," Scientific reports, vol. 7, no. 1, p. 42717, 2017.

[131] S. Dallakyan and A. J. Olson, "Small-molecule library screening by docking with PyRx," in Chemical biology: methods and protocols: Springer, 2014, pp. 243-250.

[132] K. Singh, M. S. Barwa, and P. Tyagi, "Synthesis, characterization and biological studies of Co (II), Ni (II), Cu (II) and Zn (II) complexes with bidentate Schiff bases derived by heterocyclic ketone," European Journal of Medicinal Chemistry, vol. 41, no. 1, pp. 147-153, 2006.

[133] M. Rajasekar, J. Mary, M. Sivakumar, S. S. Ravichandran, and D. Srinivasan, "Recent advances in organic fluorophore-based Schiff base metal complexes: Applications in biomedicine and related fields," Results in Chemistry, p. 102166, 2025.

[134] M. Durgun et al., "Synthesis, characterisation, biological evaluation and in silico studies of sulphonamide Schiff bases," Journal of enzyme inhibition and medicinal chemistry, vol. 35, no. 1, pp. 950-962, 2020.

[135] C. M. Da Silva et al., "Schiff bases: A short review of their antimicrobial activities," Journal of Advanced research, vol. 2, no. 1, pp. 1-8, 2011.

[136] M. A. Mohamed, J. Jaafar, A. Ismail, M. Othman, and M. Rahman, "Fourier transform infrared (FTIR) spectroscopy," in Membrane characterization: Elsevier, 2017, pp. 3-29.

[137] Z. H. Chohan, S. H. Sumrra, M. H. Youssoufi, and T. B. Hadda, "Metal based biologically active compounds: Design, synthesis, and antibacterial/antifungal/cytotoxic properties of triazole-derived Schiff bases and their oxovanadium (IV) complexes," European journal of medicinal chemistry, vol. 45, no. 7, pp. 2739-2747, 2010.

[138] F. Ibadi et al., "Organotin complexes with Schiff's base ligands: insights into their cytotoxic effects on lung cancer cells," Journal of Umm Al-Qura University for Applied Sciences, pp. 1-17, 2024.

[139] M. Bunzel and M. H. Penner, "Basic Principles of Spectroscopy," in Nielsen's Food Analysis: Springer, 2024, pp. 65-75.

[140] R. Nyquist, "Sulfoxides, Sulfones, Sulfates, Monothiosulfates, Sulfonyl Halides, Sulfites, Sulfonamides, Sulfonates, and N-Sulfinyl Anilines," Interpreting Infrared, Raman, and Nuclear Magnetic Resonance Spectra; Elsevier: Amsterdam, The Netherlands, pp. 85-117, 2001.

[141] F. Dai, Q. Zhuang, G. Huang, H. Deng, and X. Zhang, "Infrared spectrum characteristics and quantification of OH groups in coal," ACS omega, vol. 8, no. 19, pp. 17064-17076, 2023.

[142] L. Boubakri et al., "Synthesis and catalytic applications of palladium N-heterocyclic carbene complexes as efficient pre-catalysts for Suzuki–Miyaura and Sonogashira coupling reactions," New Journal of Chemistry, vol. 41, no. 12, pp. 5105-5113, 2017.

[143] B. Bakchi et al., "An overview on applications of SwissADME web tool in the design and development of anticancer, antitubercular and antimicrobial agents: A medicinal chemist's perspective," Journal of Molecular Structure, vol. 1259, p. 132712, 2022/07/05/ 2022, doi: https://doi.org/10.1016/j.molstruc.2022.132712.

[144] C. A. Lipinski, F. Lombardo, B. W. Dominy, and P. J. Feeney, "Experimental and computational approaches to estimate solubility and permeability in drug discovery and development settings," Advanced Drug Delivery Reviews, vol. 64, pp. 4-17, 2012/12/01/ 2012, doi: https://doi.org/10.1016/j.addr.2012.09.019.

[145] C. A. Lipinski, "Capter 11 Filtering in Drug Discovery," in Annual Reports in Computational Chemistry, vol. 1: Elsevier, 2005, pp. 155-168.

[146] M. Pathak, H. Ojha, A. K. Tiwari, D. Sharma, M. Saini, and R. Kakkar, "Design, synthesis and biological evaluation of antimalarial activity of new derivatives of 2,4,6-s-triazine," Chemistry Central Journal, vol. 11, no. 1, p. 132, 2017/12/19 2017, doi: 10.1186/s13065-017-0362-5.

[147] E. M. Gerlach, M. A. Korkmaz, I. Pavlinov, Q. Gao, and L. N. Aldrich, "Systematic Diversity-Oriented Synthesis of Reduced Flavones from -Pyrones

to Probe Biological Performance Diversity," ACS Chemical Biology, vol. 14, no. 7, pp. 1536-1545, 2019/07/19 2019, doi: 10.1021/acschembio.9b00294.

[148] C.-Y. Jia, J.-Y. Li, G.-F. Hao, and G.-F. Yang, "A drug-likeness toolbox facilitates ADMET study in drug discovery," Drug Discovery Today, vol. 25, no. 1, pp. 248-258, 2020/01/01/ 2020, doi: https://doi.org/10.1016/j.drudis.2019.10.014.

[149] D. F. Veber, S. R. Johnson, H.-Y. Cheng, B. R. Smith, K. W. Ward, and K. D. Kopple, "Molecular Properties That Influence the Oral Bioavailability of Drug Candidates," Journal of Medicinal Chemistry, vol. 45, no. 12, pp. 2615-2623, 2002/06/01 2002, doi: 10.1021/jm020017n.

[150] P. R. Andrews, D. J. Craik, and J. L. Martin, "Functional group contributions to drug-receptor interactions," Journal of Medicinal Chemistry, vol. 27, no. 12, pp. 1648-1657, 1984/12/01 1984, doi: 10.1021/jm00378a021.

[151] I. Ahmad, H. Khan, M. U. Amin, S. Khalid, T. Behl, and N. Ur Rahman, "An Overview on the Anticancer Potential of Punarnavine: Prediction of Drug-Like Properties," Oncologie (Tech Science Press), vol. 23, no. 3, 2021.

[152] A. Daina, O. Michielin, and V. Zoete, "iLOGP: a simple, robust, and efficient description of n-octanol/water partition coefficient for drug design using the GB/SA approach," Journal of chemical information and modeling, vol. 54, no. 12, pp. 3284-3301, 2014.

[153] T. Ginex, J. Vazquez, E. Gilbert, E. Herrero, and F. J. Luque, "Lipophilicity in drug design: An overview of lipophilicity descriptors in 3D-QSAR studies," Future medicinal chemistry, vol. 11, no. 10, pp. 1177-1193, 2019.

[154] M. Nabati, H. Sabahnoo, and V. Bodaghi-Namileh, "Molecular structure Determination and stability parameters study of 99mTc-MDP (technetium 99m Methylene diphosphonate) cold kit and analysis of its binding to osteocalcin receptor as a bone scan agent," Chem Methodol, vol. 4, pp. 297-310, 2019.

[155] Y. C. Martin, "A bioavailability score," Journal of medicinal chemistry, vol. 48, no. 9, pp. 3164-3170, 2005.

[156] J. B. Baell and G. A. Holloway, "New substructure filters for removal of pan assay interference compounds (PAINS) from screening libraries and for their exclusion in bioassays," Journal of medicinal chemistry, vol. 53, no. 7, pp. 2719-2740, 2010.

[157] R. Brenk et al., "Lessons learnt from assembling screening libraries for drug discovery for neglected diseases," ChemMedChem: Chemistry Enabling Drug Discovery, vol. 3, no. 3, pp. 435-444, 2008.

[158] S. J. Teague, A. M. Davis, P. D. Leeson, and T. Oprea, "The design of leadlike combinatorial libraries," Angewandte Chemie International Edition, vol. 38, no. 24, pp. 3743-3748, 1999.

[159] O. OECD, "423-Guidelines for the testing of chemicals Acute oral toxicity-Fixed dose procedure," Animals (Basel), 2001.

[160] P. Banerjee, A. O. Eckert, A. K. Schrey, and R. Preissner, "ProTox-II: a webserver for the prediction of toxicity of chemicals," Nucleic acids research, vol. 46, no. W1, pp. W257-W263, 2018.

[161] H. Kaji, N. Nagai, M. Nishizawa, and T. Abe, "Drug delivery devices for retinal diseases," Advanced drug delivery reviews, vol. 128, pp. 148-157, 2018.

[162] M. Chen et al., "Toward predictive models for drug-induced liver injury in humans: are we there yet?," Biomarkers in medicine, vol. 8, no. 2, pp. 201-213, 2014.

[163] O. R. Kolawole and K. Kashfi, "NSAIDs and cancer resolution: new paradigms beyond cyclooxygenase," International journal of molecular sciences, vol. 23, no. 3, p. 1432, 2022.

[164] T. Joshi, P. Sharma, T. Joshi, and S. Chandra, "In silico screening of anti-inflammatory compounds from Lichen by targeting cyclooxygenase-2," Journal of Biomolecular Structure and Dynamics, vol. 38, no. 12, pp. 3544-3562, 2020.

[165] P. H. Araújo et al., "Identification of potential COX-2 inhibitors for the treatment of inflammatory diseases using molecular modeling approaches," Molecules, vol. 25, no. 18, p. 4183, 2020.

[166] G. I. Lambrou, K. Hatziagapiou, and S. Vlahopoulos, "Inflammation and tissue homeostasis: The NF-κB system in physiology and malignant progression," Molecular Biology Reports, vol. 47, no. 5, pp. 4047-4063, 2020.

[167] N. D. Perkins, "Integrating cell-signalling pathways with NF-κB and IKK function," Nature reviews Molecular cell biology, vol. 8, no. 1, pp. 49-62, 2007.

[168] T. Huxford and G. Ghosh, "A structural guide to proteins of the NF-κB signaling module," Cold Spring Harbor perspectives in biology, vol. 1, no. 3, p. a000075, 2009.

[169] T. Huxford, A. Hoffmann, and G. Ghosh, "Understanding the logic of IκB: NF-κB regulation in structural terms," NF-kB in Health and Disease, pp. 1-24, 2010.

[170] S. Prasad, K. Phromnoi, V. R. Yadav, M. M. Chaturvedi, and B. B. Aggarwal, "Targeting inflammatory pathways by flavonoids for prevention and treatment of cancer," Planta medica, vol. 76, no. 11, pp. 1044-1063, 2010.

[171] A. ABDELMADJID et al., "Synthesis, crystal structure, electrochemical, theoretical studies and antioxidant activities of new Schiff base," Journal of Molecular Structure, vol. 1227, p. 129368, 2021.

[172] A. Xing, D. Zeng, and Z. Chen, "Synthesis, crystal structure and antioxidant activity of butylphenol Schiff bases: Experimental and DFT study," Journal of Molecular Structure, vol. 1253, p. 132209, 2022.

[173] E. H. Anouar et al., "Antioxidant properties of phenolic Schiff bases: structure–activity relationship and mechanism of action," Journal of computer-aided molecular design, vol. 27, pp. 951-964, 2013.

[174] M. S. Rana et al., "Antioxidant activity of Schiff base ligands using the DPPH scavenging assay: an updated review," RSC advances, vol. 14, no. 45, pp. 33094-33123, 2024.

[175] P. Baral, S. Udit, and I. M. Chiu, "Pain and immunity: implications for host defence," Nature Reviews Immunology, vol. 19, no. 7, pp. 433-447, 2019.

[176] S. Hannoodee and D. N. Nasuruddin, "Acute inflammatory response," in StatPearls [Internet]: StatPearls Publishing, 2024.

[177] S. P. Gawade, "Acetic acid induced painful endogenous infliction in writhing test on mice," Journal of pharmacology & pharmacotherapeutics, vol. 3, no. 4, p. 348, 2012.

[178] M. A. Alblihed, "Astragalin attenuates oxidative stress and acute inflammatory responses in carrageenan-induced paw edema in mice," Molecular Biology Reports, vol. 47, no. 9, pp. 6611-6620, 2020.

[179] Y. Nomier et al., "Ethnopharmacological evaluation of Poppy seed oil in combination with Tramadol on behavioral paradigm and on dopamine, and cytokines levels," European Review for Medical & Pharmacological Sciences, vol. 27, no. 5, 2023.